TECHNICAL REPORT SL-87-10

VULNERABILITY EVALUATION OF THE KEYWORKER BLAST SHELTER

by

Thomas R. Slawson

Structures Laboratory

DEPARTMENT OF THE ARMY
Waterways Experiment Station, Corps of Engineers
PO Box 631, Vicksburg, Mississippi 39180-0631

April 1987
Final Report

Prepared for Federal Emergency Management Agency
Washington, DC 20472

Destroy this report when no longer needed. Do not return it to the originator.

The findings in this report are not to be construed as an official Department of the Army position unless so designated by other authorized documents.

The contents of this report are not to be used for advertising, publication, or promotional purposes. Citation of trade names does not constitute an official endorsement or approval of the use of such commercial products.

TECHNICAL REPORT SL-87-10

VULNERABILITY EVALUATION OF THE KEYWORKER BLAST SHELTER

by

Thomas R. Slawson

Structures Laboratory

DEPARTMENT OF THE ARMY
Waterways Experiment Station, Corps of Engineers
PO Box 631, Vicksburg, Mississippi 39180-0631

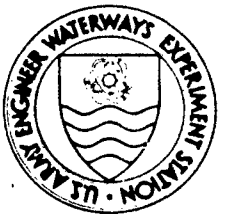

April 1987
Final Report

Prepared for Federal Emergency Management Agency
Washington, DC 20472

AD-A182 508

Unclassified
SECURITY CLASSIFICATION OF THIS PAGE

REPORT DOCUMENTATION PAGE

Form Approved
OMB No. 0704-0188
Exp. Date: Jun 30, 1986

1a. REPORT SECURITY CLASSIFICATION: Unclassified	1b. RESTRICTIVE MARKINGS
2a. SECURITY CLASSIFICATION AUTHORITY	3. DISTRIBUTION/AVAILABILITY OF REPORT: Approved for public release; distribution unlimited.
2b. DECLASSIFICATION/DOWNGRADING SCHEDULE	
4. PERFORMING ORGANIZATION REPORT NUMBER(S): Technical Report SL-87-10	5. MONITORING ORGANIZATION REPORT NUMBER(S)
6a. NAME OF PERFORMING ORGANIZATION: USAEWES Structures Laboratory; 6b. OFFICE SYMBOL (If applicable): WESSS	7a. NAME OF MONITORING ORGANIZATION
6c. ADDRESS (City, State, and ZIP Code): PO Box 631, Vicksburg, MS 39180-0631	7b. ADDRESS (City, State, and ZIP Code)
8a. NAME OF FUNDING/SPONSORING ORGANIZATION: Federal Emergency Management Agency; 8b. OFFICE SYMBOL (If applicable)	9. PROCUREMENT INSTRUMENT IDENTIFICATION NUMBER
8c. ADDRESS (City, State, and ZIP Code): Washington, DC 20472	10. SOURCE OF FUNDING NUMBERS: PROGRAM ELEMENT NO. / PROJECT NO. / TASK NO / WORK UNIT ACCESSION NO

11. TITLE (Include Security Classification)
Vulnerability Evaluation of the Keyworker Blast Shelter

12. PERSONAL AUTHOR(S)
Slawson, T. R.

13a. TYPE OF REPORT	13b. TIME COVERED	14. DATE OF REPORT (Year, Month, Day)	15. PAGE COUNT
Final report	FROM _____ TO _____	April 1987	114

16. SUPPLEMENTARY NOTATION
Available from National Technical Information Service, 5285 Port Royal Road, Springfield, VA 22161.

17. COSATI CODES		
FIELD	GROUP	SUB-GROUP

18. SUBJECT TERMS (Continue on reverse if necessary and identify by block number)
Blast effect; Structural design; Explosions; Soil-structure interaction; Nuclear blast shelters; Shallow-buried structures

19. ABSTRACT (Continue on reverse if necessary and identify by block number)

The 100-man Keyworker blast shelter that survived MINOR SCALE (a high explosive event) was retested using the High Explosive Simulation Technique (HEST) in August 1986. The test was conducted at White Sands Missile Range, N. Mex. The existing structure sustained minor damage (1/8-inch permanent midspan deflection) during MINOR SCALE at the predicted 75-psi peak overpressure level, and a retest was proposed to investigate the shelter's large deformation behavior.

The shelter was tested using a 1-MT nuclear weapon simulation at 130- to 160-psi (depending on the duration of the simulation). The shelter survived the test with large plastic roof deformations ranging from 8 to 17 inches at roof midspan. The failure mode of the shelter roof was very ductile, and the shelter had adequate reserve capacity to withstand large deformations without catastrophic failure.

(Continued)

20. DISTRIBUTION/AVAILABILITY OF ABSTRACT	21. ABSTRACT SECURITY CLASSIFICATION
☒ UNCLASSIFIED/UNLIMITED ☐ SAME AS RPT ☐ DTIC USERS	Unclassified
22a. NAME OF RESPONSIBLE INDIVIDUAL	22b. TELEPHONE (Include Area Code) / 22c. OFFICE SYMBOL

DD FORM 1473, 84 MAR — 83 APR edition may be used until exhausted. All other editions are obsolete.

SECURITY CLASSIFICATION OF THIS PAGE
Unclassified

19. ABSTRACT (Continued).

Survivability of occupants and mechanical equipment at this overpressure was investigated. The mechanical equipment inside the shelter was fully functional after the test e cept for the roof-mounted fluorescent light fixtures. In-structure shock was within acceptable limits for shelter occupants, and high-speed movies of the mannequin movement reinforced this conclusion.

Based on this test result, it is concluded that the shelter performed as designed in the buried configuration under ideal backfill conditions. Additional scale model tests validated the shelter design in the bermed configuration and in various backfill types.

PREFACE

The research reported herein was sponsored by the Federal Emergency Management Agency (FEMA) through the US Army Engineer Division, Huntsville (HND), in support of the Keyworker Blast Shelter Program. Mr. Jim Jacobs, FEMA, was the program monitor.

Testing was conducted by personnel of the Structures Laboratory (SL), US Army Engineer Waterways Experiment Station (WES), under the general supervision of Messrs. Bryant Mather, Chief, SL, and James T. Ballard, Assistant Chief, SL. Chief of the Structural Mechanics Division (SMD) during this investigation was Dr. Jimmy P. Balsara. The project was managed by Dr. Sammy A. Kiger of the Research Group (SMD). Messrs. Stanley C. Woodson and James L. Davis (SMD) supervised the experiment. Mr. Thomas R. Slawson (SMD) prepared this report. Electronic data recovery was performed by Mr. Herman P. Parks, Calibration and Standards Section, Instrumentation Services Division, WES. The report was edited by Ms. Lee T. Byrne, Information Products Division, Information Technology Laboratory, WES.

COL Allen F. Grum, USA, was the previous Director of WES. COL Dwayne G. Lee, CE, is the present Commander and Director. Dr. Robert W. Whalin is the Technical Director.

CONTENTS

CONTENTS (CONCLUDED)

LIST OF ILLUSTRATIONS

LIST OF TABLES

CONVERSION FACTORS, NON-SI TO SI (METRIC) UNITS OF MEASUREMENT

Non-SI units of measurement used in this report can be converted to SI (metric) units as follows:

Multiply	By	To Obtain
cubic feet	0.02831685	cubic metres
degrees (angle)	0.01745329	radians
feet	0.3048	metres
g's (standard free fall)	9.80665	metres per second squared
inches	25.4	millimetres
kilotons (nuclear equivalent of TNT)	4.184	terajoules
megatons (nuclear equivalent of TNT)	4.184	petajoules
pounds (force) per square inch	6.4757	kilopascals
pounds (mass)	0.4535924	kilograms
pound (mass) per cubic foot	16.01846	kilograms per cubic metre
tons (2,000 pounds, mass)	907.1847	kilograms

VULNERABILITY EVALUATION OF THE KEYWORKER BLAST SHELTER

CHAPTER 1

INTRODUCTION

1.1 BACKGROUND

At the time this study was initiated, several civil defense policy options were being analyzed for protection of industrial capability and key workers. One option under consideration called for a program of construction of blast shelters to protect key workers remaining in high-risk areas during a national security crisis. In support of this option, the Federal Emergency Management Agency (FEMA) tasked the US Army Engineer Division, Huntsville (HND), to design the 100-man Keyworker blast shelter. The design required an earth-covered shelter to resist the radiation and blast effects of a 1-MT nuclear detonation at the 50-psi peak overpressure level. The first design was based on conventional blast shelter design procedures that neglect soil-structure interaction.

The design of the 100-man Keyworker blast shelter has evolved from the original overly conservative design to its present form based on experimental and analytical investigations performed by the US Army Engineer Waterways Experiment Station (WES) and the HND. Reductions in construction costs as the result of labor and material savings and less stringent backfill specifications were made without adversely affecting the structural performance. The design modifications were validated using small-scale static and dynamic tests during the design process. A prototype demonstration test of the shelter was conducted in MINOR SCALE, a high explosive (HE) 8-KT nuclear simulation. The shelter survived at the predicted 75-psi* peak overpressure level (measured pressures were approximately 60 psi) with minor damage (1/8-inch permanent midspan roof deformation).

This report describes the retest of the prototype shelter using the High-Explosive Simulation Technique (HEST) to simulate the airblast component of a large-yield nuclear detonation.

---

* A table of factors for converting non-SI units of measurement to SI (metric) units is presented on page v.

1.2 OBJECTIVES

The objectives of this test were to study the large deformation behavior of the Keyworker blast shelter and to study the in-structure shock environment during an overload condition.

1.3 SCOPE

The prototype shelter that survived the MINOR SCALE HE event with negligible damage was retested in a HEST environment. The predicted simulation for the test was a 1-MT yield at 160-psi peak overpressure. The shelter was tested in fully functional form as in MINOR SCALE. Also, instrumented anthropomorphic mannequins were used to study occupant survivability. They were placed in sitting and standing positions, and the motions were recorded using high-speed photography and acceleration data. The diesel generator and air moving equipment were tested pretest and posttest to investigate equipment survivability.

CHAPTER 2

TEST PROCEDURES

2.1 GENERAL

The prototype Keyworker blast shelter used in this study was constructed during FY 85 on White Sands Missile Range (WSMR) in New Mexico for the Defense Nuclear Agency (DNA) sponsored HE event, MINOR SCALE. The structure incurred negligible damage during the MINOR SCALE test in June 1985. A retest of the structure was performed on 12 August 1986 using the HEST to simulate the nuclear airblast environment. The development of the HEST procedure is described by Wampler and others (1978), and its use in similar tests is described by Kiger (1981).

A HEST test involves the detonation of high explosives distributed in a charge cavity on the ground surface above the structure. The charge cavity is covered with soil overburden to momentarily confine the blast pressure to simulate the peak overpressure and overpressure decay of a nuclear detonation. This chapter describes the structural model, the test procedure, and the instrumentation.

2.2 STRUCTURAL DETAILS

Construction and structural details for the shelter are given by Woodson and Slawson (1986). Construction drawings for the shelter were provided by HND. Floor plan and elevation views of the shelter are shown in Figure 2.1. A pretest view of the shelter before backfilling is shown in Figure 2.2. The three-bay shelter design had the following nominal details:

1. Clear span of 10 feet, 11-1/2 inches.
2. Clear height of 8 feet, 6 inches.
3. Wall and floor thickness of 9 inches.
4. Average roof thickness of 10-1/4 inches.
5. Average span-to-thickness (L/t) ratio of 12.8.
6. Average effective depth (d) to tension steel of 7-3/8 inches at the slab midspan (measured from the compression face, top, of the slab to the centroid of the tension steel), which yields an average tensile steel ratio of 0.010 at midspan.

7. Average depth (d') to the compression steel of 3-3/8 inches at the slab midspan (measured from the compression face, top, of the slab to the centroid of the compression steel), which yields an average compression steel ratio of 0.0033 at midspan.

8. Average tension (top) and compression (bottom) steel ratios at the roof support of 0.011 and 0.0036, respectively.

9. Average roof span-to-effective depth (L/d) ratio of 17.8.

10. Transverse steel ratios of approximately 0.002 in the roof, walls, and floor.

11. American Society for Testing and Materials (ASTM) Grade 60 reinforcing steel.

12. Concrete design strength of 3,000 psi.

13. Depth-of-burial (DOB) of 4 feet.

Roof reinforcement consisted of No. 6 truss and straight bars spaced at 6 inches on center. A truss bar was formed by bending a straight bar so that it would provide tension reinforcement at all locations along the roof span (i.e., located near the bottom face of the slab at midspan and near the top face of the slab at the supports). Two truss bars, a top straight bar, and a bottom straight bar provided the reinforcement in a typical 18-inch section of the roof slab. Exterior wall principal reinforcement consisted of No. 5 vertical bars spaced at 6 inches on center in each face of the wall. No. 3 single-leg stirrups were spaced at 12 inches on center with alternate rows staggered 6 inches in the exterior walls. Interior wall principal reinforcement consisted of No. 3 vertical bars spaced at 12 inches on center with no stirrups.

The shelter for Minor Scale contained the mechanical equipment required to circulate air to sustain up to 100 occupants. This equipment included a Deutz Model F1/2L511 6-KW diesel generator for electrical power, two fans with a capacity of 5,000 cfm each for air intake and exhaust, a chain-operated butterfly valve rated at 150 psi to seal the air exhaust stack during the button-up mode, and duct work to carry intake air to each bay. Also included were fluorescent and incandescent lighting.

2.3 INSTRUMENTATION

Recorded electronic data include: (1) airblast pressure; (2) roof and wall interface pressure; (3) soil stress; (4) free-field, structure, and mannequin accelerations; (5) and structure deflections.

Instrumentation locations are shown in Figures 2.3 and 2.4. Test data were recorded on 32-channel Sangamo Sabre III and V FM magnetic tape recorders located in an instrumentation trailer approximately 1,000 feet from the shelter. A zero-time channel was recorded on each data tape to establish a common time reference for the data. The data were recorded at 120 in/s, digitized at 200 kHz, and plotted. The data plots are presented in Appendix A. Recovered data was very good. The only nonusable data record was from gage D1.

In addition to the recorded electronic data, the responses of the mannequins were monitored by high-speed photography. A pretest view of the mannequins is shown in Figure 2.5.

2.3.1 Airblast Pressure Gages

Ten Kulite Model HKS-11-375 airblast pressure (AB) gages with ranges of 5,000 psi were used to measure blast pressure at eight locations on the ground surface around and above the shelter.

2.3.2 Interface Pressure Gages

Twenty Kulite Model VM-750-5 interface pressure (IF) gages with ranges of 200 and 500 psi were used at locations on the shelter roof and on one wall to measure soil-roof/wall interface stresses.

2.3.3 Soil Stress Gages

Eleven Kulite Model LQV-080-LR soil stress (SE) gages were used to measure the vertical free-field stress at locations ranging from near the ground surface to near the base of the shelter. These gages had ranges of 200 psi.

2.3.4 Accelerometers

Sixteen Endevco accelerometers were used to measure free-field, structure, and mannequin accelerations. Two Model 2262C accelerometers (AFF- 1,-2) were used to measure vertical accelerations at the roof and floor levels of the shelter in the free-field. These gages had ranges of 1,000 g's. Four Model 2262CA gages (AF-1 to AF-4) with ranges of 200 g's were used to measure vertical floor accelerations. Four Model 2262C gages (AR-1 to AR-4) with ranges of 1,000 g's were used to measure vertical roof accelerations.

Triaxial acceleration measurements were made on the mannequins using Model 2262C accelerometers with ranges of 25 g's. Mannequin 1 was standing with the accelerometers (AM1-X, -Y, -Z) mounted on the outside of its left ankle. Mannequin 2 was sitting on a bottom bunk with the accelerometers (AM2-X, -Y, -Z) mounted in its chest cavity. The X and Z measurements were mutually perpendicular horizontal components of acceleration, while the Y measurement was the vertical component of acceleration (see Figure 2.4).

2.3.5 Deflection Gages

Roof (D-1 to D-4) and wall (DW-1) deflection measurements were made using Celesco Model PT-101-10A-7559 high-frequency position/displacement transducers with ranges of 10 inches. Gages were located at roof and floor midspans in all three bays of the structure for relative roof-floor deflection measurements and at midheight, midlength of one bay for wall displacement measurement.

2.3.6 High-Speed Photography

High-speed photography was used inside the shelter to monitor the response of the mannequins. The two cameras used were Locams (manufactured by Redlake Co., Cambel, Calif.), running at approximately 400 frames per second.

2.4 TEST CONFIGURATION

The test configuration is shown in Figure 2.6. The test procedure included instrumentation of the structure and free-field, backfilling to a depth of 4 feet above the shelter roof, constructing the charge cavity, covering the charge cavity with sand overburden, and detonation of the charge. Figures 2.7 through 2.9 document test preparation.

The HEST procedure consists of the detonation of high explosive primacord (pentaerythritol tetranitrate, or PETN) in a charge cavity constructed on the ground surface above the structure. The 60-foot-square by 4-foot-thick charge cavity consisted of a wooden framing system covered with plywood. The 195 strands of 400-gr/ft primacord were uniformly distributed at midheight of the charge cavity. Each strand of primacord was detonated simultaneously at one end by strands of 100-gr/ft primacord that were wrapped around a blasting cap. The pressure generated by the detonation was momentarily confined by 4 feet of sand overburden that covered the charge cavity. The depth of the charge cavity, the height of the overburden, and the charge density

(0.0464 pounds of explosive per cubic foot of charge cavity volume) were designed to simulate the peak overpressure and pressure decay of a 1-MT nuclear detonation at 160-psi peak overpressure.

The procedure for testing the structure called for the air intake and exhaust to be closed (button-up mode) during the test since blast valves were not included for this structure.

2.5 STRUCTURAL MATERIAL PROPERTIES

Steel reinforcement and concrete strengths for the shelter were reported by Woodson and Slawson (1986) for the shelter as tested in MINOR SCALE. Specifications for the shelter called for ASTM Grade 60 reinforcing steel and 3,000-psi concrete (compressive strength at 28 days). Based on tensile tests on seven random samples, the roof steel (No. 6 bars) had mean yield, ultimate, and rupture strengths of 61.6, 95.5, and 80.4 ksi, respectively. The corresponding standard deviations for these values were 1.27, 0.53, and 1.34 ksi.

Five random samples of the wall principal steel (No. 5 bars) were tested in tension until rupture. The mean yield, ultimate, and rupture strengths were 75.2, 115.4, and 98.1 ksi, respectively. The corresponding standard deviations were 0.88, 1.09, and 2.44 ksi.

The roof and walls were cast from 10 batches of concrete. The mean 28-day concrete compressive strength for the roof and walls was 2,260 psi with a standard deviation of 280 psi. Concrete ages ranged from approximately 2 to 4 months by the time the shelter was tested during MINOR SCALE (27 June 1985). At that time, the mean concrete compressive strength was 3,240 psi with a standard deviation of 480 psi. This increase in strength was greater than expected. An additional 14 months elapsed before the HEST test was performed (concrete ages of 16 to 18 months). A conservative estimate (from a design perspective) of the concrete compressive strength on test day was taken as 3,300 psi since no concrete testing was performed at that time.

2.6 BACKFILL MATERIAL PROPERTIES AND TEST BED PREPARATION

The backfill consisted of a 2-foot-thick concrete sand blanket around the structure with blow sand filling the remainder of the excavation to a level 4 feet above the shelter roof. The backfill was placed in 8-inch layers and compacted to at least 95 percent of the soil's maximum Proctor density.

Compaction was provided by a Bomrg BW160RD1 roller/compactor and a Dynapac Model CM-10 gasoline-powered vibrator. Density and moisture content were controlled during backfill placement using a Troxler nuclear density gage.

The concrete sand was a locally obtained sand made from crushed rock material that classified as a brown sand (SP) by the Unified Soil Classification System (USCS) (US Army Corps of Engineers 1960) with a maximum Proctor dry density of 110.9 lb/ft^3 and an optimum moisture content of 8.5 percent. Based on the results of six samples during backfill placement, the mean wet density, dry density, and moisture content of the concrete sand were 118.1 lb/ft^3, 109.6 lb/ft^3, and 7.8 percent, respectively. The corresponding standard deviations were 2.0 lb/ft^3, 1.7 lb/ft^3, and 0.7 percent. The concrete sand was compacted to 99 percent of its maximum Proctor density. The results of direct shear tests indicated that the sand had an angle of internal friction of 36 degrees.

The blow sand was processed from on-site material. It classified as a brown silty sand (SP-SM) by the USCS and had an angle of internal friction of 32 degrees (based on direct shear tests). The maximum Proctor dry density was 106.2 lb/ft^3, and the optimum moisture content was 8.8 percent. Based on the results of 36 samples during backfill placement, the mean wet density, dry density, and moisture content of the blow sand were 112.1 lb/ft^3, 101.7 lb/ft^3, and 10.2 percent, respectively. The corresponding standard deviations were 4.3 lb/ft^3, 3.1 lb/ft^3, and 2.9 percent. The blow sand was compacted to 95 percent of its maximum Proctor density.

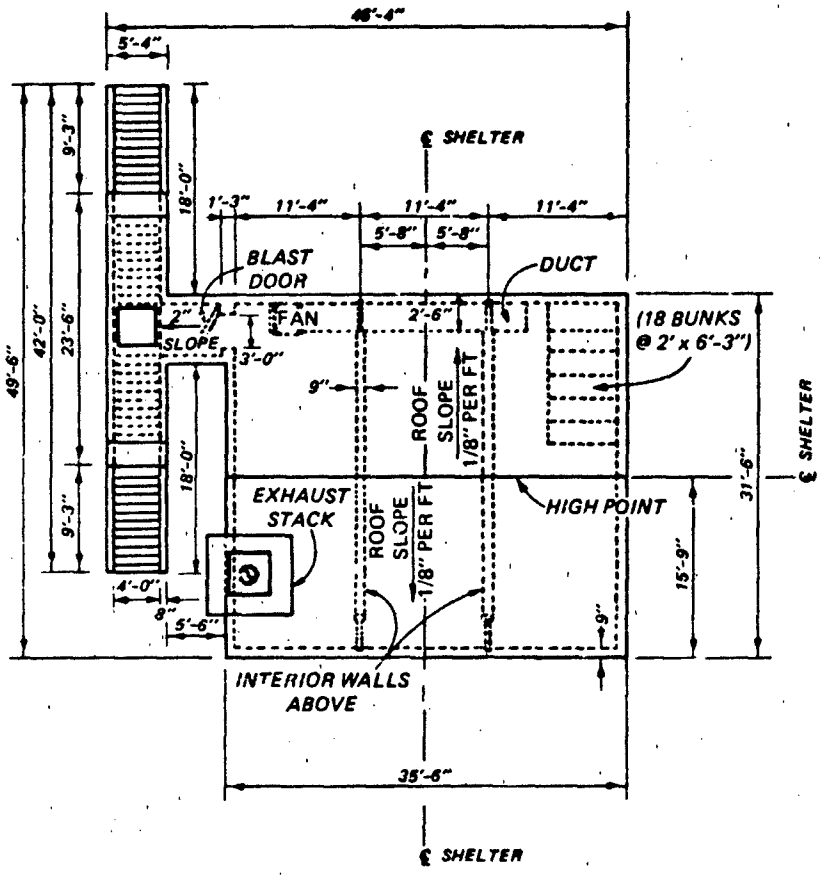

PLAN VIEW

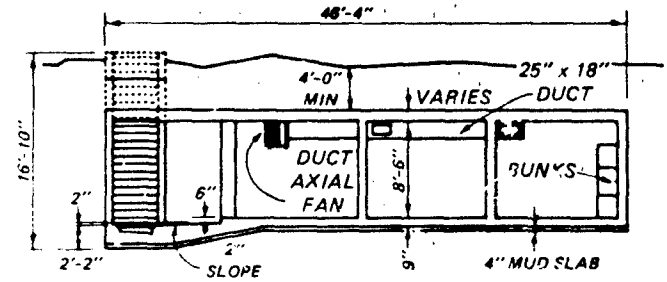

ELEVATION

Figure 2.1. Floor plan and elevation.

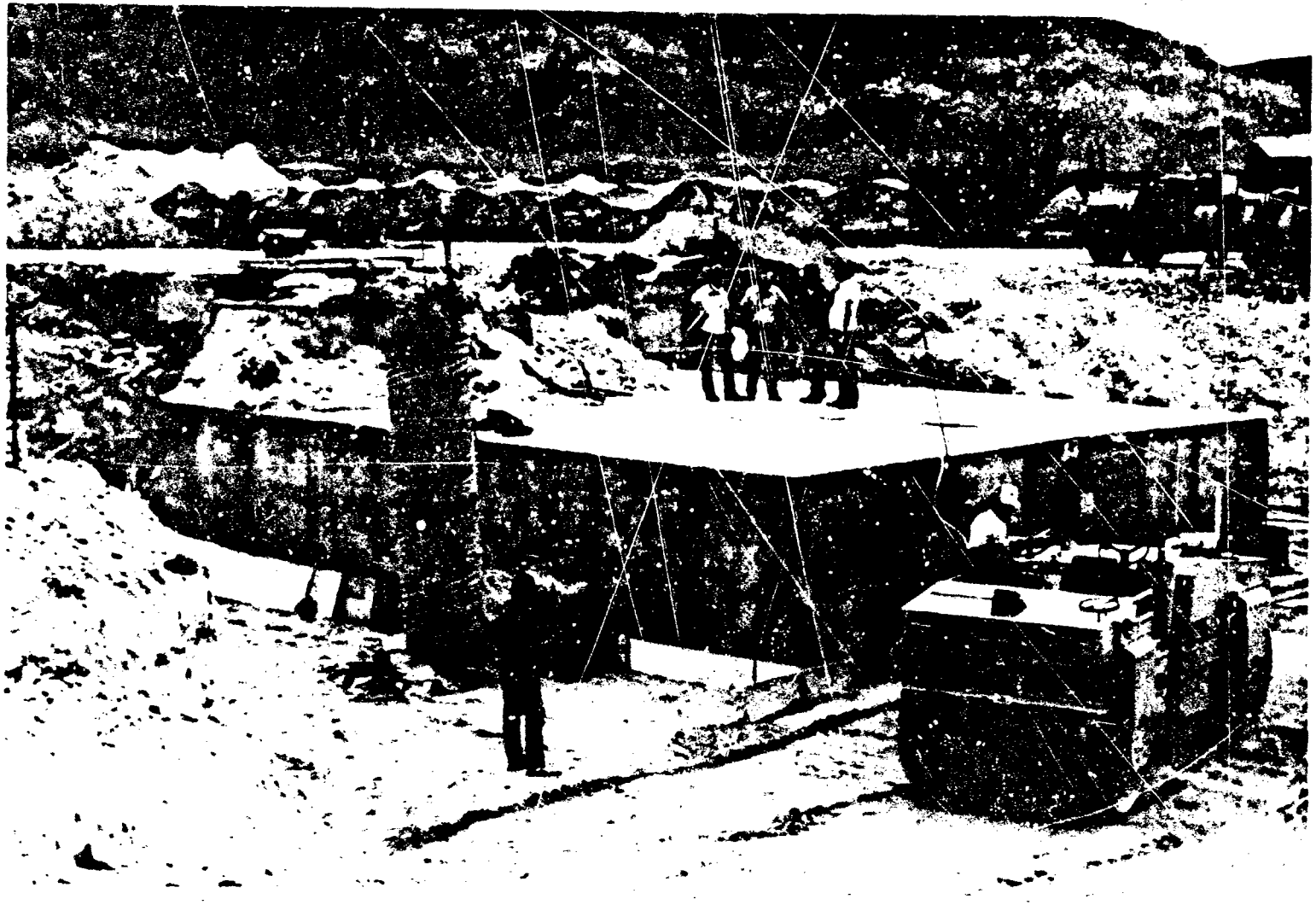

Figure 2.2. Pretest view of the shelter.

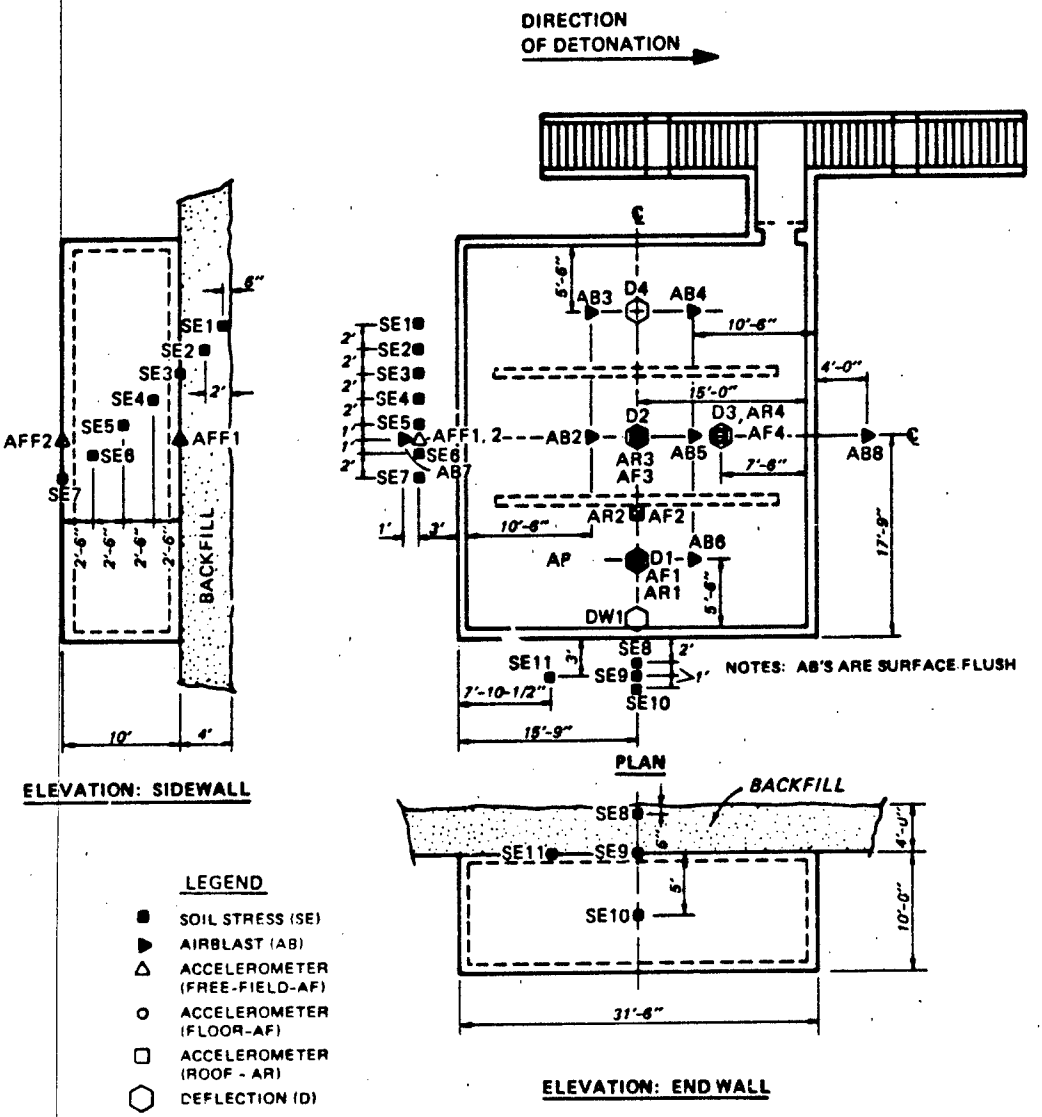

Figure 2.3. Instrumentation plan (Sheet 1 of 2).

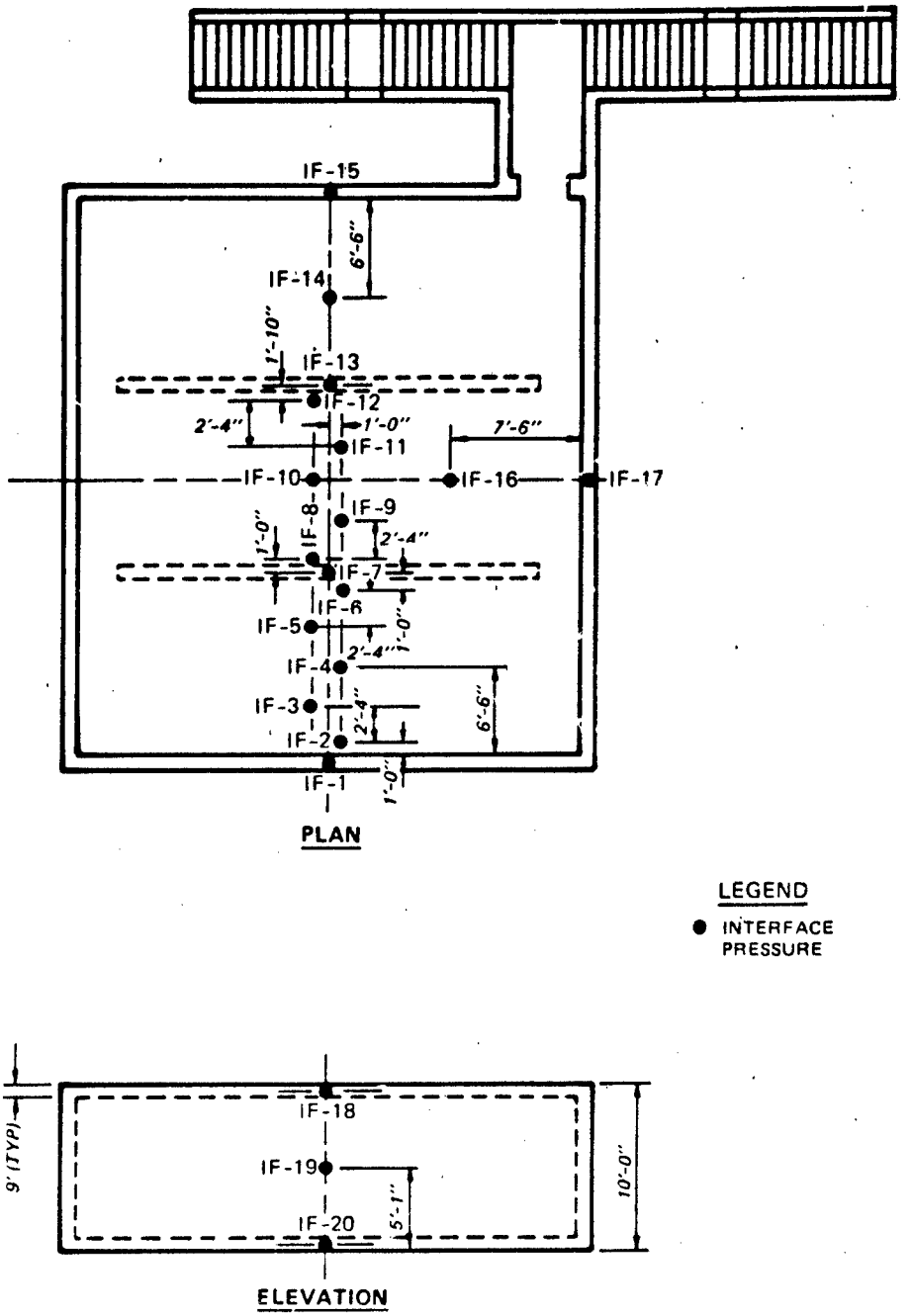

Figure 2.3. Instrumentation plan (Sheet 2 of 2).

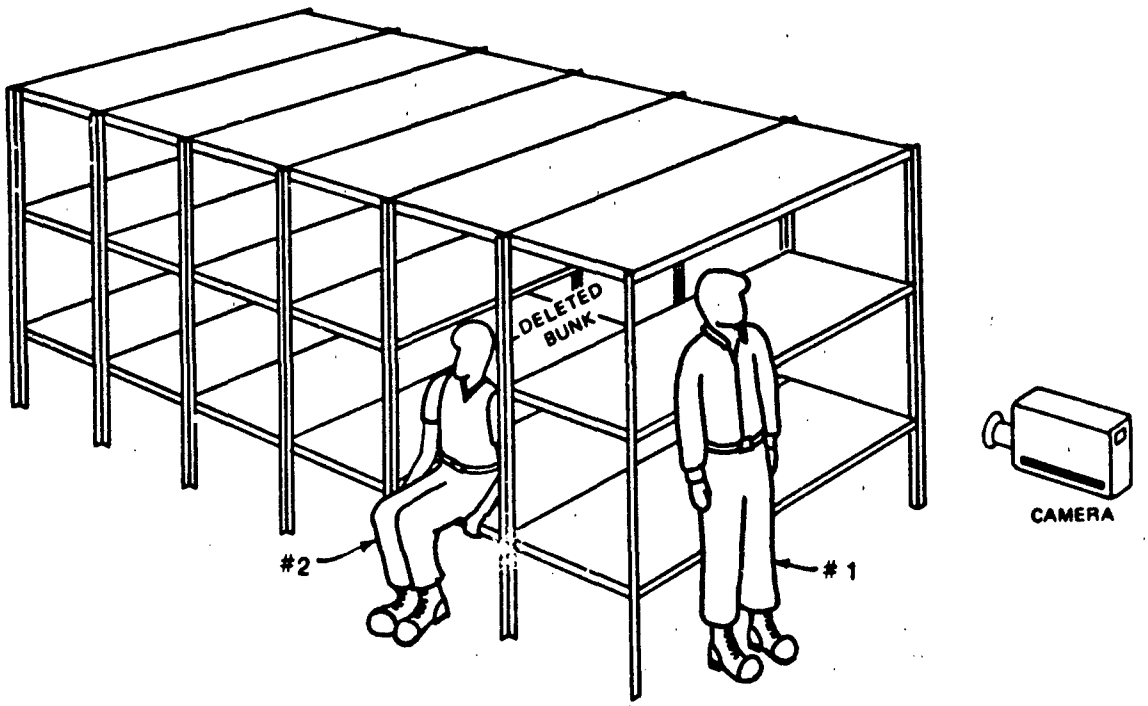

a. Bunks and camera.

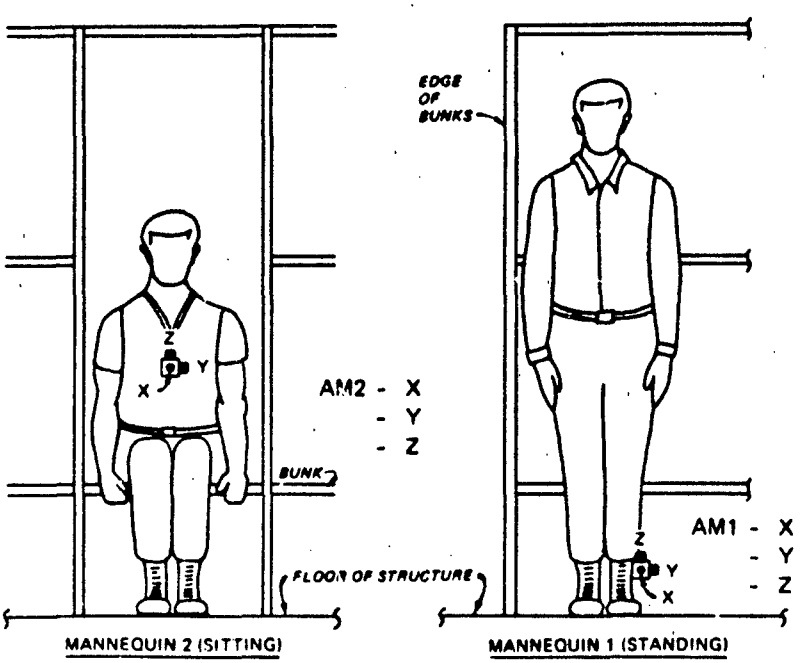

b. Mannequins and gages.

Figure 2.4. Mannequin instrumentation plan and camera location (See Figure 2.1 for bunk location in shelter).

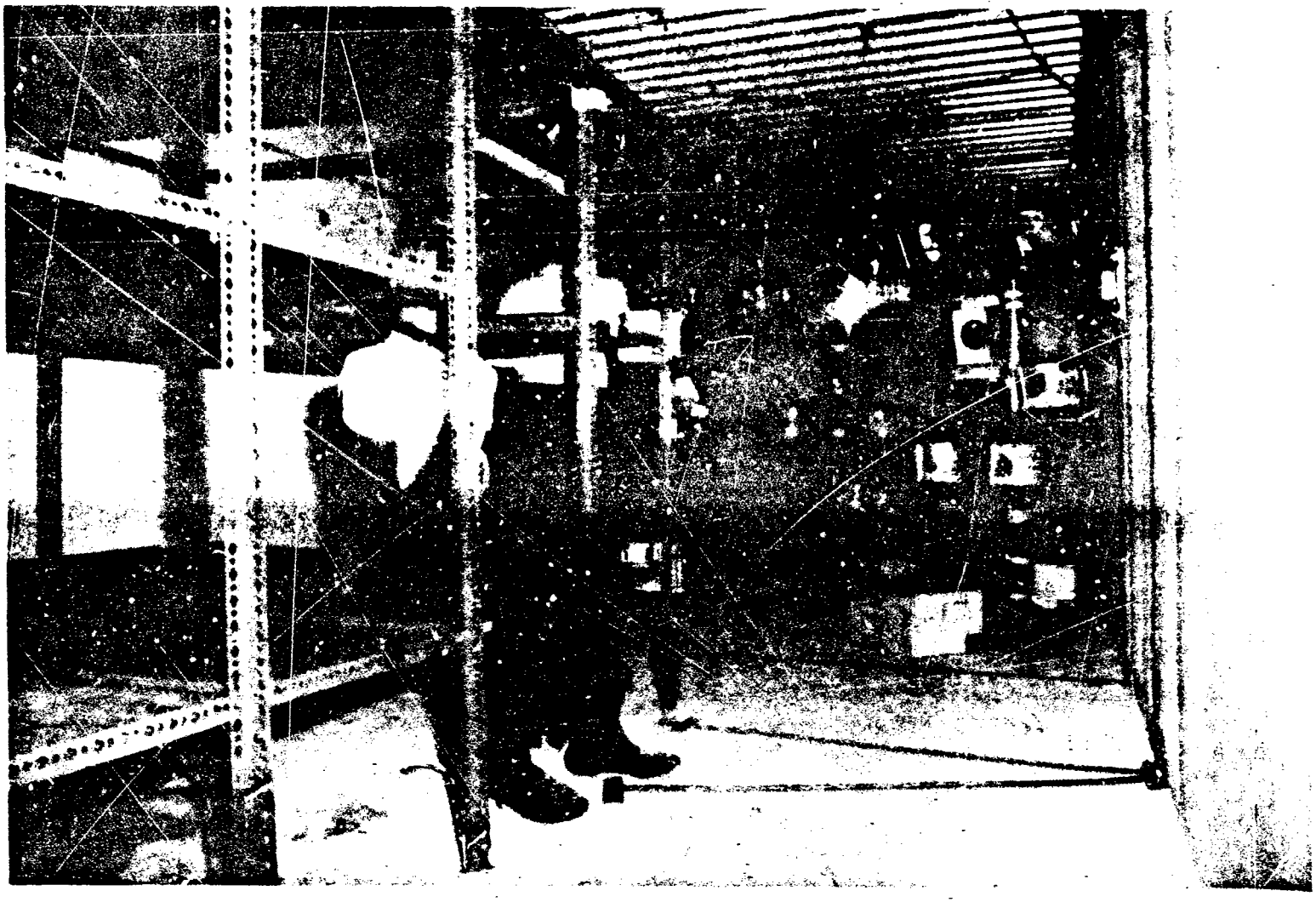

Figure 2.5. View of the instrumented mannequins showing the camera setup.

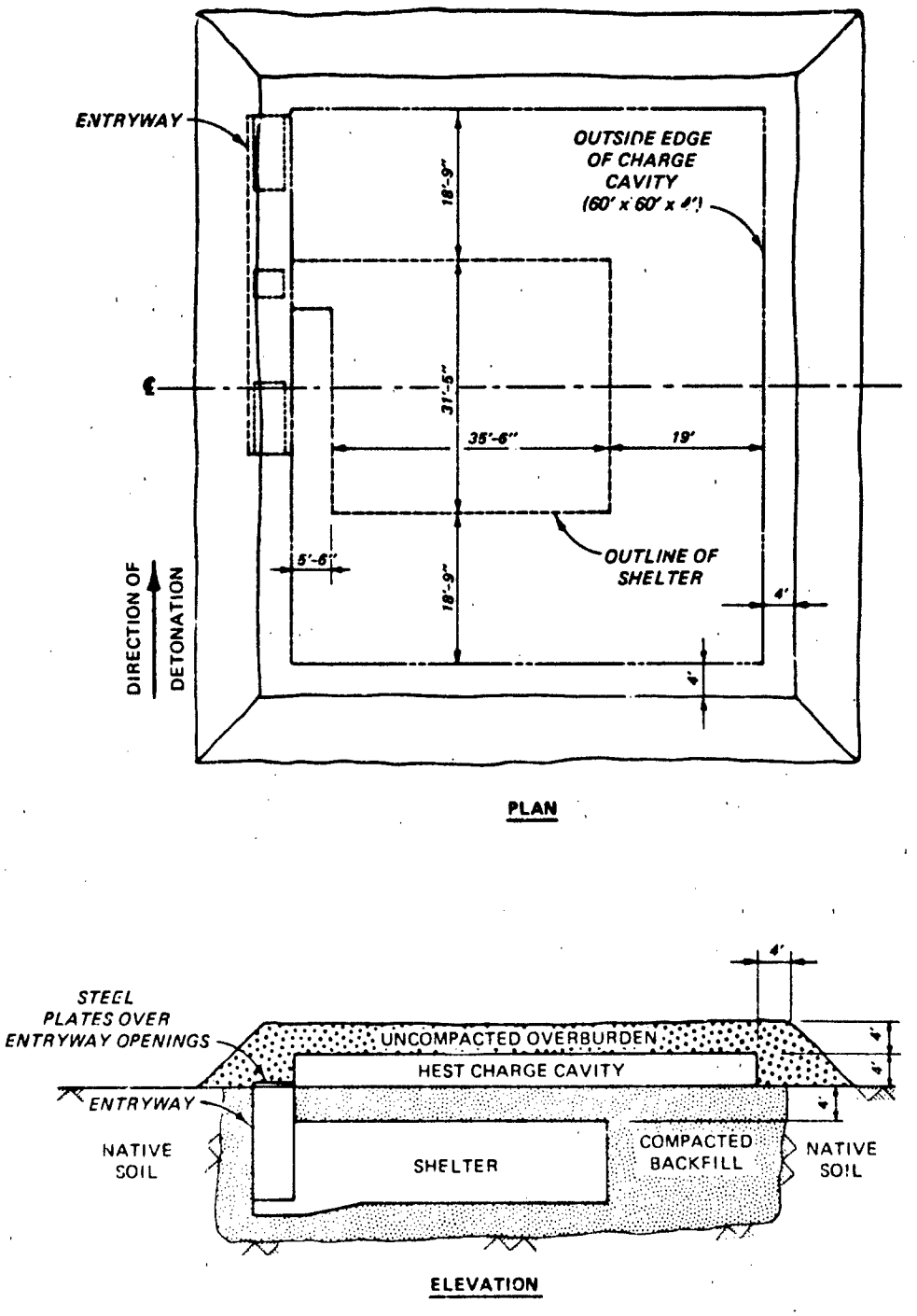

Figure 2.6. Test configuration.

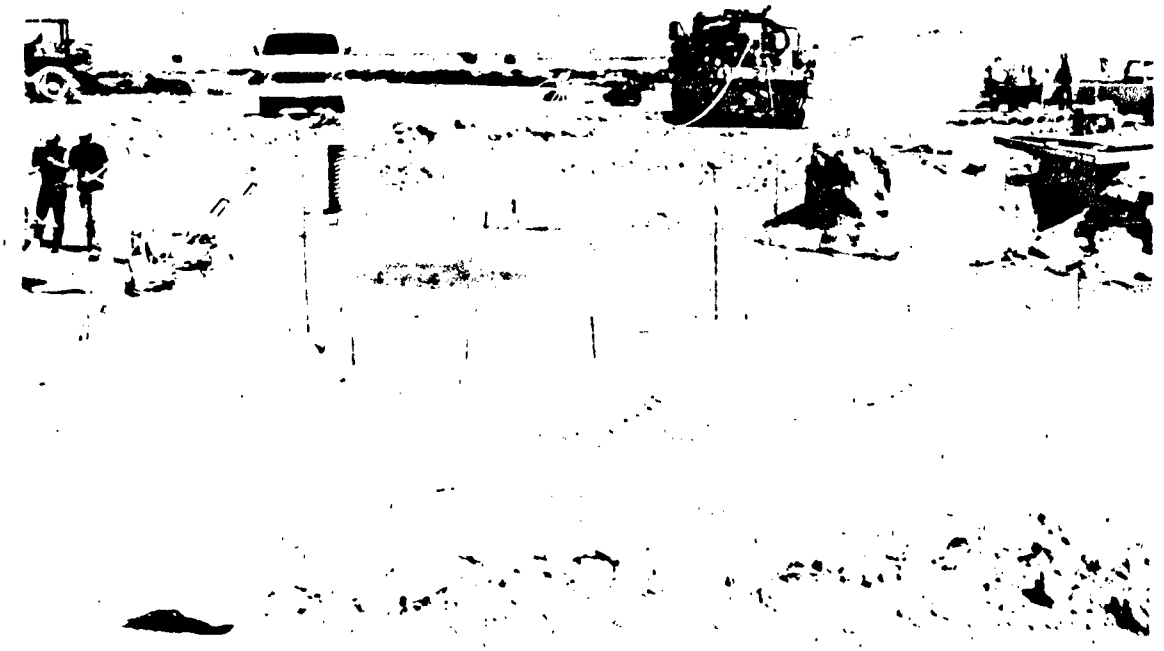

Figure 2.7. Backfilling at the roof level of the structure.

Figure 2.8. Construction of the BEST cavity (primacord placement).

a. Pretest.

b. Detonation.

Figure 2.9. Detonation of the HEST charge cavity.

CHAPTER 3

TEST RESULTS

3.1 STRUCTURAL DAMAGE

The HEST test of the prototype shelter was performed on the structure that survived the MINOR SCALE HE event. The condition of the shelter prior to the HEST test was essentially undamaged.

Structural damage during the HEST retest of the shelter was significant. Roof deflection profiles for each bay of the shelter are shown in Figure 3.1 (bay 3 is closest to the entryway). The maximum permanent roof deflection was approximately 17 inches for bay 1, 8 inches for bay 2, and 13 inches for bay 3. The exterior bays (1 and 3) received more damage than the interior bay (2) as expected. The roof response mode is described as a combination of shear and flexure. Overall views of the damaged roof are shown in Figures 3.2 and 3.3. No roof steel appeared to be broken in the exposed areas.

For bay 1, the embedded angle to wall connection failed as the result of large shear deformations of the roof slab at the exterior wall. The angle (shown in Figure 3.4) supports the metal roof decking. The maximum shear deformation of the roof slab at the face of the exterior wall was approximately 10-1/2 inches. At the interior support, approximately 7-3/4 inches of shear deformation occurred in the first 15 inches of the clear span. Shear deformation accounted for approximately 54 percent of the total permanent deflection (17 inches). An interior view of the roof slab for bay 1 is shown in Figure 3.5.

Shear response accounted for approximately 44 percent of the total permanent deformation (8 inches) of bay 2. Measured shear deformations of 3-1/2 inches were noted at each wall for the interior bay. The shear deformation occurred over an area that extended 15 to 16 inches from the face of the walls. Figure 3.6 shows a posttest interior view of bay 2.

Bay 3 behaved almost identically to bay 1. The embedded angle connection failed over nearly the entire length of the exterior wall. Approximately 9-1/2 inches of shear response occurred in the roof slab at the face of the exterior wall, and approximately 6-1/2 inches of shear deformation occurred over the first 16 inches of the span from the face of the interior wall. Shear deformation accounted for approximately 62 percent of the total

permanent midspan deflection. An interior view of bay 3 is shown in Figure 3.7, and a view of the exposed top roof reinforcement at the exterior wall of bay 3 is shown in Figure 3.8.

The walls and floor slabs survived with only minor cracking. The entryway was severely damaged during this test, as shown in Figures 3.2 and 3.9. However, the test configuration did not load the entryway in the same manner as a nuclear detonation. The tops of the entryway shafts were covered with steel plates to support the soil overburden covering the HEST cavity. The HEST cavity did not cover the entryway openings but did extend to the edge of the entryway. Therefore, only the sides of the entryway closest to the shelter were loaded. In a nuclear event, all sides and the interior of the entryway would be loaded. The entryway was still usable after the test except that it was filled with debris from the HEST cavity (mostly overburden soil). The HEST test did not retest the blast door.

The metal decking on the underside of the roof separated from the wall above the blast door, as shown in Figure 3.10. The connection of the embedded angle to the wall failed. This allowed crushed concrete to fall inside the shelter.

In general, the metal decking was very successful in its dual role of providing roof construction formwork and preventing concrete rubble from falling from the damaged roof slab.

3.2 DAMAGE TO NONSTRUCTURAL AND SUPPORT SYSTEMS

The stud wall that isolated the generator failed as a result of excessive roof deflection (see Figure 3.7). Although this failure was not important structurally, it would lead to excessive noise levels inside the shelter bays for occupants as described by Woodson and Slawson (1986).

The exhaust stack/roof slab connection was distressed, as shown in Figure 3.11. The exhaust penetration detail was critical because of the large masses suspended there. The combined weight of the exhaust fan, butterfly valve, and connector was approximately 1,100 pounds. Although damage did occur at the exhaust penetration, the exhaust system was functional after the test. The generator and fuel tank were undamaged during the test.

Another area of concern was the intake fan support, which attached the 260-pound intake fan to the shelter. This detail survived with only minor

concrete cracking. Roof-mounted electrical conduits and fluorescent light fixtures failed during the test as the result of excessive roof deflection.

3.3 RIGID-BODY MOTION

WSMR performed pretest and posttest surveys on the four corners of the roof of the shelter. The survey indicated that the structure moved 1-1/2 inches downward during the test. Damage to the floor slab (minor cracking) did not indicate that this much rigid-body motion occurred.

3.4 MANNEQUIN MOVEMENT

The final positions of the mannequins were unchanged from pretest locations. High-speed photography was used to monitor mannequin motion during the test. The camera setup and mannequin locations are shown in Figure 2.5. The two cameras viewing the mannequin motion operated at approximately 400 frames per second. Analysis of the high-speed film is included in Chapter 4.

3.5 RECOVERED DATA

Data for this test included electronic instrumentation and high-speed photography. Data recovery was very good for the airblast pressure gages, soil stress gages, accelerometers, interface pressure gages, and deflection gages. All recovered data are presented in Appendix A. The data are referenced to a common zero time and are displayed with time in milliseconds as the abscissa.

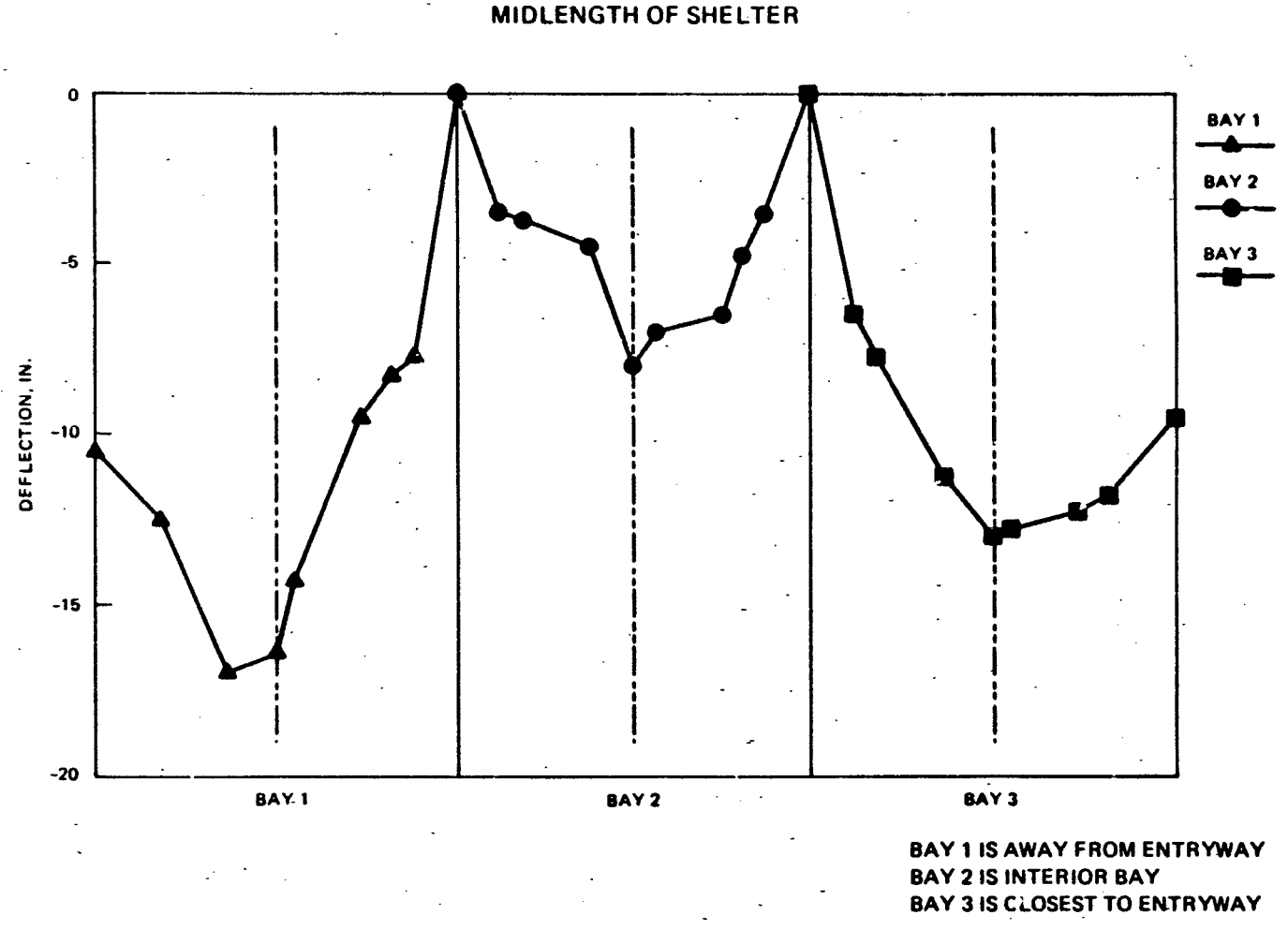

Figure 3.1. Roof deflection profiles.

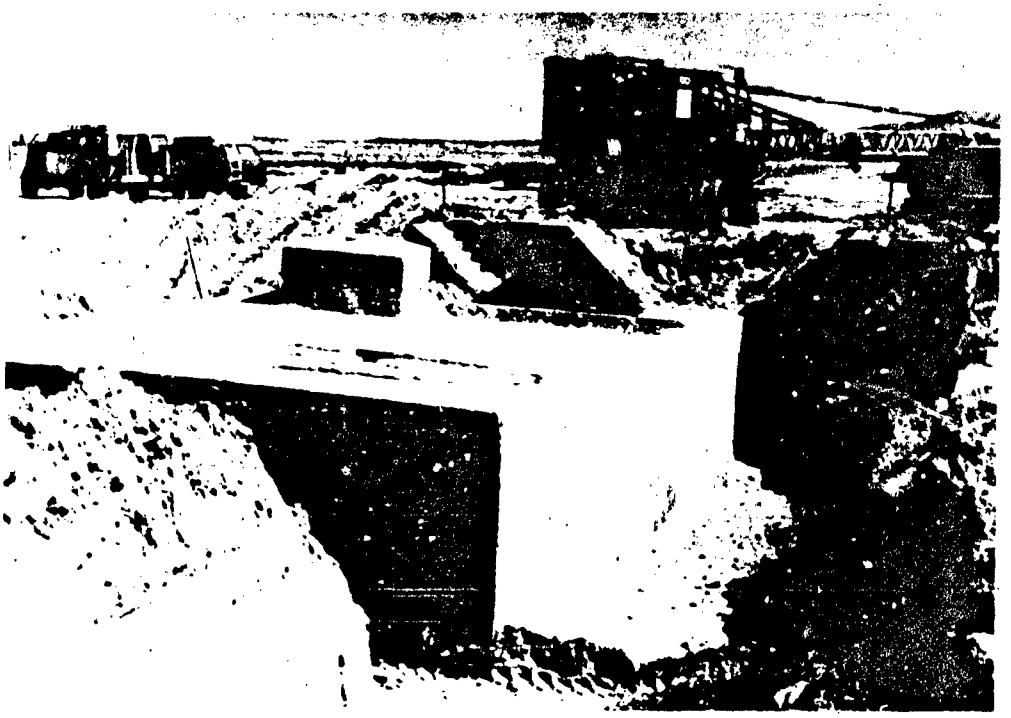

Figure 3.2. Posttest view of the shelter showing entryway damage.

Figure 3.3. Posttest view of the shelter roof.

Figure 3.4. Interior view of bay 1 showing the failure of the embedded angle to wall connection.

Figure 3.5. Interior view of bay 1.

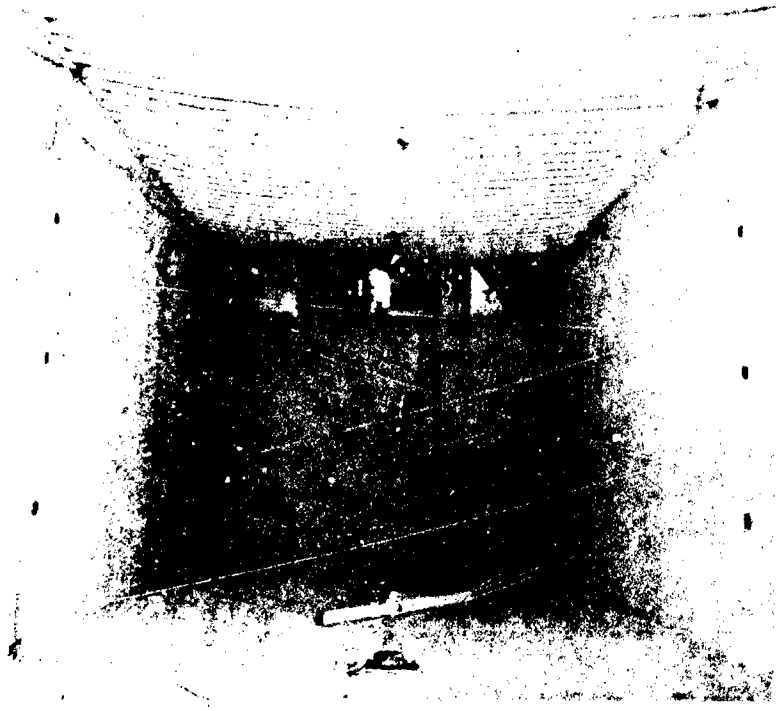

Figure 3.6. Interior view of bay 2.

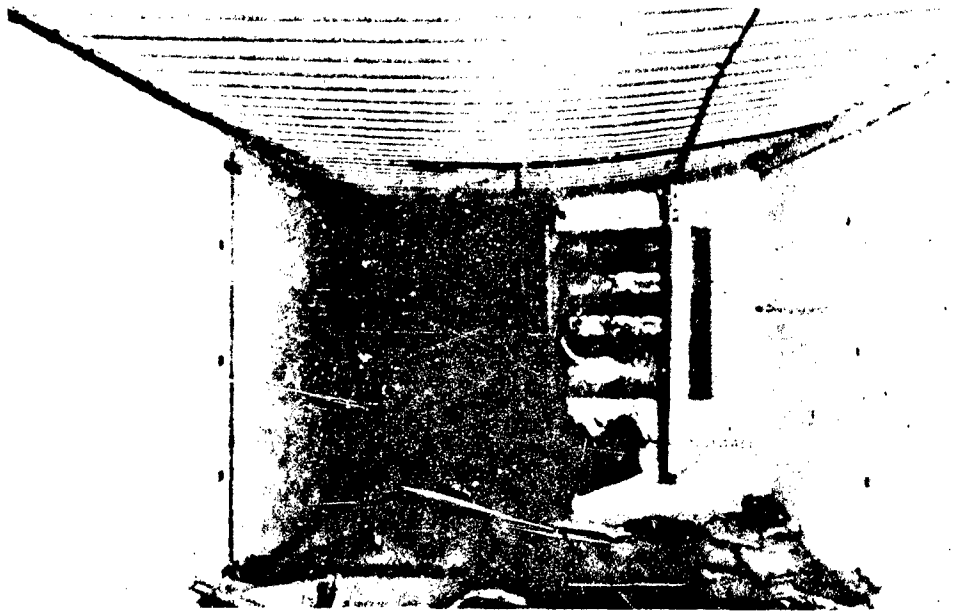

Figure 3.7. Interior view of bay 3.

Figure 3.8. Exposed top of roof reinforcement, bay 3.

Figure 3.9. Interior view of entryway damage.

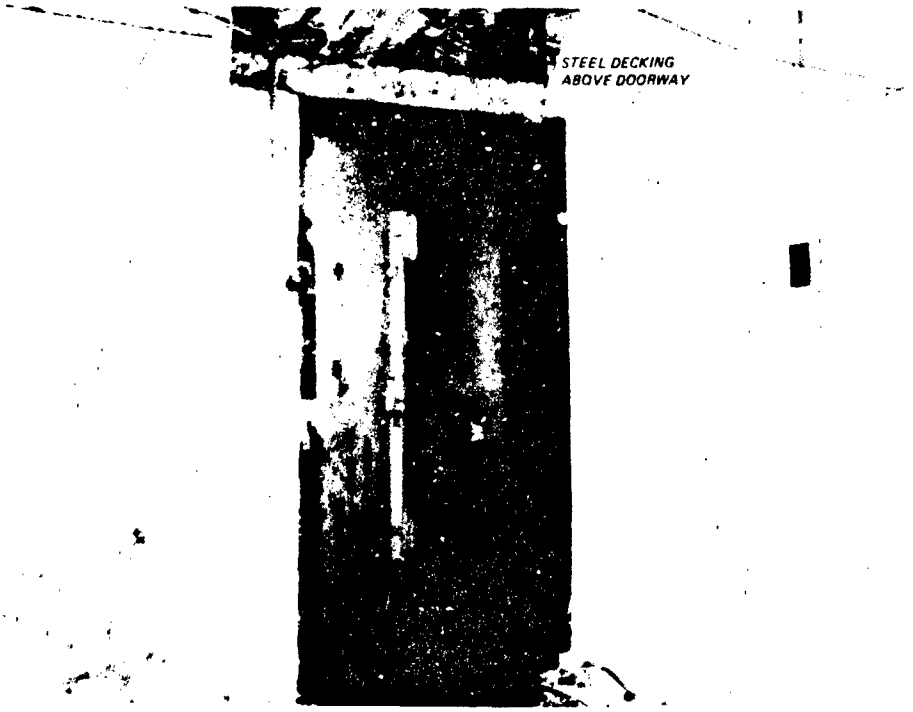

Figure 3.10. Damage above the blast door.

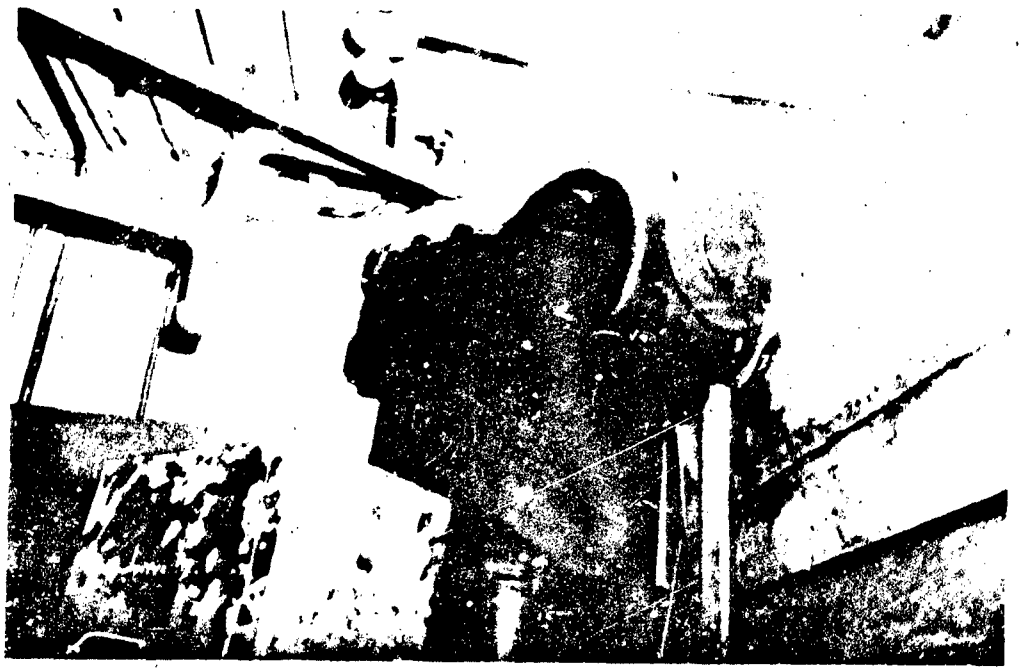

Figure 3.11. Posttest view of the exhaust stack.

CHAPTER 4

ANALYSIS

4.1. ANALYSIS OF FREE-FIELD AND STRUCTURE LOADING DATA

The VSBS computer program (Kiger, Slawson, and Hyde 1984) used to predict roof response requires the input of structure, backfill, and loading parameters. From this data, the single-degree-of-freedom (SDOF) model of the shelter roof is formulated. Calculations of the resistance function and the effective roof loading require additional calculated or input variables. This chapter analyzes the recovered data to determine the experimental values of nuclear weapon simulation, loading wave velocity, lateral soil pressure coefficient, roof reflection factor, attenuation factor, arching factor, and load factor. The experimentally observed variables are compared with calculated or assumed values used in the VSBS program, and response calculations are presented. In addition, in-structure shock and survivability are investigated.

4.1.1 Nuclear Weapon Simulation

Estimates of the nuclear weapon yield and peak pressure that best fit the recovered airblast pressure records are required to define the ground surface loading function. The weapon simulations were determined by comparing the data records with the Speicher and Brode (1981) definitions of the pressure-time histories of various yield surface bursts. Best fits of yield and peak overpressure were determined for each pressure record, and a collective fit of all the records was performed to determine the average simulation. In addition, the best fit peak overpressure for a 1-MT surface burst was determined since the desired simulation was 1-MT at 160 psi. The fits were made using the principle of least squares on the impulse-time record of the airblast data and the Speicher-Brode function. The procedure used is presented in more detail by Mlakar and Walker (1980) and was modified for impulse comparison by Mr. James Baylot of WES. Fits were made using 50 and 100 ms of data.

The best 50-ms fit to all the data records was 58 KT at 226-psi peak overpressure. The best 1-MT fit for 50 ms was 159-psi peak overpressure. These two fits are presented in Figure 4.1. A comparison of the pressure-time histories of the best fit and best 1-MT fit is shown in Figure 4.2. Table 4.1

summarizes the results of all the weapon fits.

4.1.2 Loading Wave Velocity

Loading wave velocities were calculated based on the arrival time of the vertical stress wave at the soil stress gages located at various depths in the free field. The gages were placed in groups for comparison. The gages in each group were located at different depths in a plane perpendicular to the direction of detonation so that the ground surface above each gage was loaded by the blast wave at the same time. The mean loading wave velocities determined from group 1 (SE-1, -2, -3, -4, -5, -6, and -7) and group 2 (SE-8, -9, and -10) were 1,150 and 1,170 ft/s, respectively. It is recommended that a loading wave velocity of 1,160 ft/s be used for structural response calculations.

4.1.3 Lateral Soil Pressure Coefficient

The lateral soil pressure coefficient (ratio of horizontal to vertical soil pressures) was determined by comparing the peak vertical free-field stresses with peak horizontal wall interface stresses at the same depth of burial. Based on a comparison of the data from gages IF-18 with SE-9 and IF-19 with SE-10, the experimental lateral soil pressure coefficient was 0.6. Stress amplification resulting from reflection at the wall-soil interface may have increased the experimental coefficient slightly. However, 0.6 is a reasonable value for the backfill used in this test.

4.1.4 Roof Reflection Factor

The loads on the roof of a buried structure are increased initially because of reflection of the loading wave. This increase in peak stress decreases rapidly as the result of tensile wave reflections from the concrete-air interface at the bottom of the roof slab and from wave interactions with the free soil surface. Therefore, the duration of the amplified stress spike is a function of the roof thickness, the loading wave velocity in the backfill and in the roof slab, the backfill material properties, and the depth of burial. The duration of the reflected spike was determined from the roof interface pressure data and was found to be approximately 4.7 ms.

The roof reflection factor was determined by comparing the peak roof interface stresses with the peak soil stress at the roof level. The mean experimental value of the roof reflection factor is 1.99. If the interface pressure gages near the supports are excluded, the mean reflection factor is 1.6.

4.1.5 Attenuation Factor

The attenuation of peak stress with increasing depth is due to both the spatial decay of the shock front and hysteretic losses in the soil. The VSBS program modifies the soil surface loading by an attenuation factor to calculate the roof loading and the thrust in the roof caused by the horizontal wall loading. For this reason, the attenuation factors at the roof level and at the midheight of the structure are required. Based on a comparison of peak soil stresses at these locations with the best fit nuclear weapon simulation at the ground surface (58 KT, 226 psi for 50 ms), experimental attenuation factors of 0.78 and 0.62 were determined at the roof level and structure midheight, respectively. The weapon simulation was used rather than actual surface pressure data since the large high-frequency spikes in the HEST loading are filtered out before the loading wave reaches the roof level.

4.1.6 Soil Arching Ratio and Load Factor

The roof loading distribution for shallow-buried structures is nonuniform in nature after the duration of the reflected spike as a result of soil structure interaction (soil arching). Soil arching is caused by shear stresses within the soil mass when relative deformations occur and is defined as the ability of a soil to transfer loads from one location to another in response to a relative displacement between the locations. This phenomenon results in lower roof interface stresses over the flexible clear span of the roof and higher stresses near the support. Soil arching and its effects upon buried structure response are discussed by Kiger, Slawson, and Hyde (1984).

The soil arching ratio is defined as the ratio of the average roof stress to the free-field stress at the roof level. Soil arching ratios for bay 1 (away from entryway) and bay 2 (interior bay) were determined from the recovered roof interface stress and free-field stress data. Soil arching ratios were calculated after the decay of the reflected spike (4.7 ms) up to the time of maximum response. The average arching ratios for this time span are 0.71 for bay 1 and 0.77 for bay 2. The results of the analyses are presented in Table 4.2, and a typical plot of soil arching ratio versus time is shown in Figure 4.3.

In a simple SDOF model, the total roof load is modified by a load factor to determine the effective roof loading. This factor depends upon the roof loading distribution and the deflected shape of the roof. Using a fully

plastic response mode and the measured roof load distribution, the load factors for bay 1 and bay 2 were calculated. The results are presented in Table 4.2, and a typical plot of load factor versus time is shown in Figure 4.4. The average load factor for bays 1 and 2 after the decay of the reflected spike and before the time of maximum response is 0.26. The load factor is also a measure of the uniformity of the load. The load factor is 0.5 for a uniform load and 0.25 for a parabolic load with zero load at midspan.

4.2 COMPARISON OF EXPERIMENTAL AND THEORETICAL PARAMETERS

Table 4.3 compares the experimentally determined loading parameters with calculated values from the VSBS (Kiger, Slawson, and Hyde 1984) computer program. Some values used by the program are required input, and suggested normal ranges are presented. The theoretical parameters agree with the experimentally determined values except for the duration of the reflected spike. The observed duration of 4.7 ms is considerably larger than the calculated value of 1 ms. The duration calculated by VSBS is governed (in this case) by tensile reflections from the concrete-air interface on the bottom of the roof slab and is empirically limited to 12 transient times (transient time equals the roof thickness divided by the wave velocity in concrete).

4.3 ROOF RESPONSE CALCULATIONS

The VSBS computer code was used to calculate maximum roof response using the weapon simulations as the input loading. The results are presented in Table 4.4. The maximum predicted roof response ranged from 6.1 to 16.3 inches for the input weapons and compares well with the observed permanent responses of 8, 13, and 17 inches for the three bays of the shelter.

4.4 IN-STRUCTURE SHOCK AND SURVIVABILITY

In-structure shock is typically represented in terms of shock spectra. Shock spectra are plots of the maximum responses, usually of relative displacement, pseudovelocity, and/or acceleration of all possible linear oscillators with a specified amount of damping to a given input base acceleration-time history. Vertical shock spectra were calculated using the recovered floor acceleration data as input to a computer program developed at WES. The

shock spectra were generated for damping ratios of 0, 5, and 10 percent of critical damping. The shock spectra are presented in Figures 4.5 through 4.8 for accelerometers AF-1 through AF-4, respectively.

Figure 4.9 compares the experimentally determined vertical shock spectra (smoothed by hand with damping of 10 percent) for the shelter floor with fragility curves for typical floor-mounted equipment (Headquarters, Department of the Army 1987). Based on the comparison of the shock spectra and fragility curves, generators and communication equipment should be shock isolated to ensure their survivability. However, the diesel generator (mounted on top of its fuel tank) in the shelter was undamaged during the test. The test results indicate that the generator will survive the design overpressure of 50 psi and has survived one overload test of 159 psi.

Crawford and others (1974) present a summary of human shock tolerance and recommend design maximum accelerations of 10 g's for a standing man at or below the frequency of 10 Hz (resonant frequency). The experimental shock spectra show that a man in the standing position (most vulnerable) would not suffer compressive fractures; however, impact injuries can occur at much lower shock levels as a result of loss of balance and falling. The high-speed movies of the mannequin motion showed that impact injury was not probable. Plots of relative mannequin movement are presented in Figure 4.10.

Table 4.1. Weapon simulation summary.

	100-ms Simulations			50-ms Simulations		
Gage	W* KT	Pso† psi	Pso for Best 1-MT Fit, psi	W KT	Pso psi	Pso for Best 1-MT Fit, psi
AB-1	21.4	270	124	52.9	222	155
AB-2	38.8	255	137	77.8	223	164
AB-3	26.5	280	134	56.5	237	165
AB-4	27.7	256	127	57.1	221	156
AB-5	26.5	264	129	52.7	229	158
AB-6	32.7	248	129	57.7	221	156
AB-7	29.4	244	124	70.3	208	152
AB-8	22.0	293	133	46.1	246	164
Avg	28.0	262	130	58.0	226	159

* W is the simulated nuclear weapon yield in kilotons TNT equivalent.
† Pso is the simulated peak overpressure in psi.

Table 4.2. Arching ratio and load factor summary.

	Average Arching Ratio				Average Load
Bay*	Using SE-3	Using SE-9	Using SE-11	Average†	Factor
1	0.98	0.65	0.51	0.71	0.26
2	1.06	0.70	0.55	0.77	0.26

* Bay 1 was located on the opposite side of the shelter from the entryway. Bay 2 was the interior bay.
† Average values are presented for the time interval after the duration of the reflected spike to the time of maximum roof response.

Table 4.3. Comparison of experimental and theoretical loading parameters.

Parameter	Experimental Value	Theoretical Value*	Comments
Loading wave velocity ft/s	1,160.0	(1,200-1,500)	Input
Lateral soil pressure coefficient	0.6	(0.5-0.6)	Input
Roof reflection factor	1.6	1.6	
Duration of reflected spike, ms	4.7	1.0	
Attenuation factor at roof level	0.78	0.87-0.98	†
Attenuation factor at wall midheight	0.62	0.77-0.96	†
Soil arching ratio	0.73	0.60	
Load factor	0.26	0.31	

* Tabular values in parentheses are normal ranges of input for the soil used in this test.

† The theoretical values of attenuation factors were based on the four mean best fit weapon simulations presented in Chapter 4.

Table 4.4. VSBS response calculations.

Weapon Yield KT	Peak Overpressure psi	Maximum Response in.*	Time of Maximum Response, ms†	Notes‡
58	226	12.0	64	a
1,000	159	16.3	75	a
28	262	11.0	61	b
1,000	130	6.1	71	b

* Maximum permanent roof deflections ranged from 8 to 17 inches.

† Maximum response occurred at 80 ms for bay 1 and at 75 ms for bay 2.

‡ a - The input weapon yield and peak overpressure were determined from 50-ms fits of the recovered data.

b - The input weapon yield and peak overpressure were determined from 100-ms fits of the recovered data.

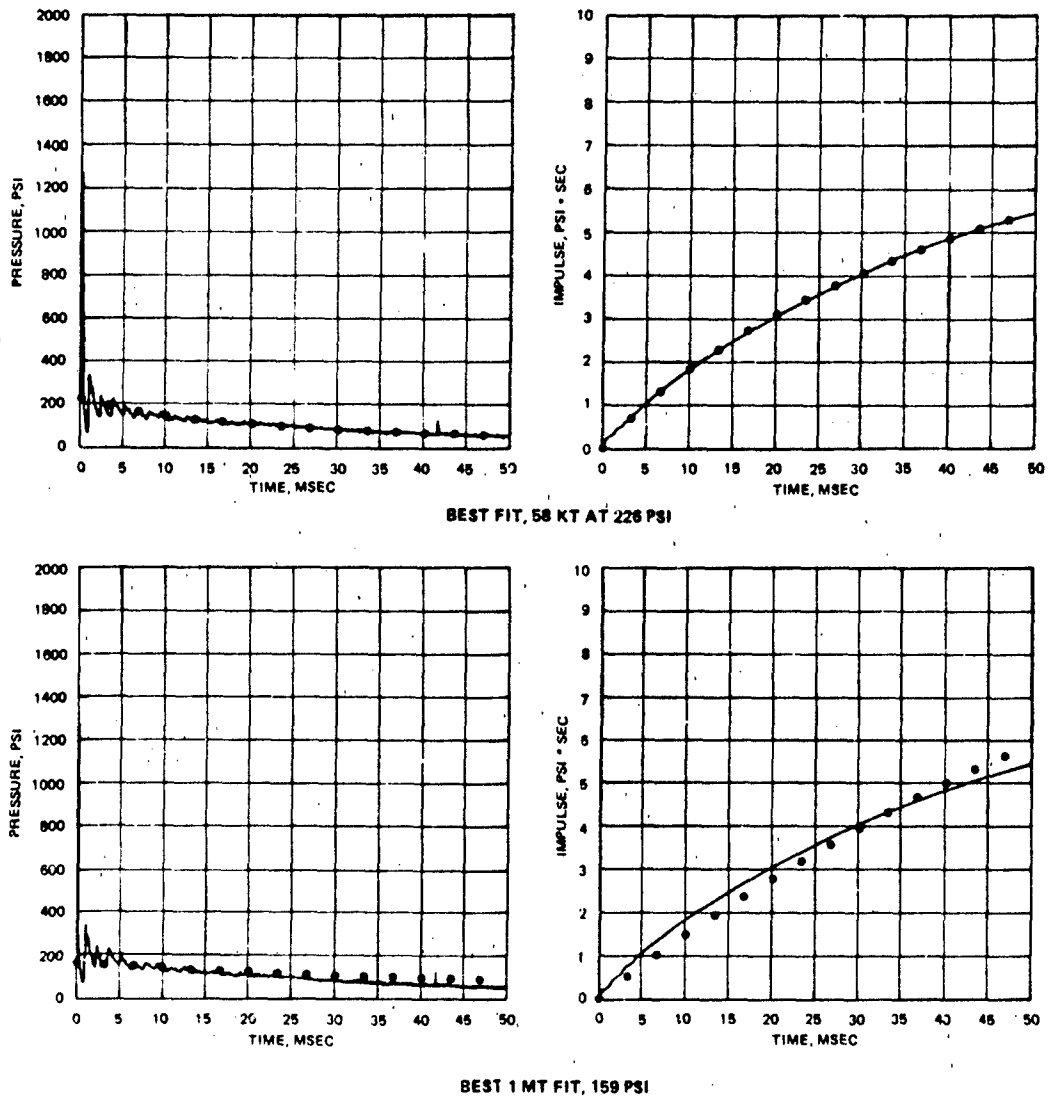

Figure 4.1. Average weapon simulations for 50 ms.

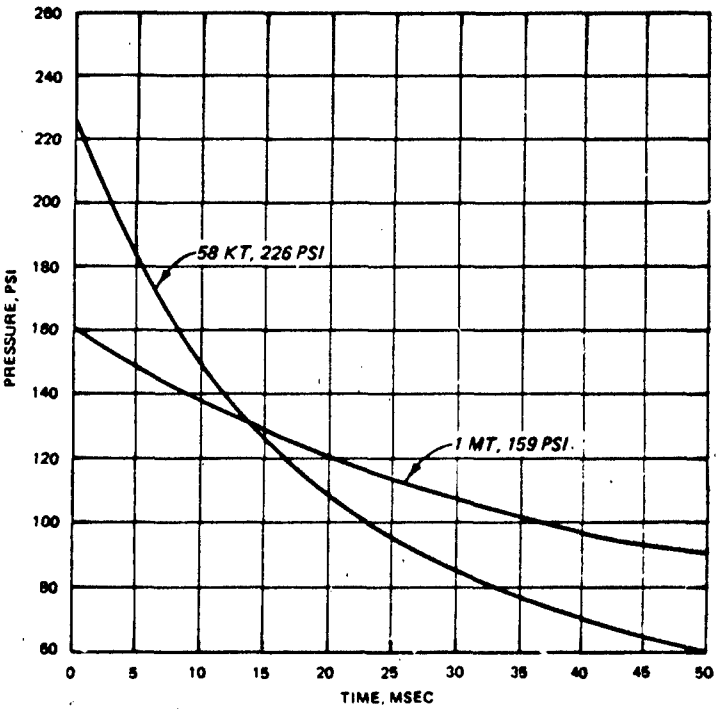

Figure 4.2. Comparison of the best fit and 1-MT best fit simulations.

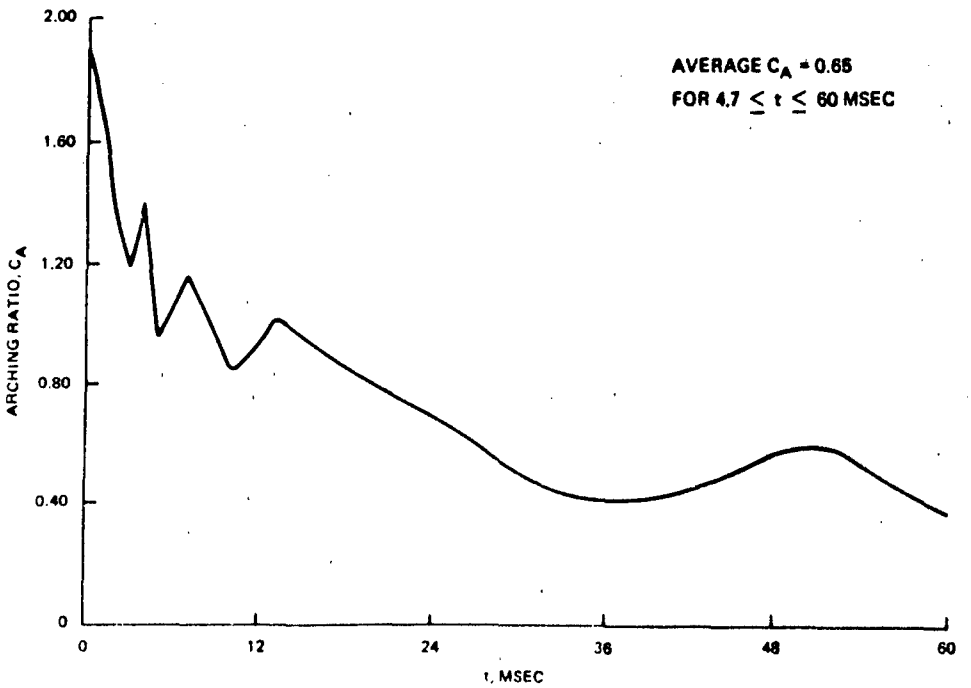

Figure 4.3. Soil arching ratio plot (bay 1 using SE-9).

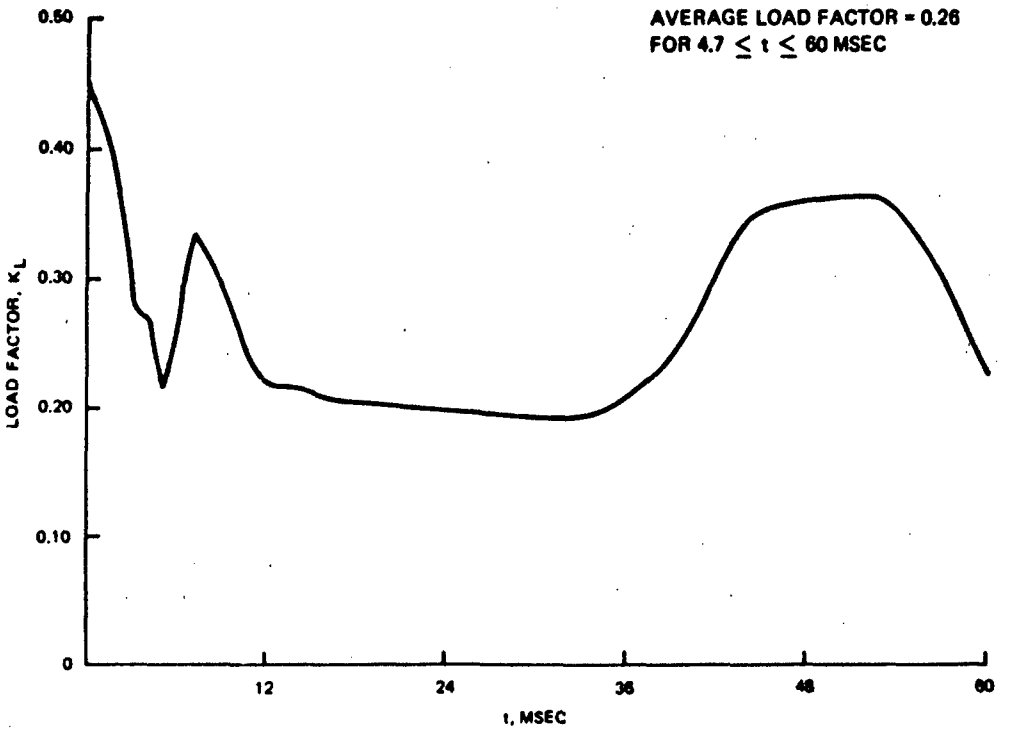

Figure 4.4. Load factor plot (bay 1).

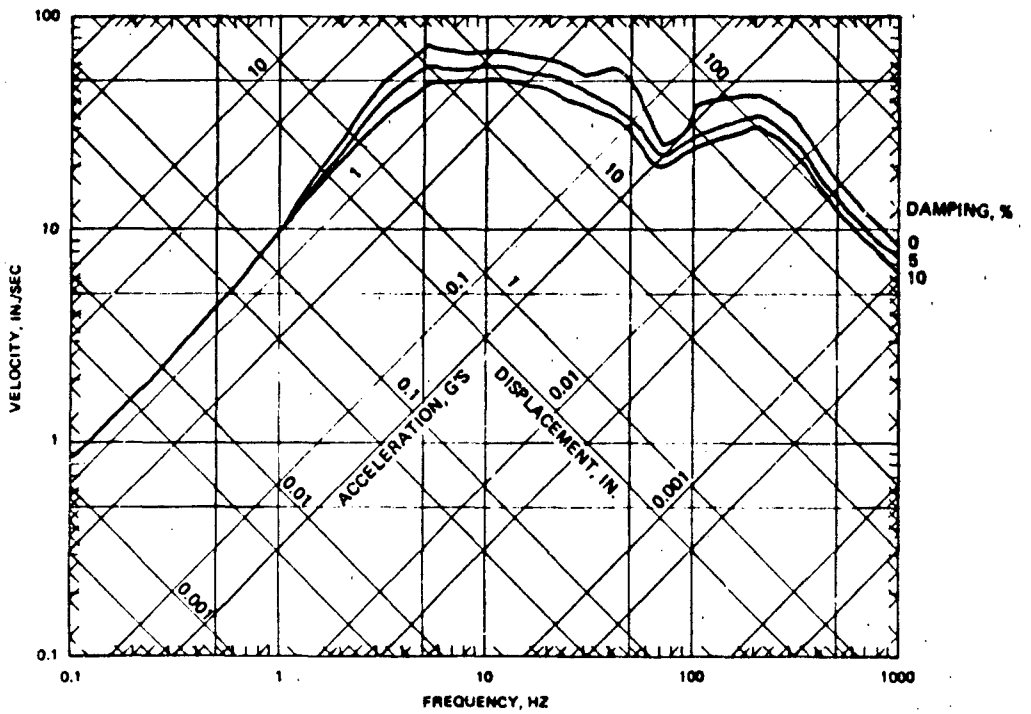

Figure 4.5. Floor shock spectra using gage AF-1.

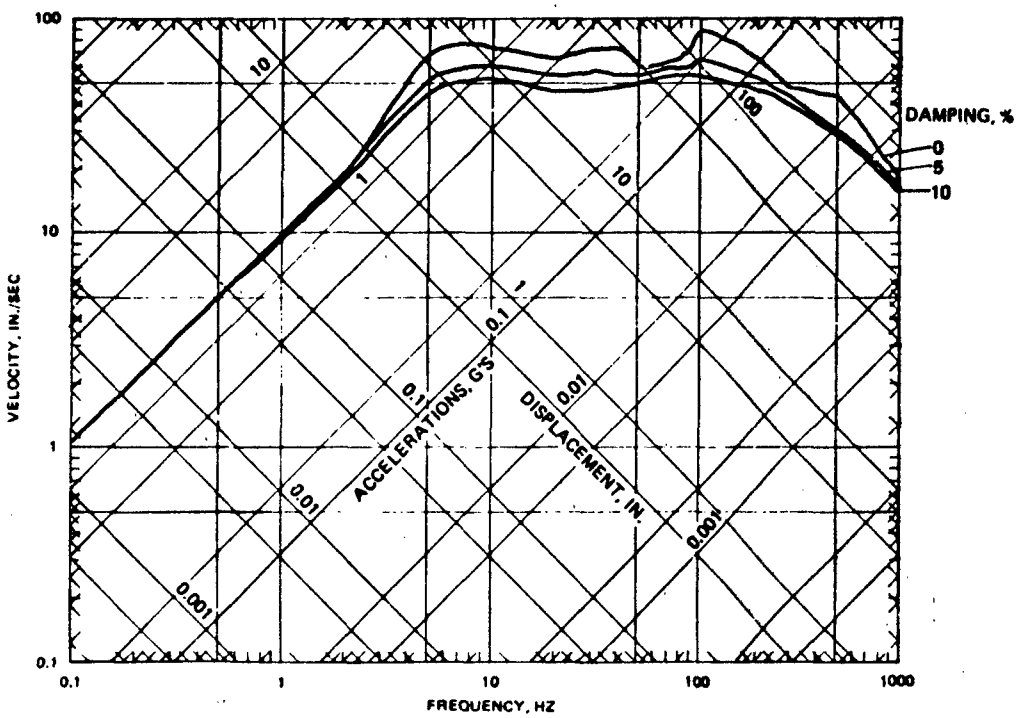

Figure 4.6. Floor shock spectra using gage AF-2.

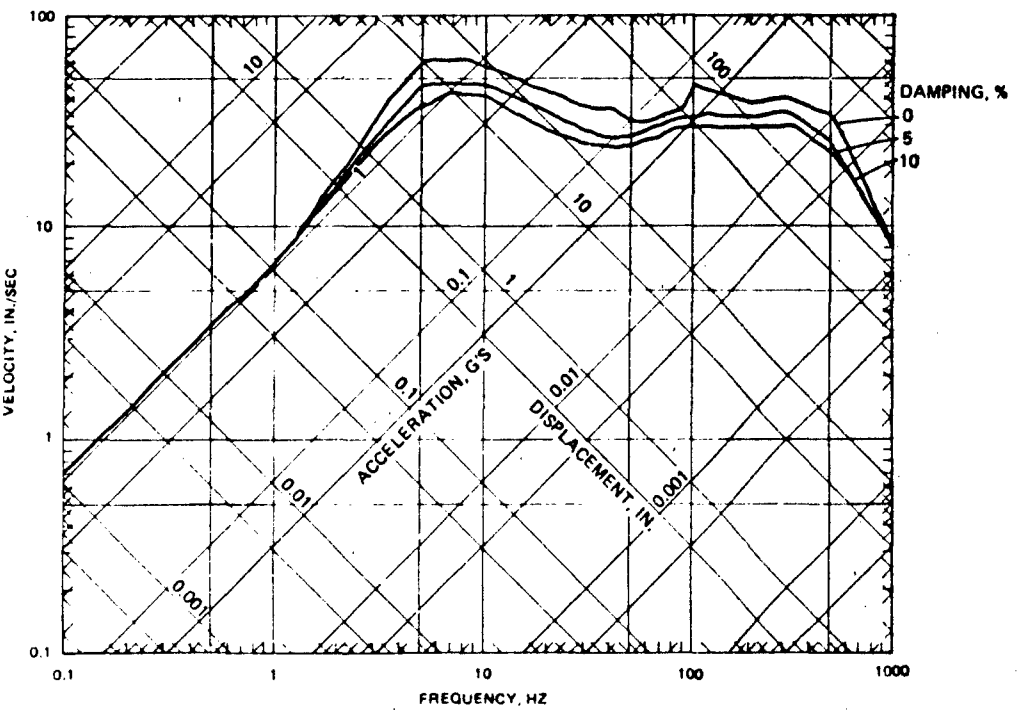

Figure 4.7. Floor shock spectra using gage AF-3.

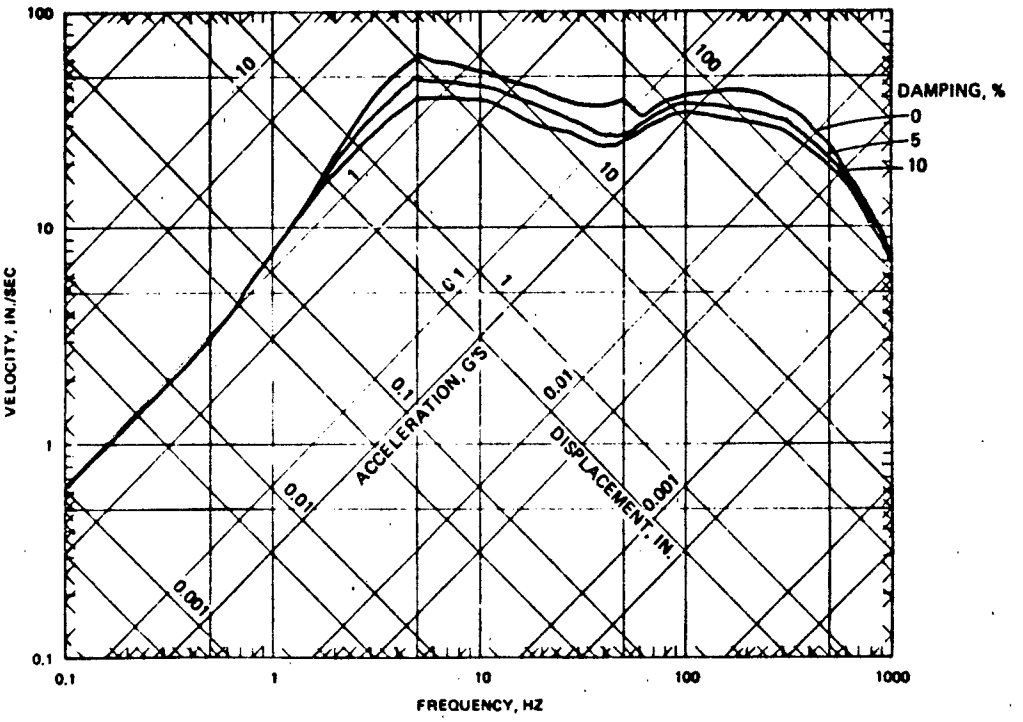

Figure 4.8. Floor shock spectra using gage AF-4.

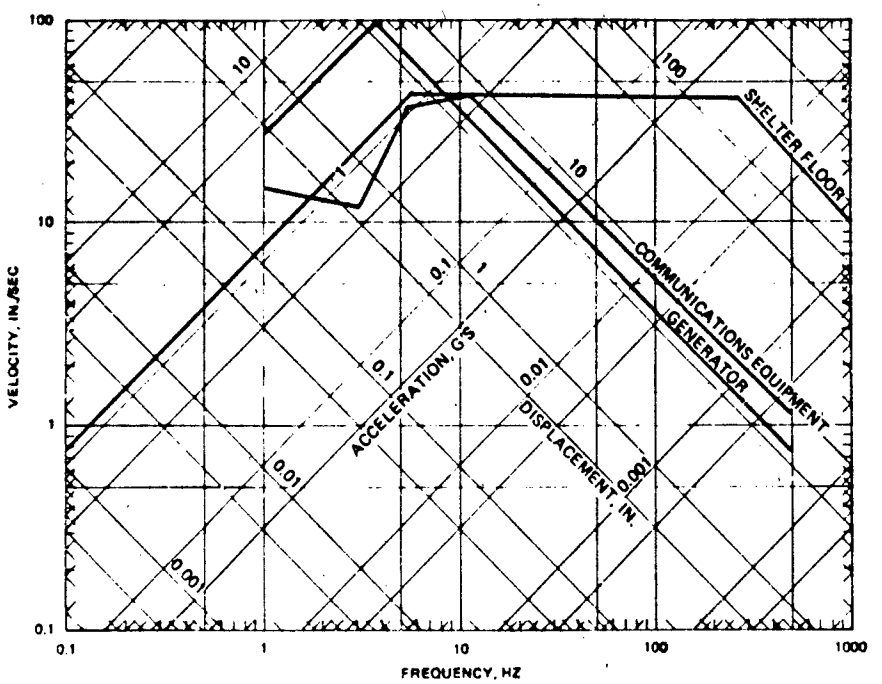

Figure 4.9. Comparison of the average experimental shock spectra (10 percent damping) with fragility curves for typical equipment.

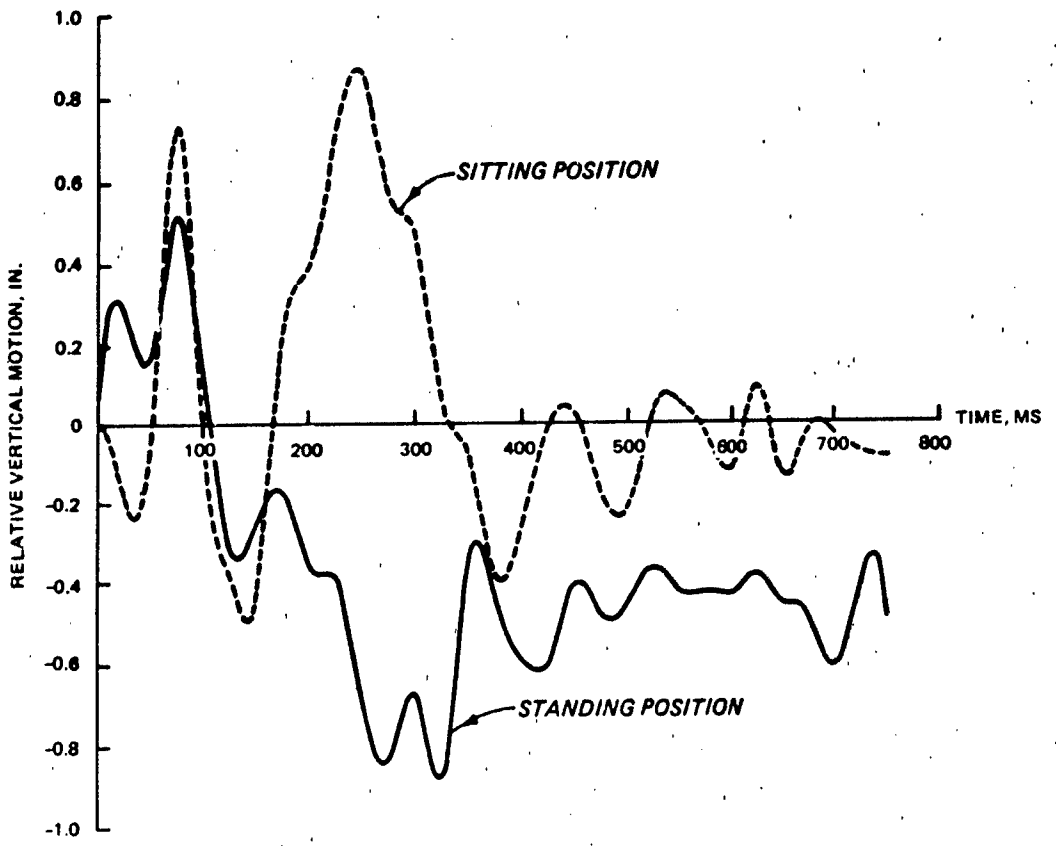

Figure 4.10. Plots of relative mannequin movement.

CHAPTER 5

CONCLUSIONS AND RECOMMENDATIONS

5.1 CONCLUSIONS

The Minor Scale and HEST tests of the prototype Keyworker blast shelter validated the structural design for the 1-MT at 50-psi nuclear threat and demonstrated that the shelter has reserve capacity to resist significant overloads (on the order of 130 to 160 psi) without catastrophic failure. The HEST test (along with the 1/4-scale tests) proves that the shelter design has adequate reserve capacity to resist the design load (1-MT, 50 psi) at sites throughout the country where site conditions may not be as good as WSMR.

Even though the shear response of the roof slab was significant, the failure mode was very ductile. The connection of the roof decking and embedded angle to the exterior shelter walls (near the doorway in particular) needs revision to prevent the embedded angle from pulling out at large roof deformations. However, this detail is adequate for the minor damage incurred at the design overpressure levels. The roof decking prevented most of the crushed concrete from falling to the floor except near the walls and doorway, as noted. Use of the roof decking protects the shelter occupants from projectile injuries caused by broken concrete when the roof is significantly damaged.

The mechanical equipment and their mounting details were adequate for the design loading and for the overload environment. During the HEST test, the lighting fixtures were detached from the roof slab, and the exhaust stack connection to the roof slab was damaged (but not to failure). These details were adequate at small roof deformations.

The entryway design proved adequate at the design overpressure but was severely damaged during the HEST test. The blast door was not retested at the higher overpressure because the HEST does not provide the dynamic overpressure phase required to test a blast door.

Occupant survivability is probable even at the 150-psi level. The generator also survived at this overpressure level. Some shock isolation may be required for communication equipment, but this was not investigated by the test.

5.2 RECOMMENDATIONS

Based on the results of this test and the scale model testing programs conducted by WES, the design of the 100-man Keyworker blast shelter should be accepted. The minor revisions suggested in this chapter make the shelter perform better at large deformations resulting from overload conditions.

The shelter has adequate structural capacity to be used at the design overpressure level for the many site conditions found throughout the country. To limit backfill conditions to those in the current data base, the backfill material should have an angle of internal friction greater than approximately 25 degrees, and compaction to 90 percent of the maximum Proctor density is recommended. For special site conditions, such as high water tables, the bermed configuration should be used. The experimental and analytical programs conducted by WES have resulted in a shelter design that can be used without a redesign for site-specific conditions in most cases. The shelter design has been experimentally validated in the buried and bermed configurations.

REFERENCES

1. Crawford, R. E., and others. 1974. "The Air Force Design Manual for Design and Analysis of Hardened Structures," Air Force Weapons Laboratory, Kirtland Air Force Base, N. Mex.

2. Headquarters, Department of the Army. 1987. "Fundamentals of Protective Design for Conventional Weapons," Technical Manual 5-855-1, Washington, DC.

3. Kiger, S. A. 1981 (Jul). "Use of a Foam HEST to Simulate Low Yield Nuclear Overpressures," Miscellaneous Paper SL-81-12, US Army Engineer Waterways Experiment Station, Vicksburg, Miss.

4. Kiger, S. A., Slawson, T. R., and Hyde, D. W. 1984 (Sep). "Vulnerability of Shallow-Buried Flat-Roof Structures; A Computational Procedure," Technical Report SL-80-7, Report 6, US Army Engineer Waterways Experiment Station, Vicksburg, Miss.

5. Mlakar, P. F., and Walker, R. E. 1980 (Sep). "Statistical Estimation of Simulated Yield and Overpressure," Shock and Vibration Bulletin, Bulletin 50, Part 2, The Shock and Vibration Center, Naval Research Laboratory, Washington, DC.

6. Speicher, S. J., and Brode, H. L. 1981 (Nov). "Airblast Overpressure Analytic Expression for Burst Height, Range, and Time Over an Ideal Surface," PSR Note 385 (with updates through Nov 1982), Pacific-Sierra Research Corporation, Santa Monica, Calif.

7. US Army Corps of Engineers. 1960. "The Unified Soil Classification System," Technical Memorandum No. 3-357, US Army Engineer Waterways Experiment Station, Vicksburg, Miss.

8. Wampler, H. W., and others. 1978. "A Status and Capability Report on Nuclear Airblast Simulation Using HEST," Proceedings of the Nuclear Blast and Shock Simulation Symposium, 28-30 November 1978, Vol 1, General Electric-TEMPO, Santa Barbara, Calif.

9. Woodson, S. C., and Slawson, T. R. 1986 (Dec). "Demonstration Test of the Keyworker Blast Shelter: Minor Scale," Technical Report SL-86-40, US Army Engineer Waterways Experiment Station, Vicksburg, Miss.

THIS PAGE IS INTENTIONALLY LEFT BLANK

APPENDIX A

RECORDED DATA

FEMA KEYWORKER
AB-1
200000. HZ CAL= 2951.
LP4/0 70% CUTOFF= 9000. HZ

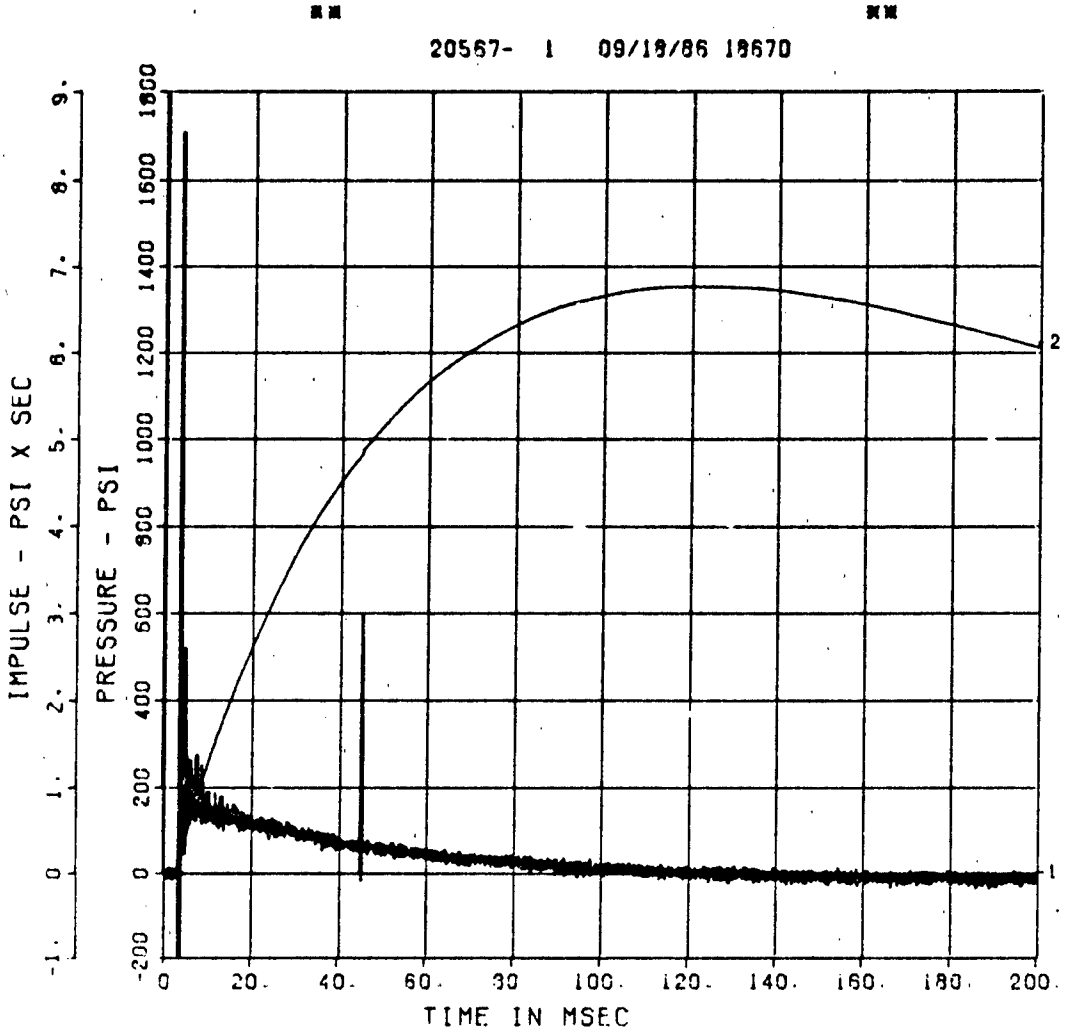

Note: The primary data plot is labeled "1" at the far right side of these plots. The pressure scale should be used for this plot. Data plots derived from the primary data are labeled "2" and/or "3," and vertical scales to the left of the primary scale should be used (i.e., impulse).

FEMA KEYWORKER
AB-2
200000. HZ CAL= 3496.
LP4/0 70% CUTOFF= 9000. HZ

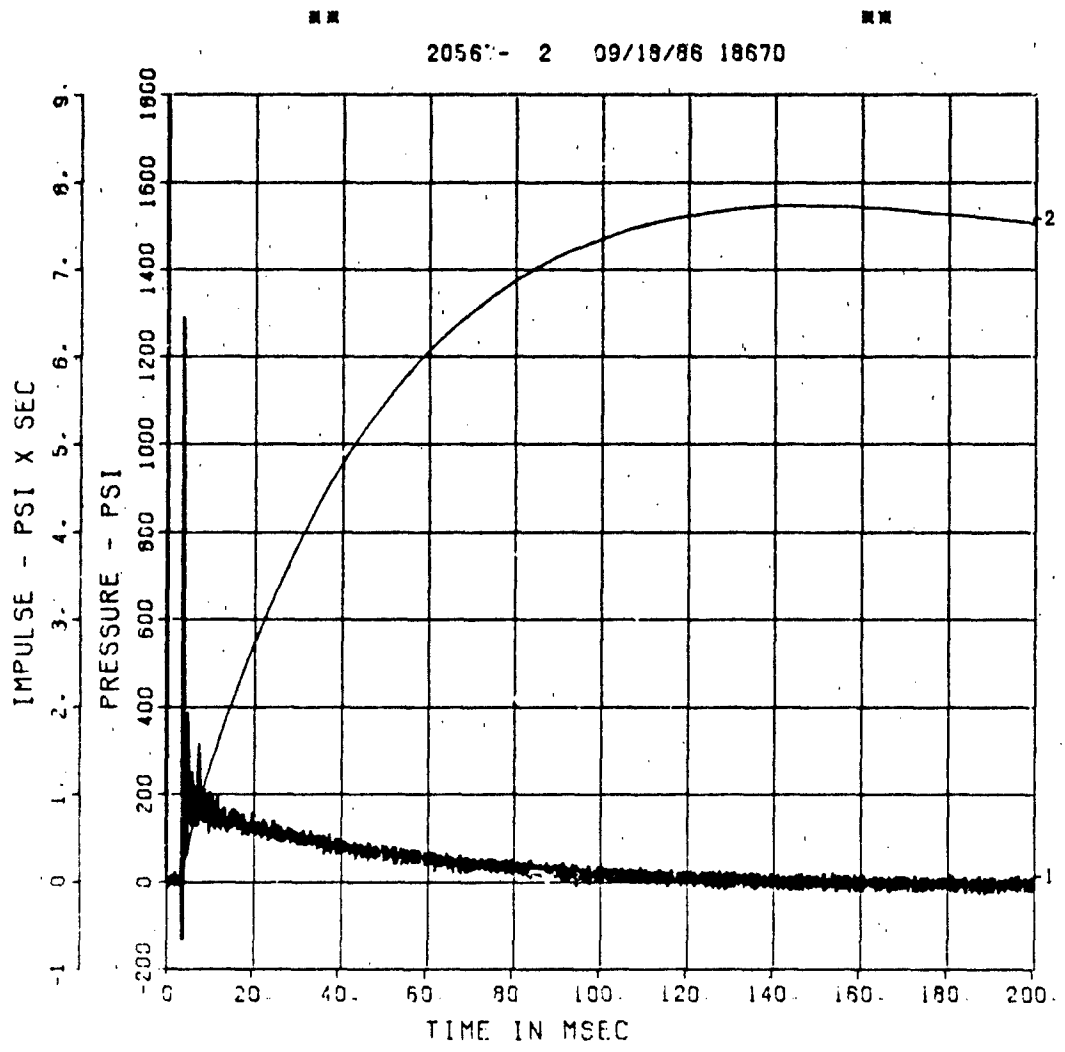

FEMA KEYWORKER
AB-3
200000. HZ CAL= 4023.
LP4/0 70% CUTOFF= 9000. HZ

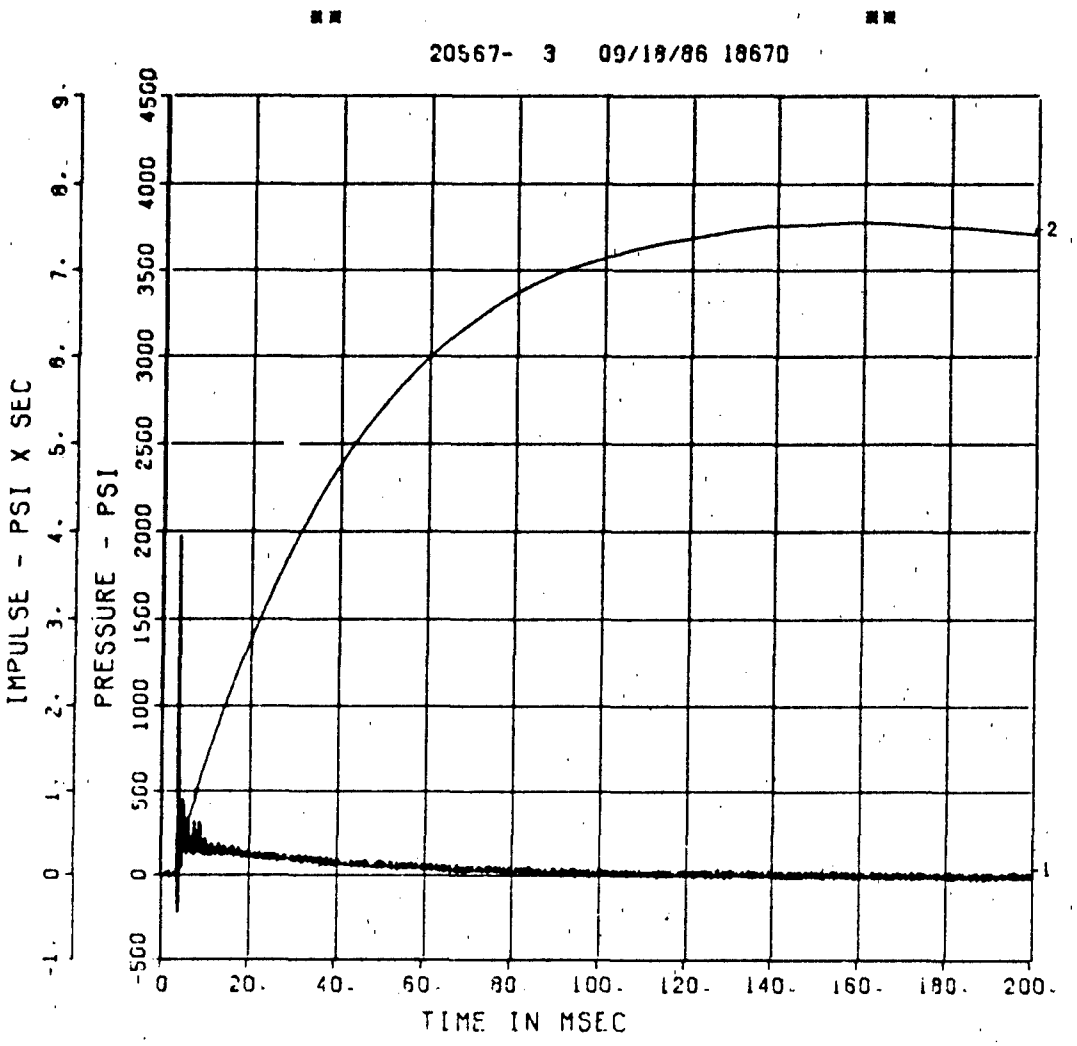

FEMA KEYWORKER
AB-4
200000. HZ CAL= 3667.
LP4/0 70% CUTOFF= 9000. HZ

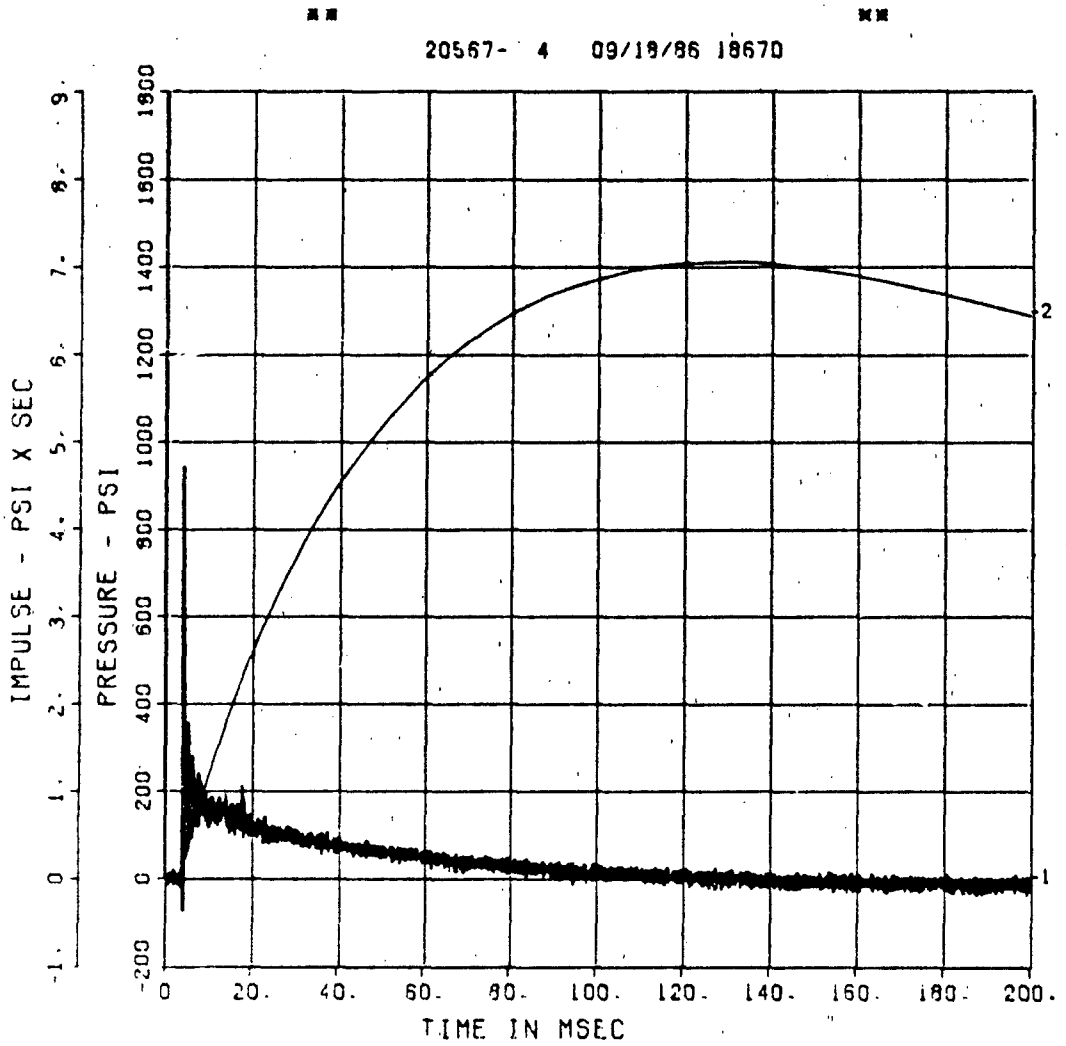

FEMA KEYWORKER
AB-5
200000. HZ CAL= 3763.
LP4/0 70% CUTOFF= 9000. HZ

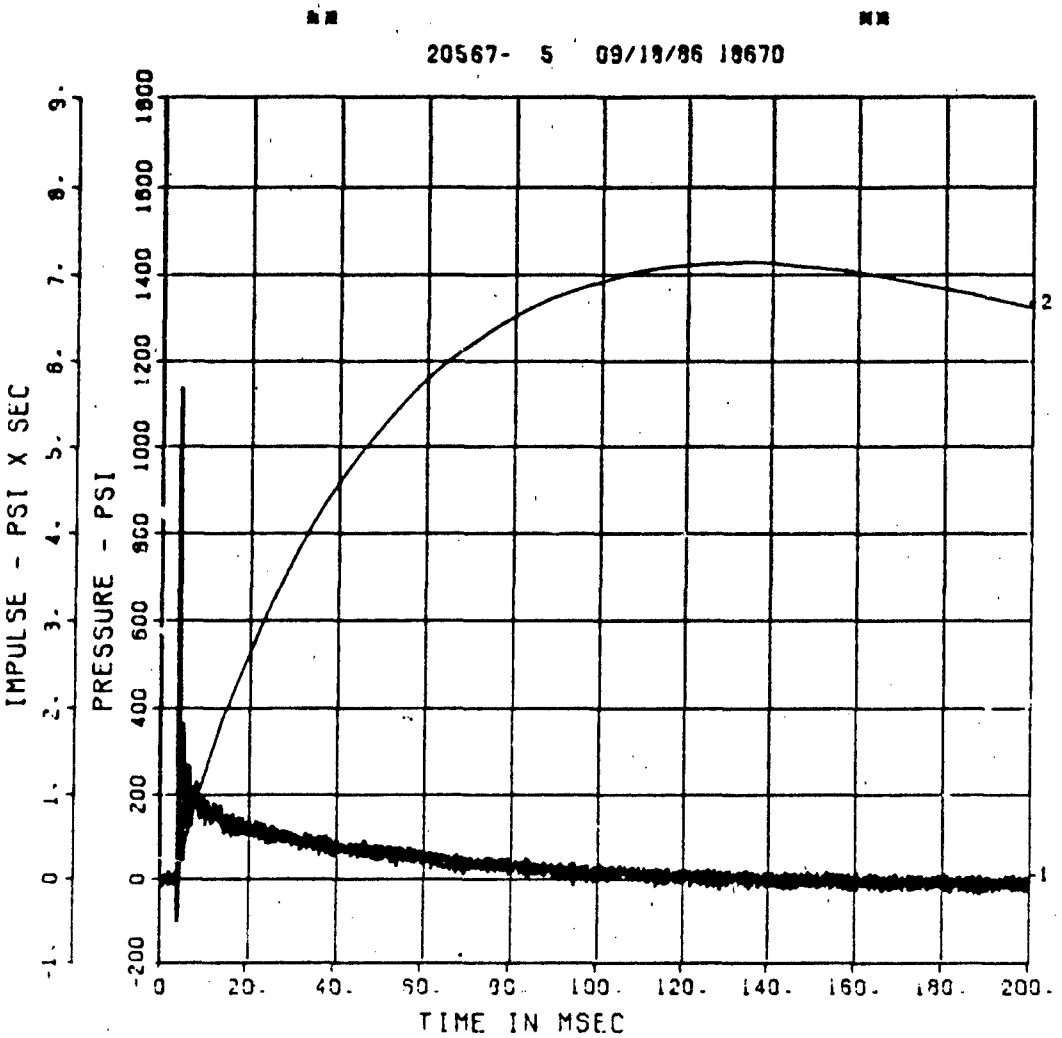

FEMA KEYWORKER
AB-6
200000. HZ CAL= 3736.
LP4/0 70% CUTOFF= 9000. HZ

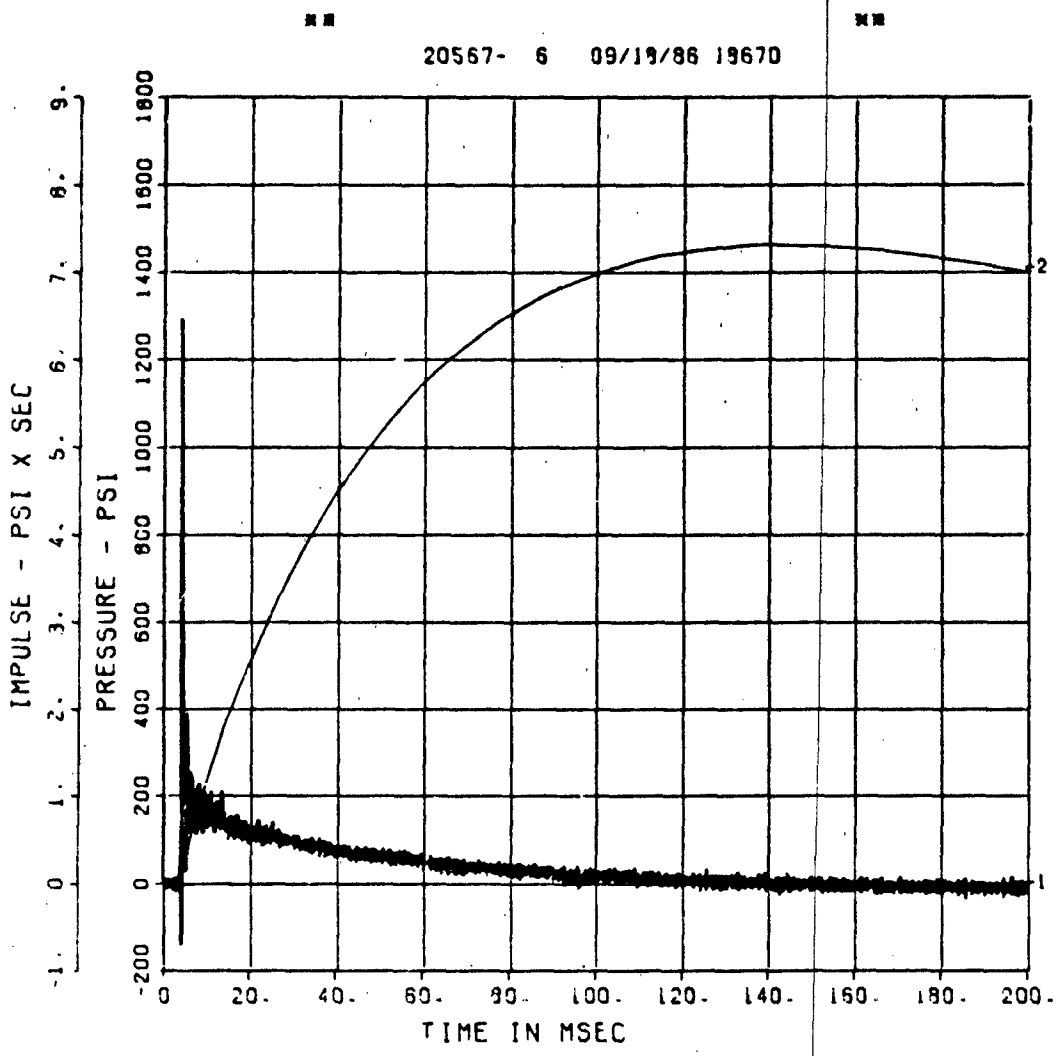

FEMA KEYWORKER
AB-7
200000. HZ CAL= 3469.
LP4/0 70% CUTOFF= 9000. HZ

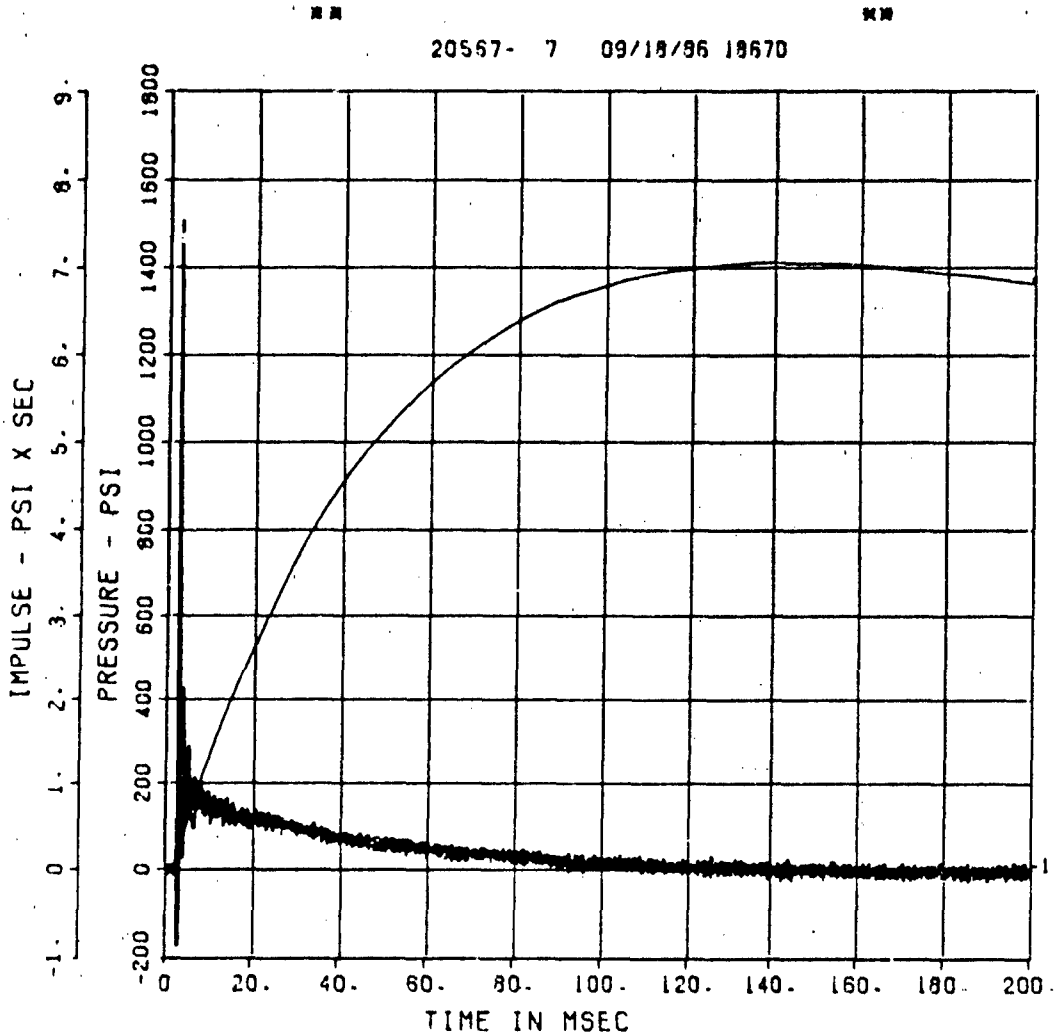

FEMA KEYWORKER
AB-8
200000. HZ CAL= 4351.
LP4/0 70% CUTOFF= 9000. HZ

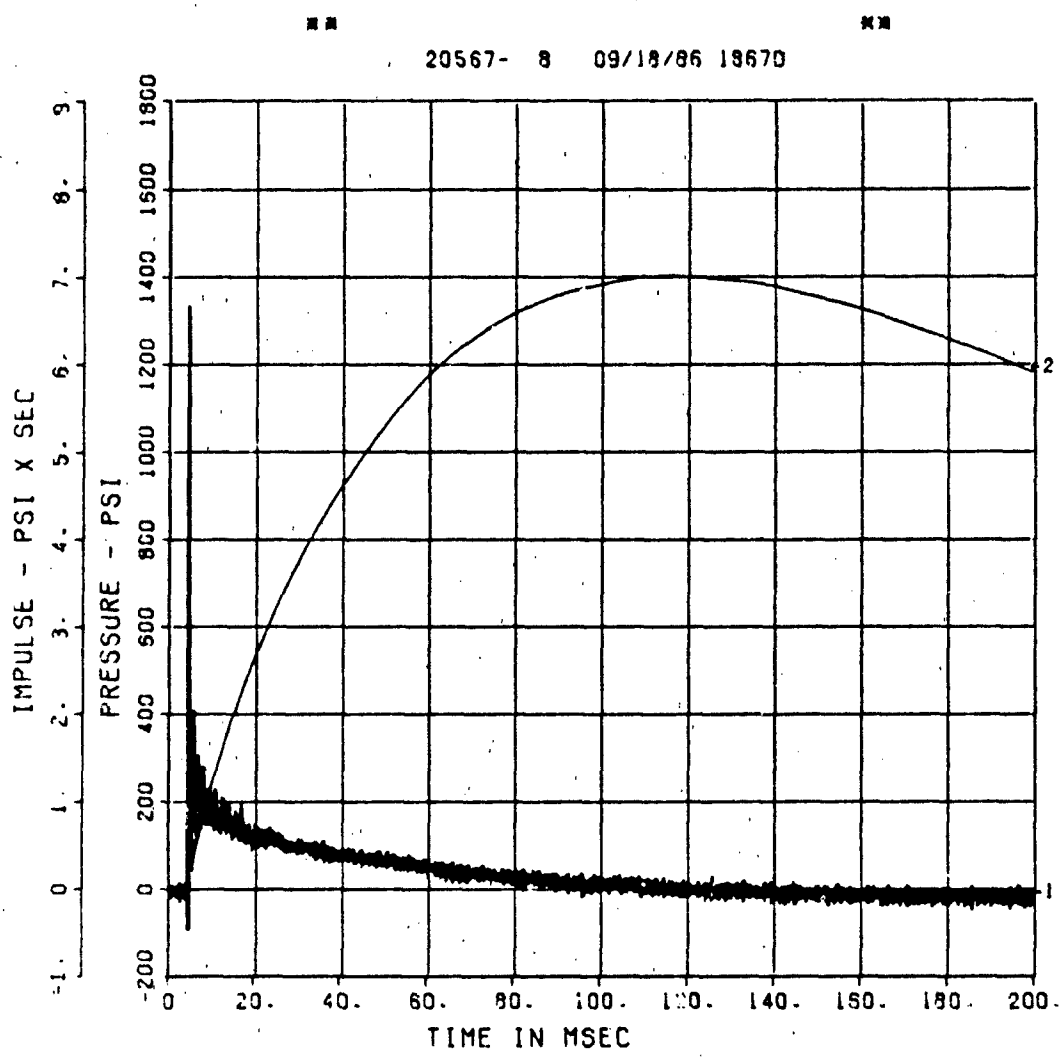

FEMA KEYWORKER
F-1
200000. HZ CAL= 550.0

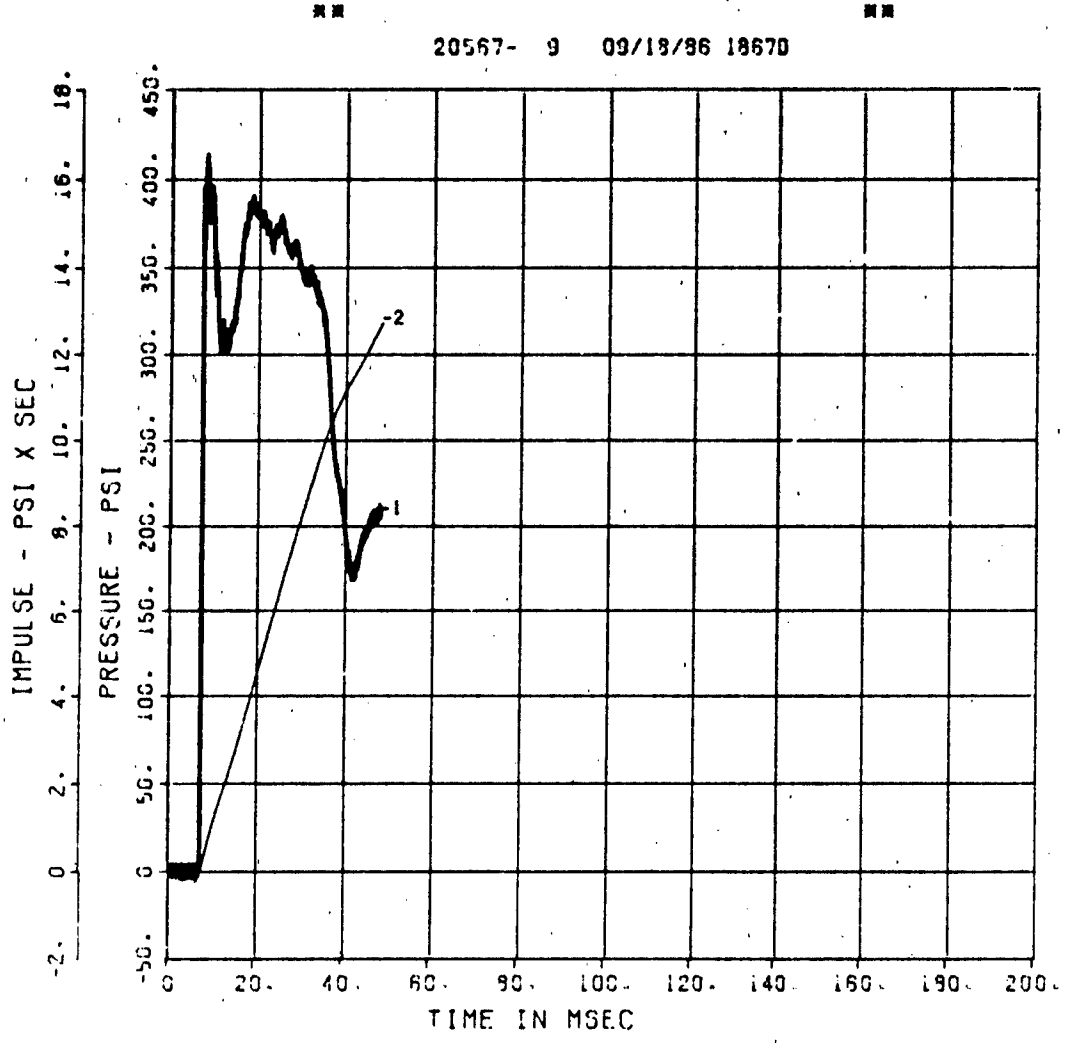

FEMA KEYWORKER
IF-2
200000. HZ CAL= 518.0

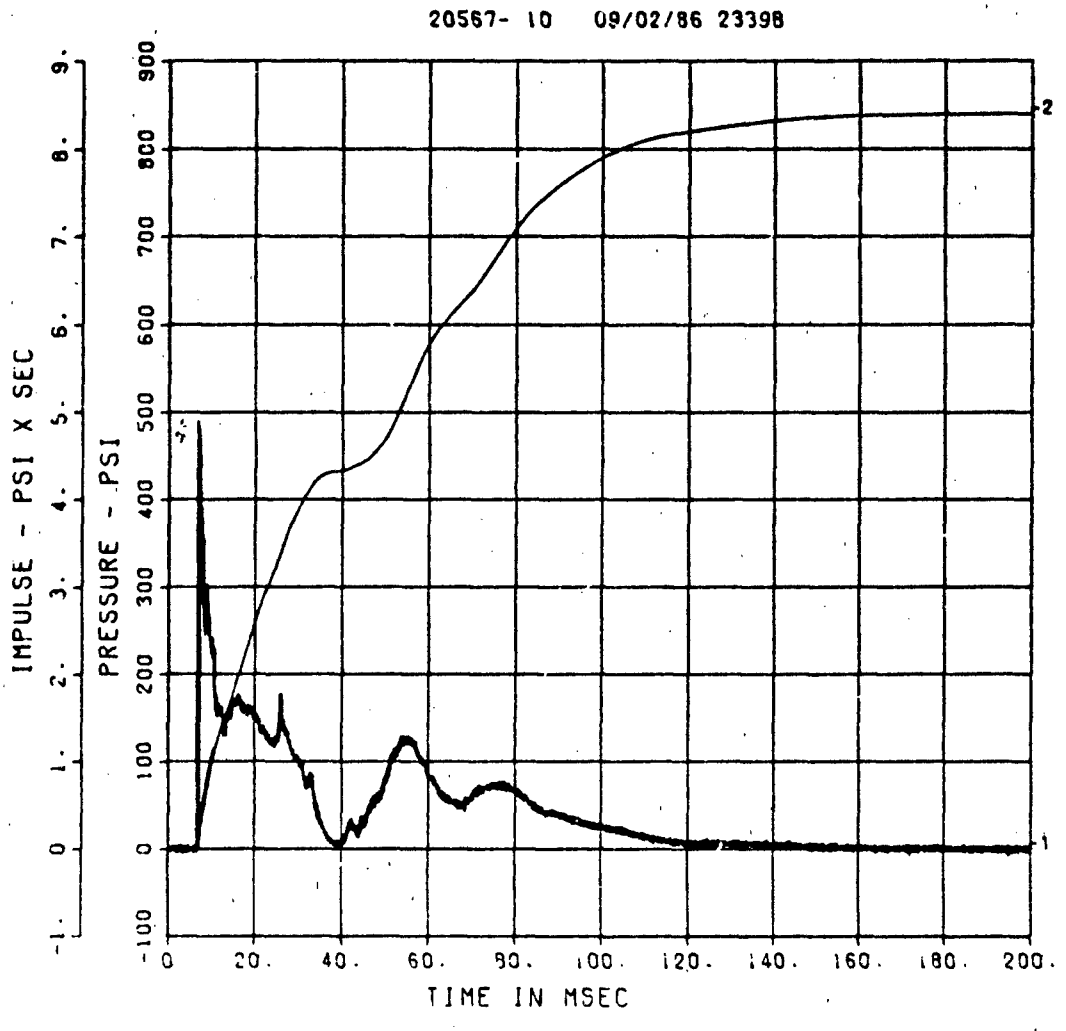

FEMA KEYWORKER
IF-3
200000. HZ CAL= 209.0

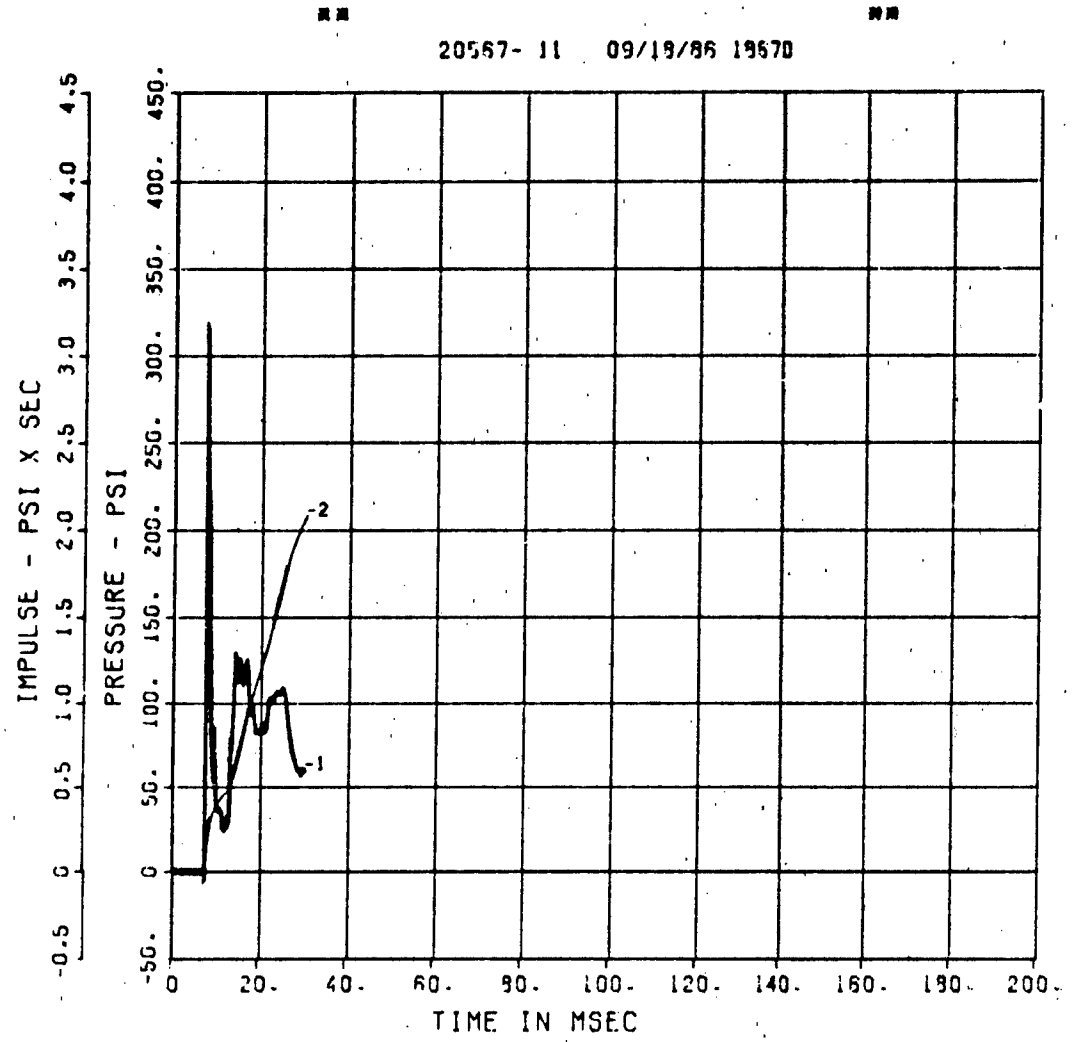

FEMA KEYWORKER
IF-4
200000. HZ CAL= 268.5

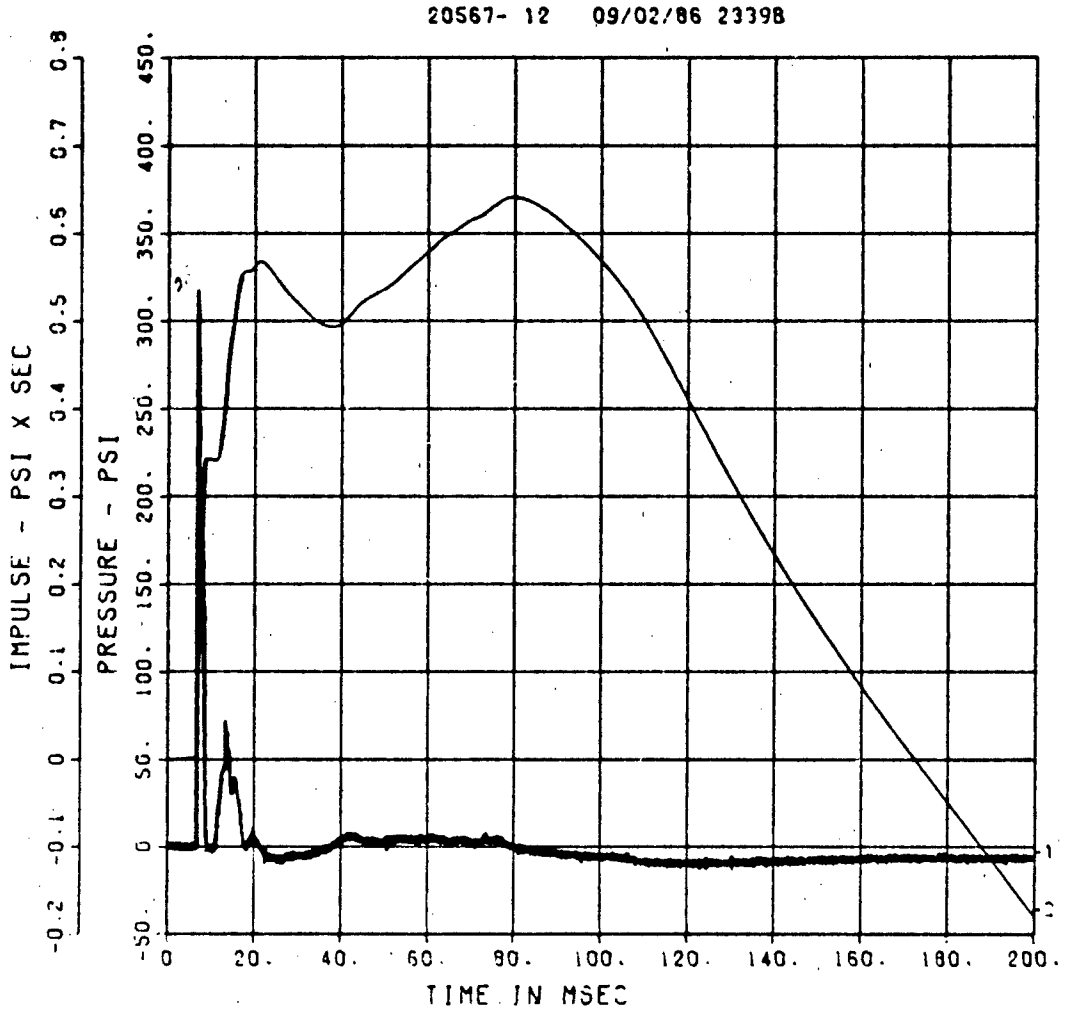

FEMA KEYWORKER
IF-5
200000. HZ CAL= 224.5

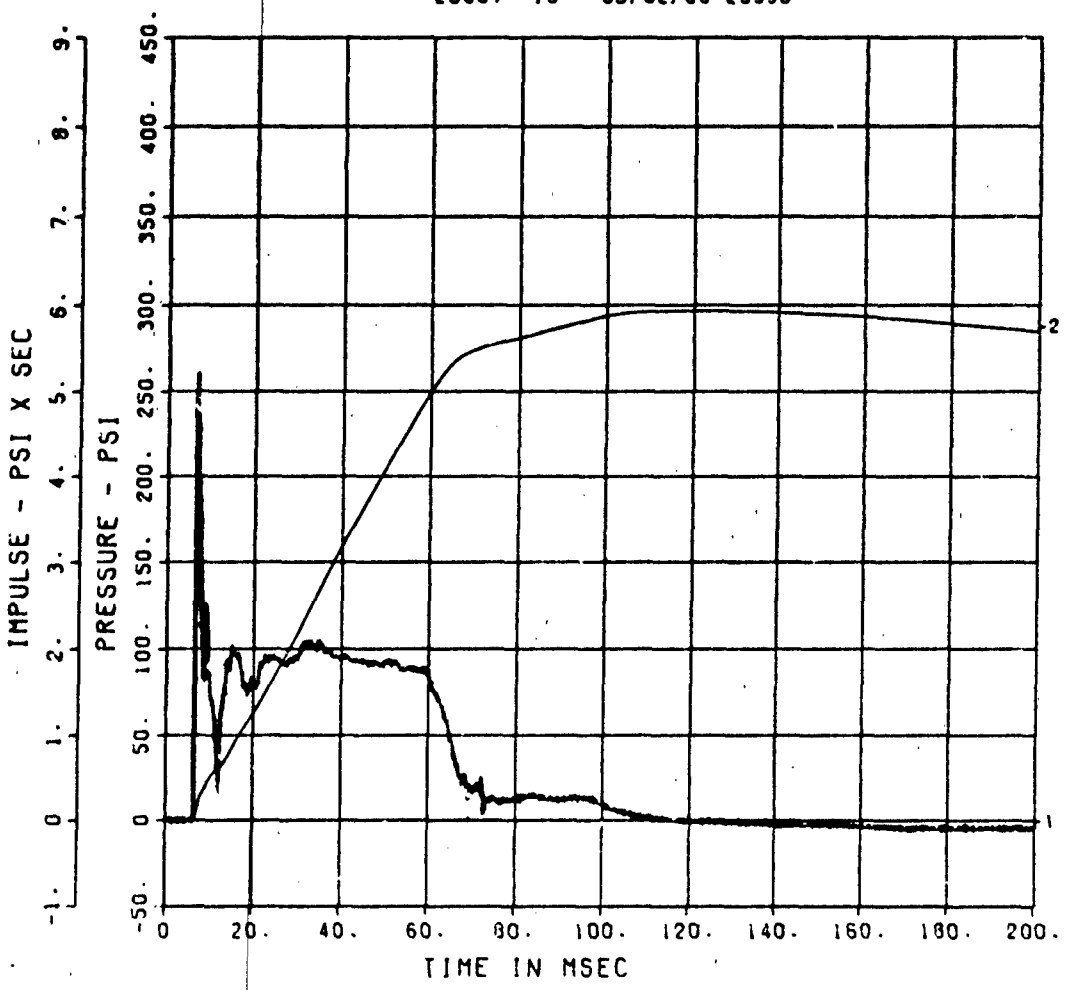

FEMA KEYWORKER
IF-6
200000. HZ CAL= 534.5

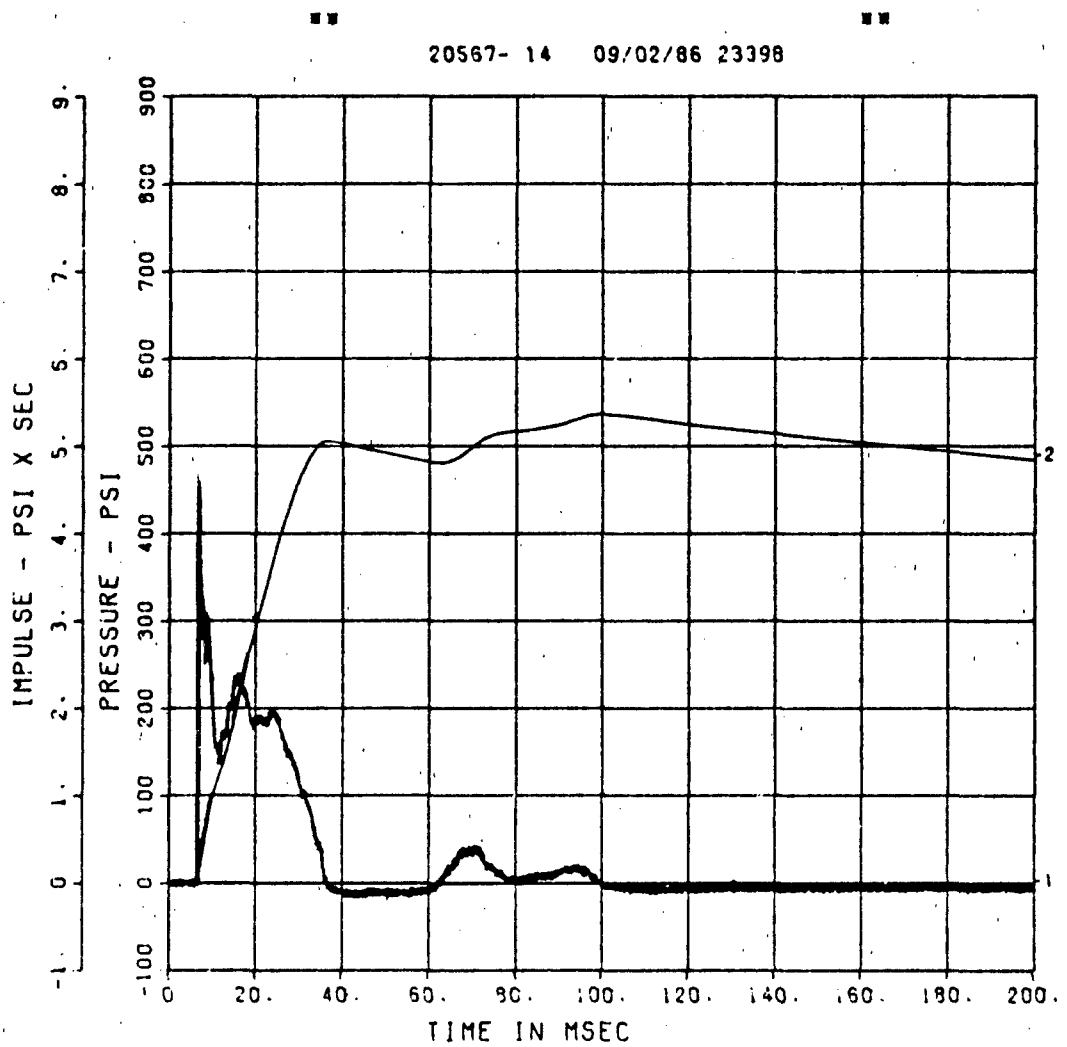

FEMA KEYWORKER
IF-7
200000. HZ CAL= 566.9

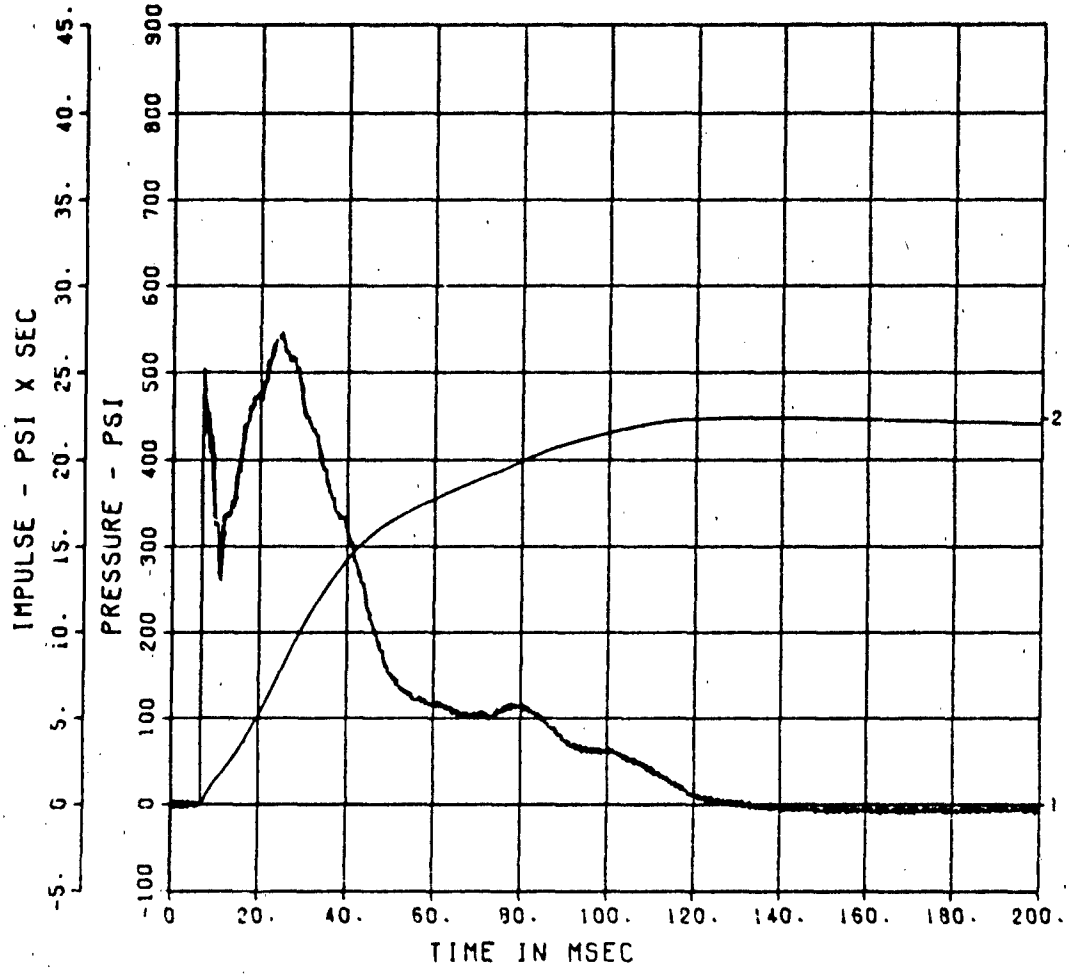

FEMA KEYWORKER
IF-8
200000. HZ CAL= 521.0

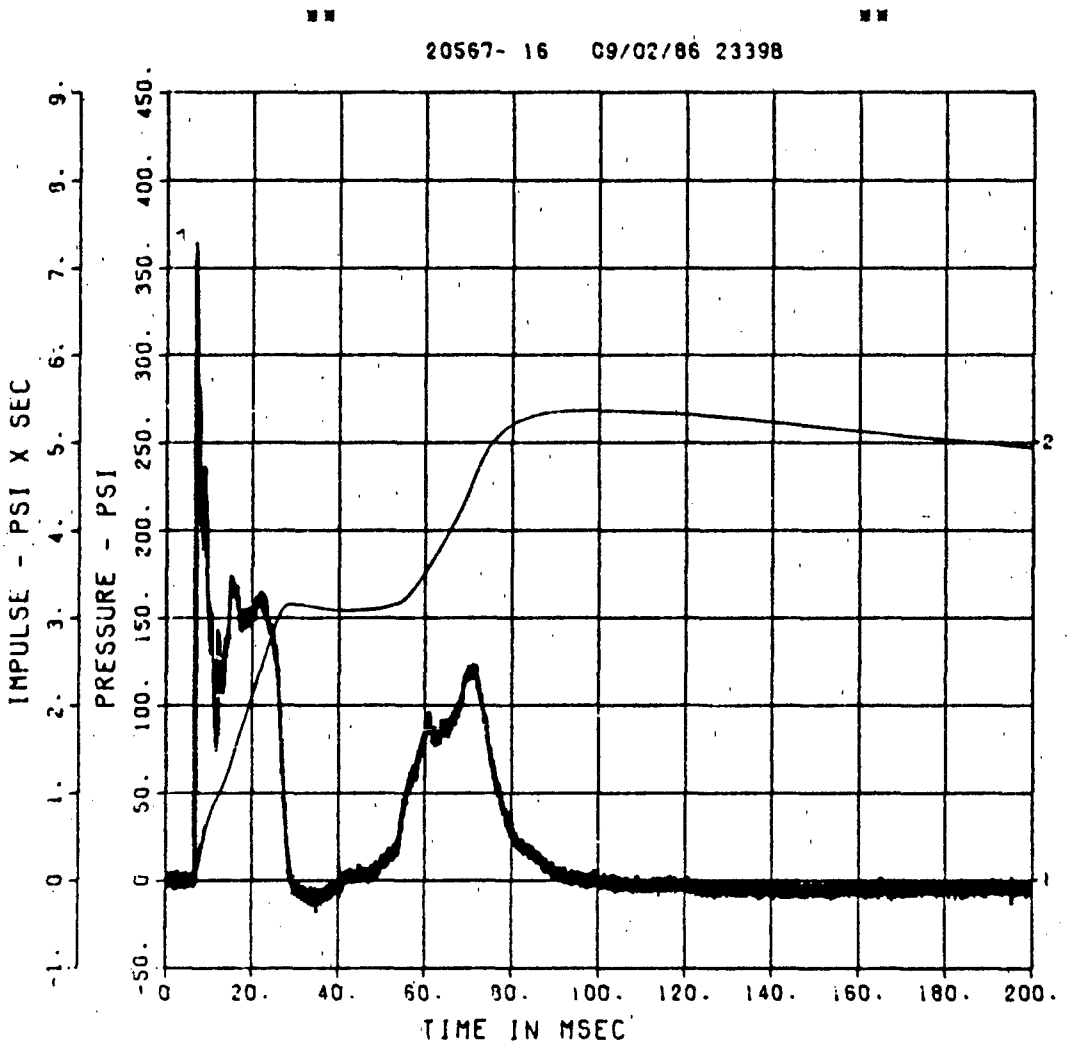

FEMA KEYWORKER
1F-9
200000. HZ CAL= 273.2

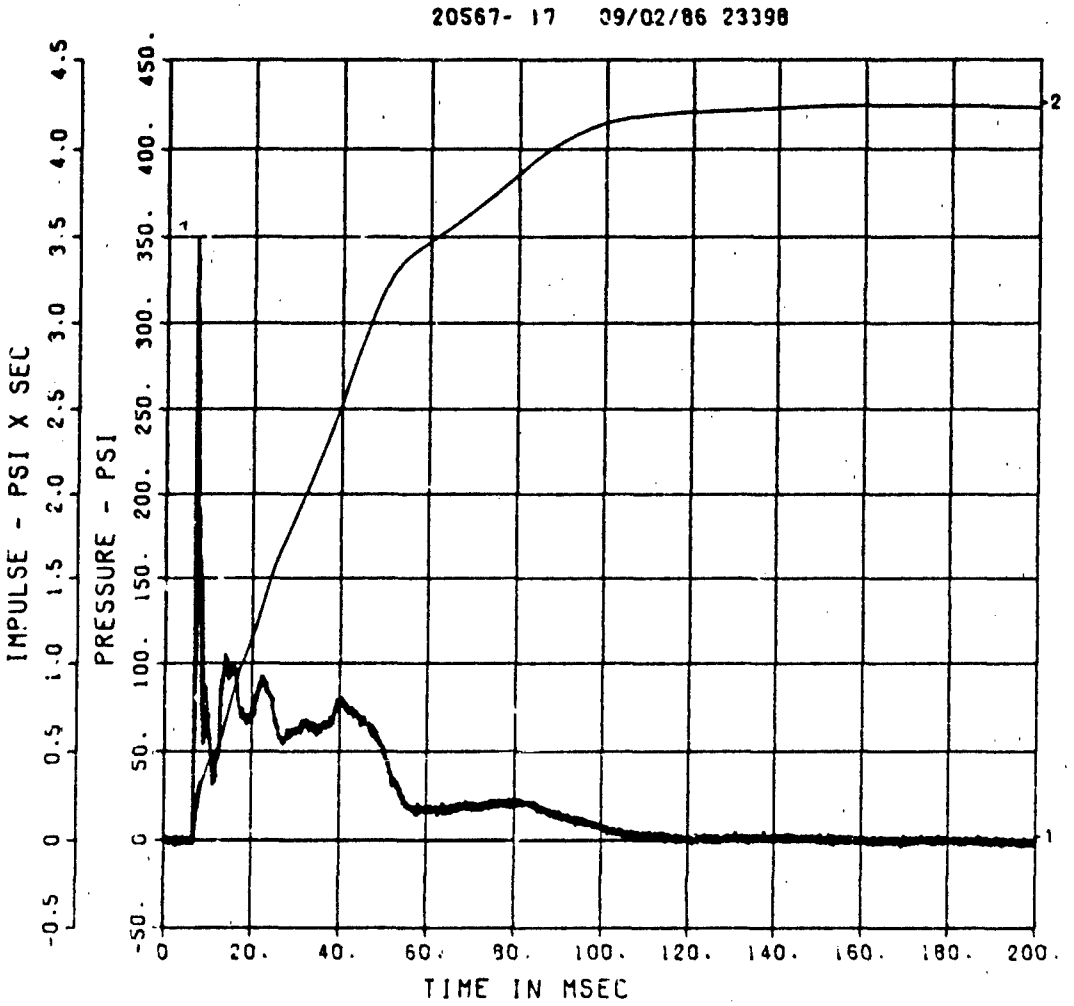

FEMA KEYWORKER
IF-10
200000. HZ CAL= 224.0

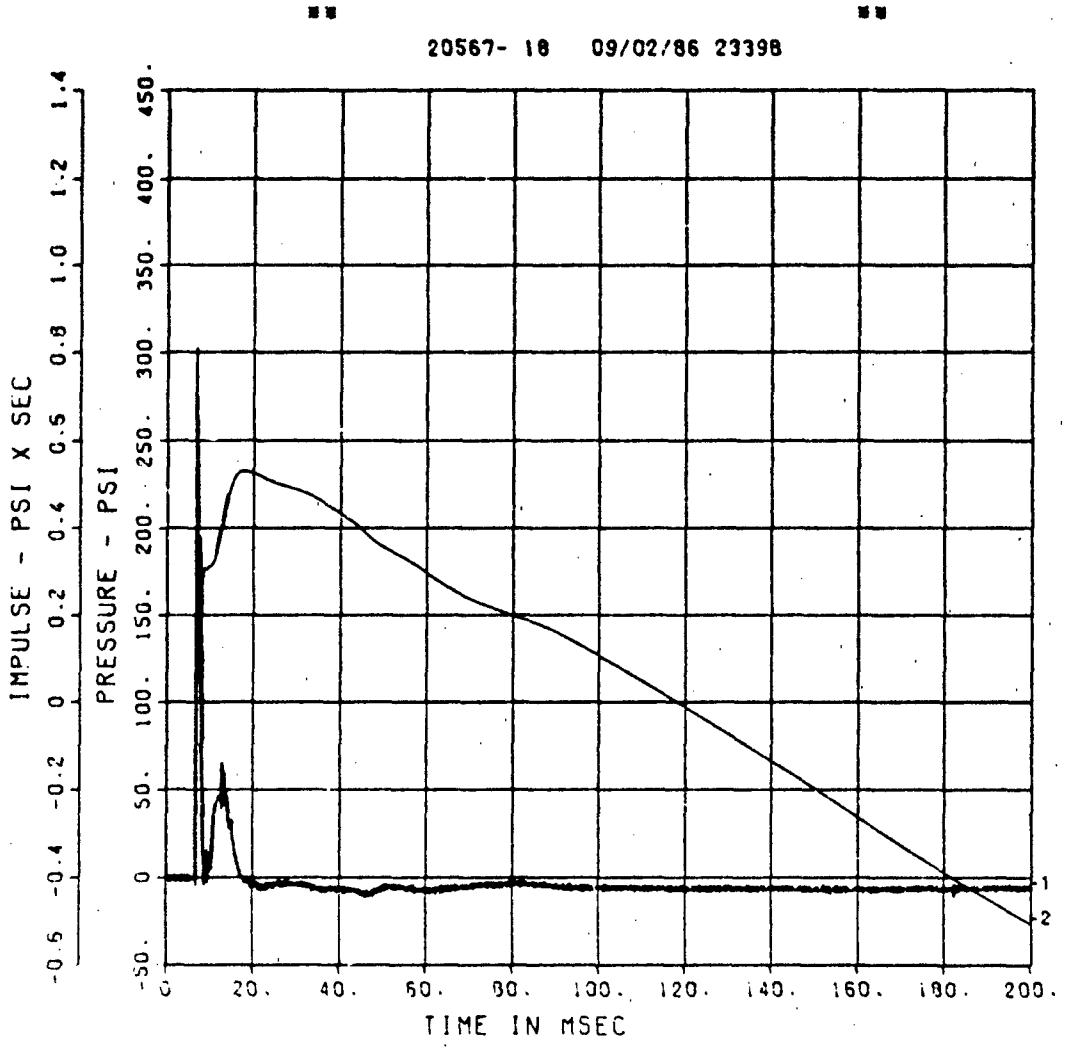

FEMA KEYWORKER
IF-11
200000. HZ CAL= 237.5

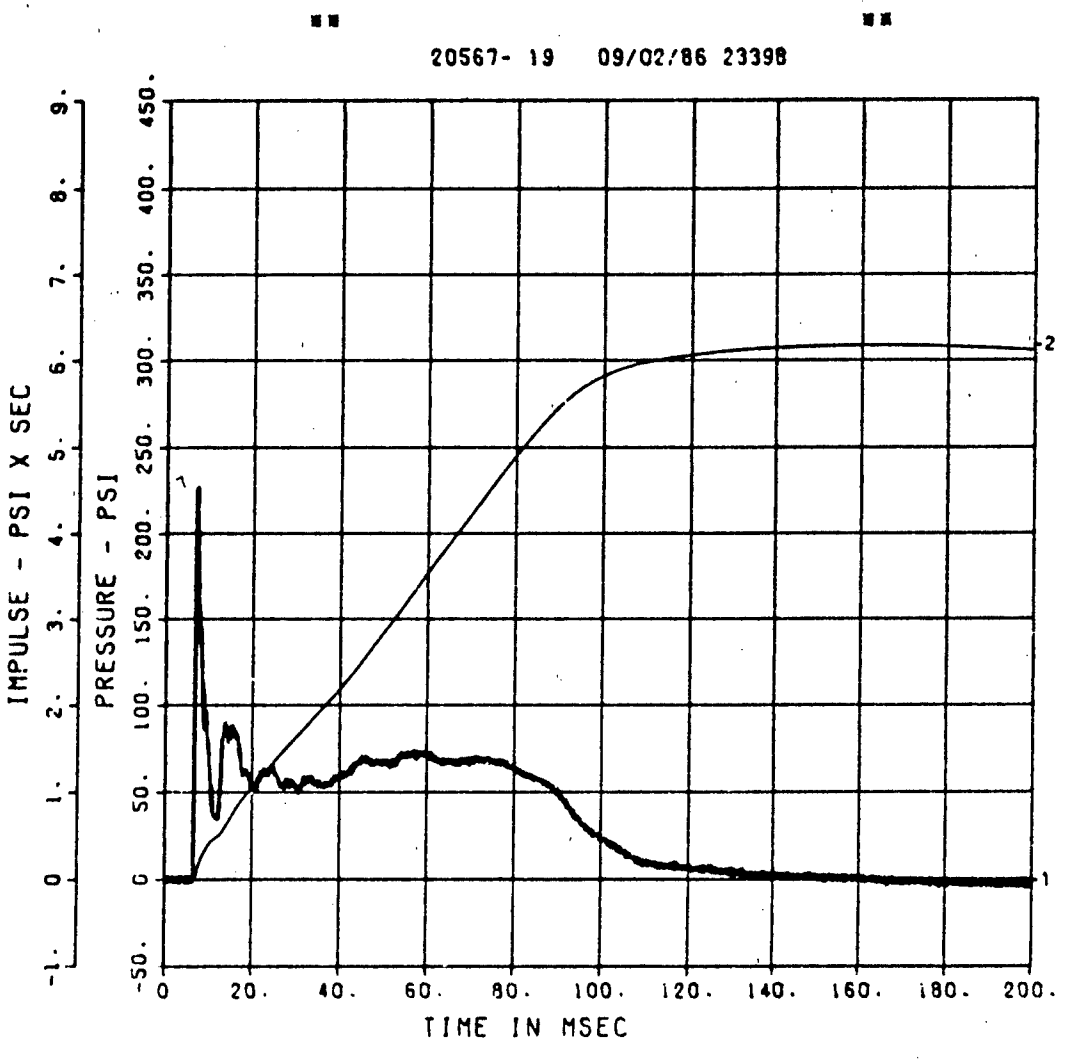

FEMA KEYWORKER
IF-12
200000. HZ CAL= 518.0

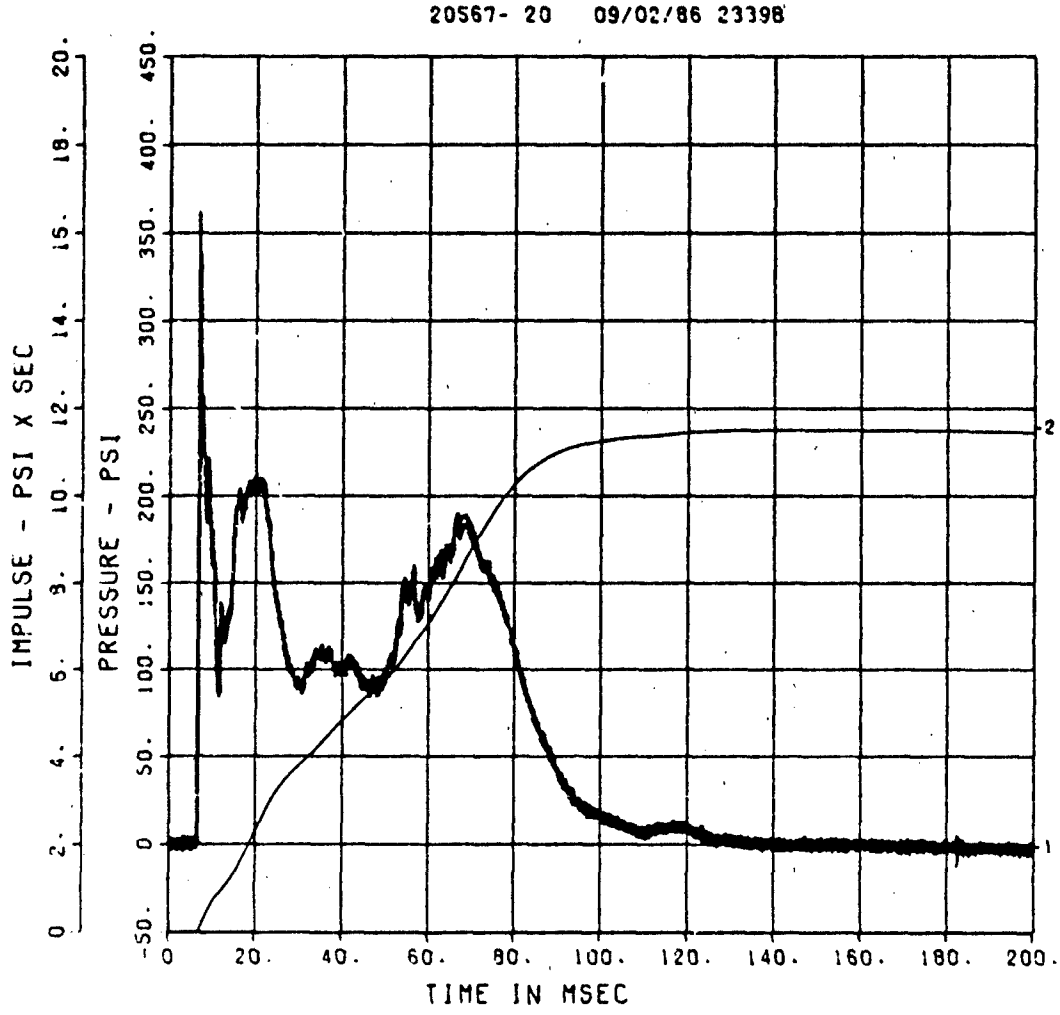

FEMA KEYWORKER
IF-13
200000. HZ CAL= 525.9

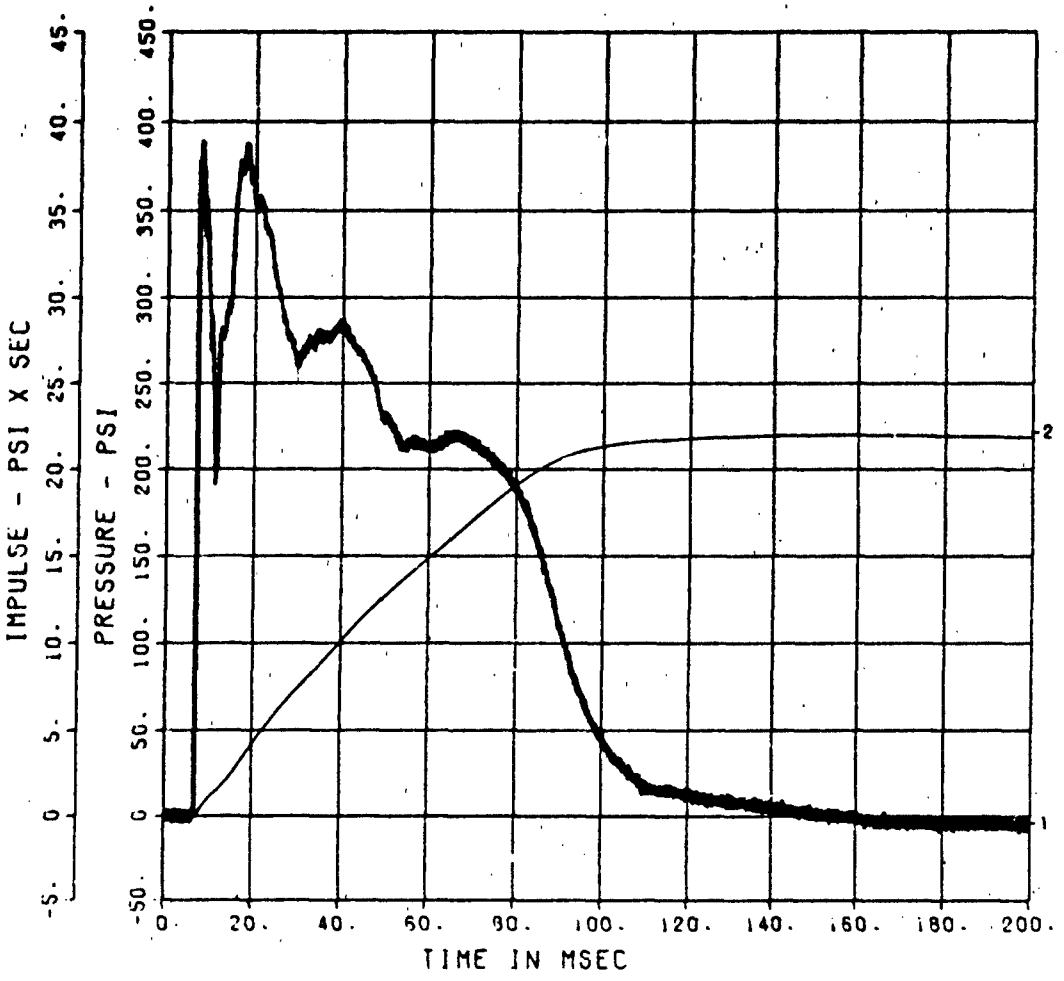

FEMA KEYWORKER
IF-14
200000. HZ CAL= 228.0

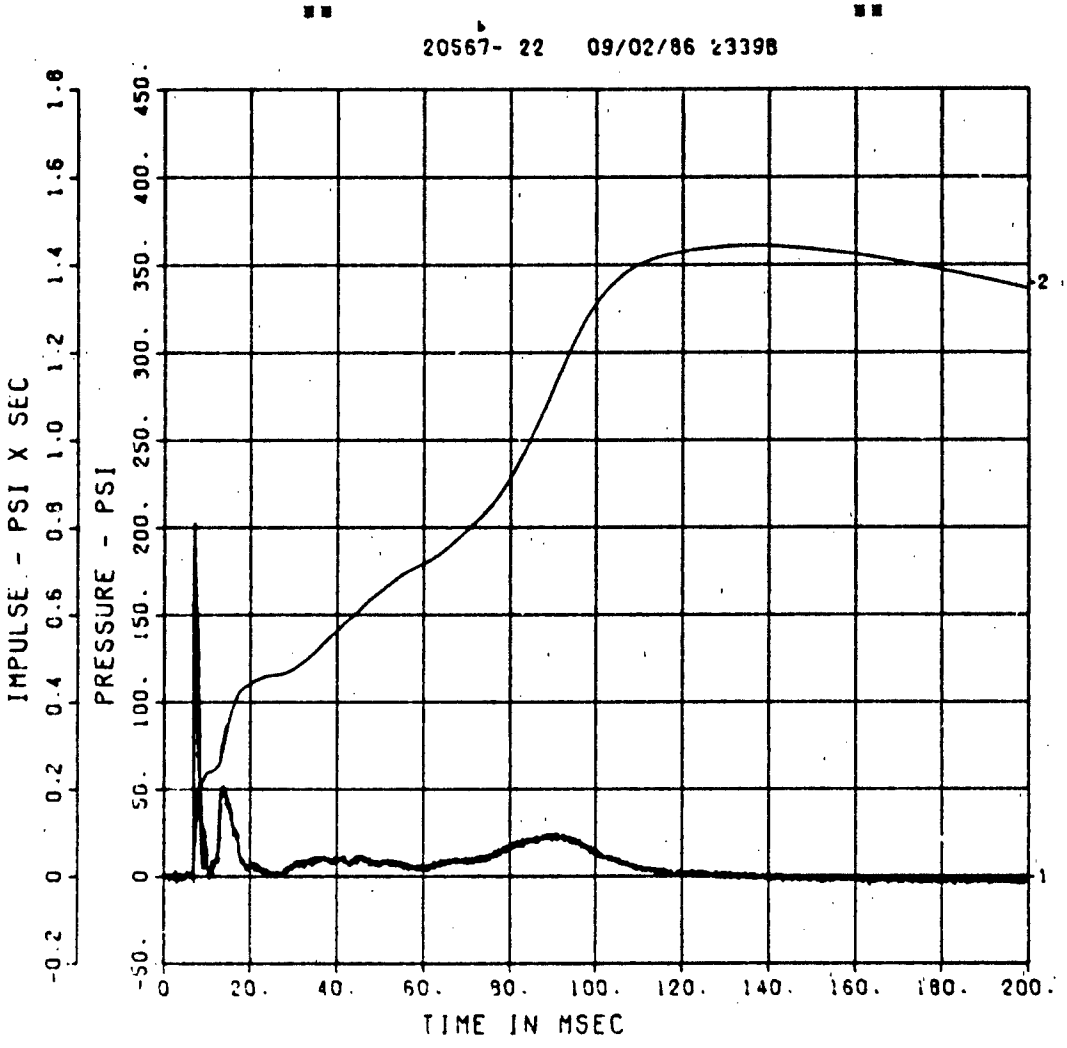

FEMA KEYWORKER
IF-15
200000. HZ CAL= 522.3

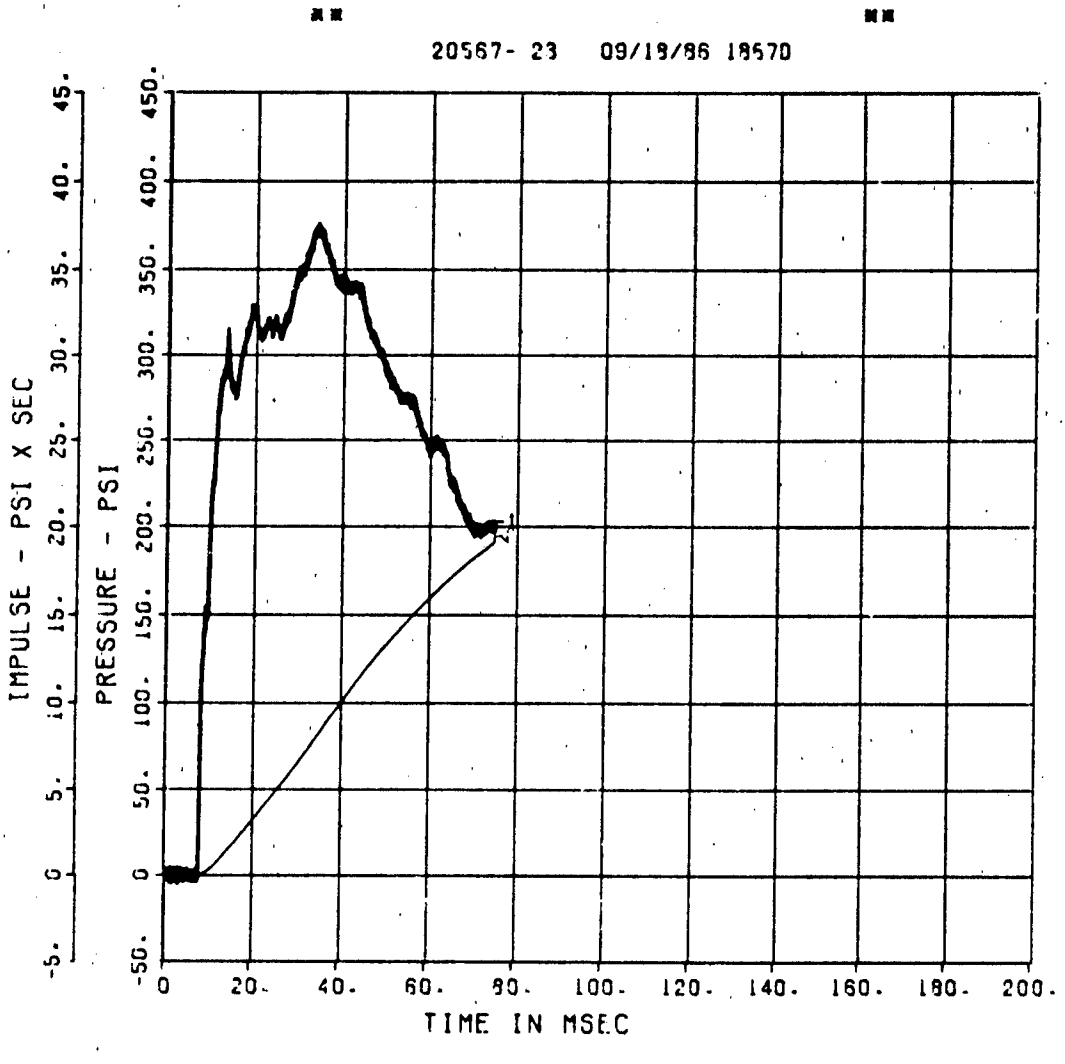

FEMA KEYWORKER
IF-16
200000. HZ CAL= 249.1

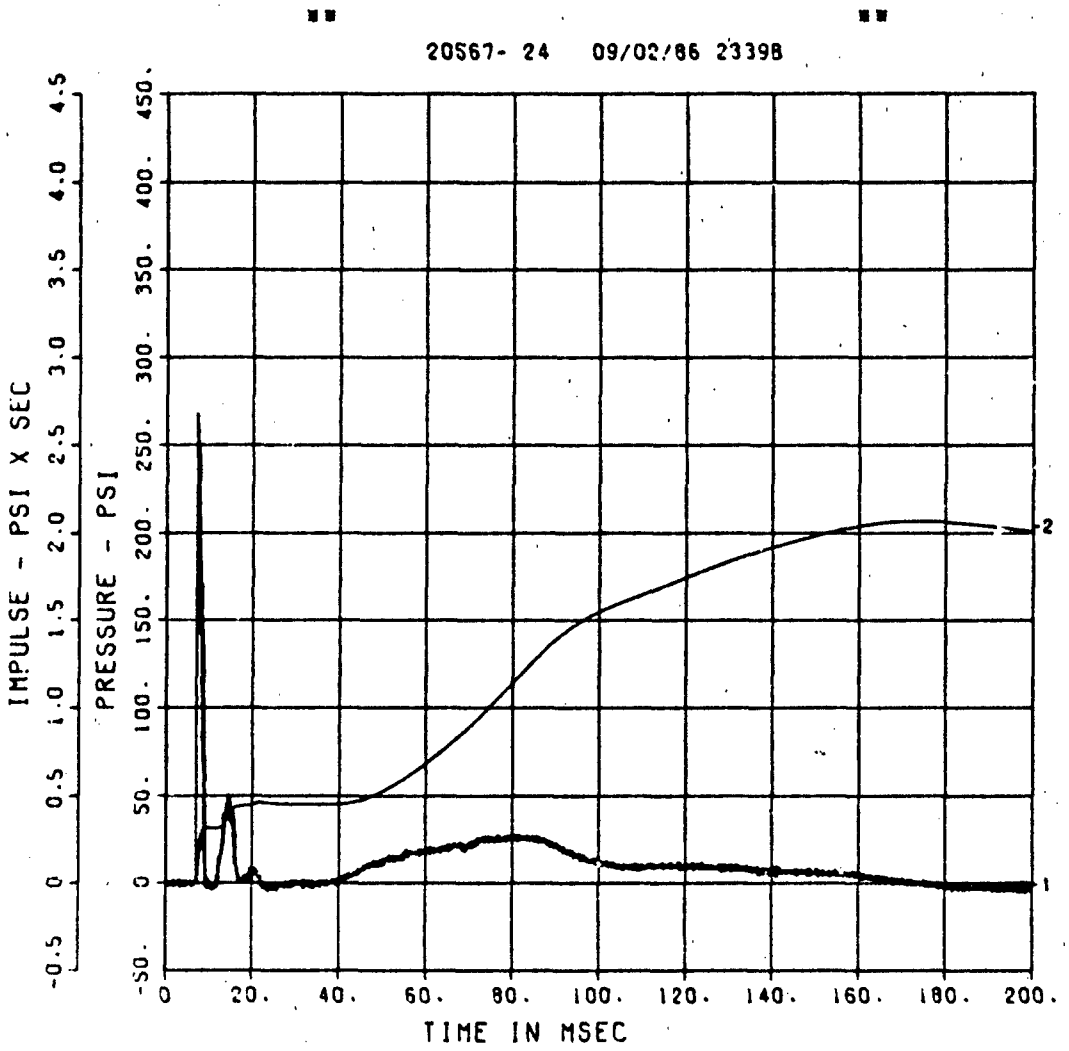

FEMA KEYWORKER
IF-17
200000. HZ CAL= 588.7

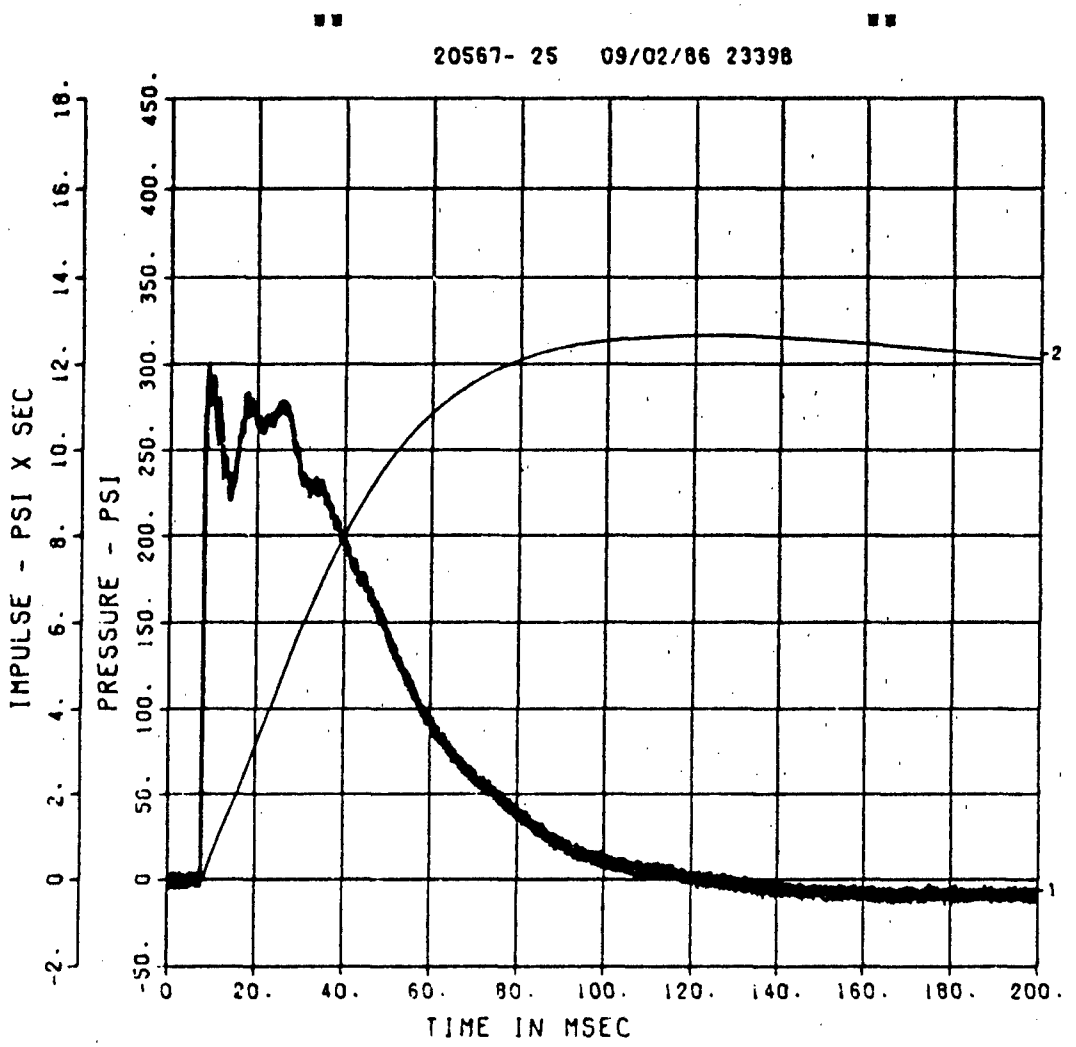

FEMA KEYWORKER
IF-18
200000. HZ CAL= 222.7

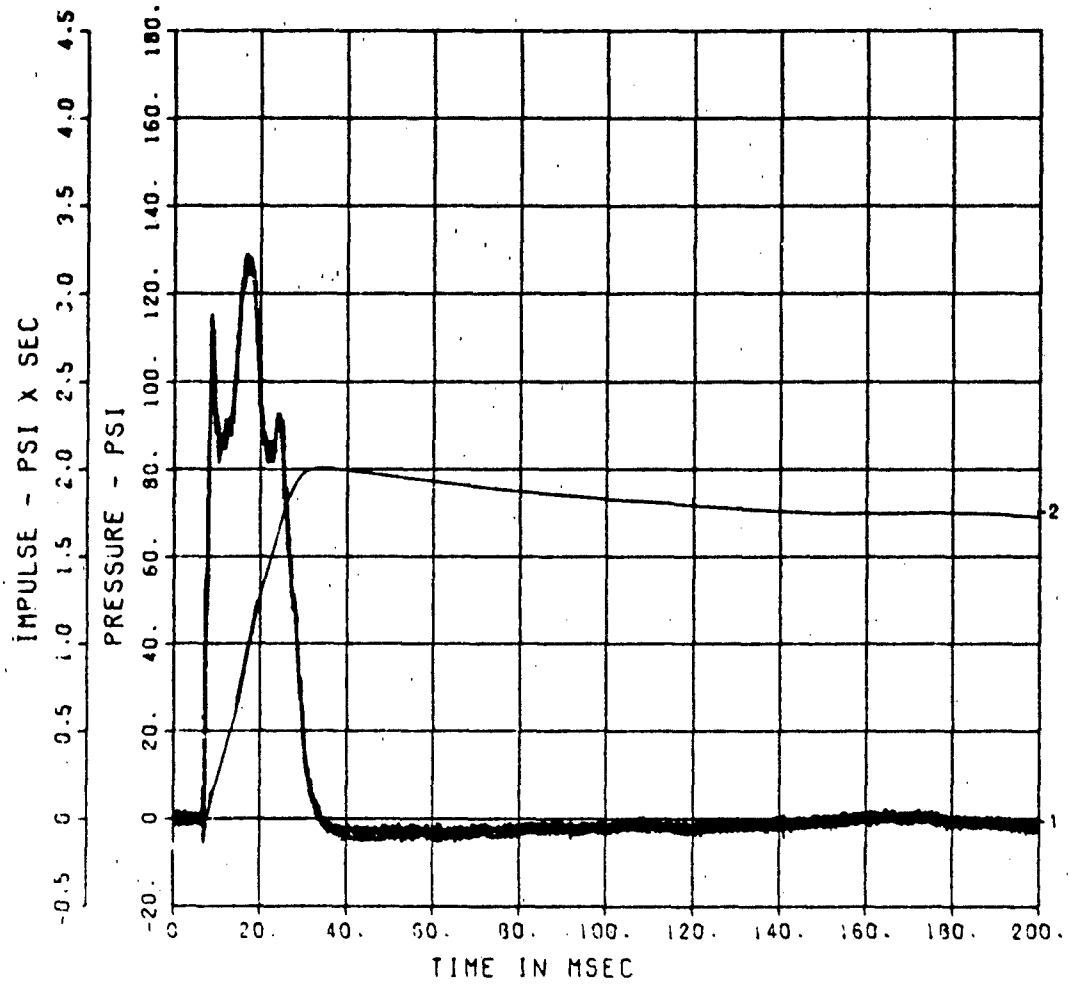

FEMA KEYWORKER
IF-19
200000. HZ CAL= 184.9

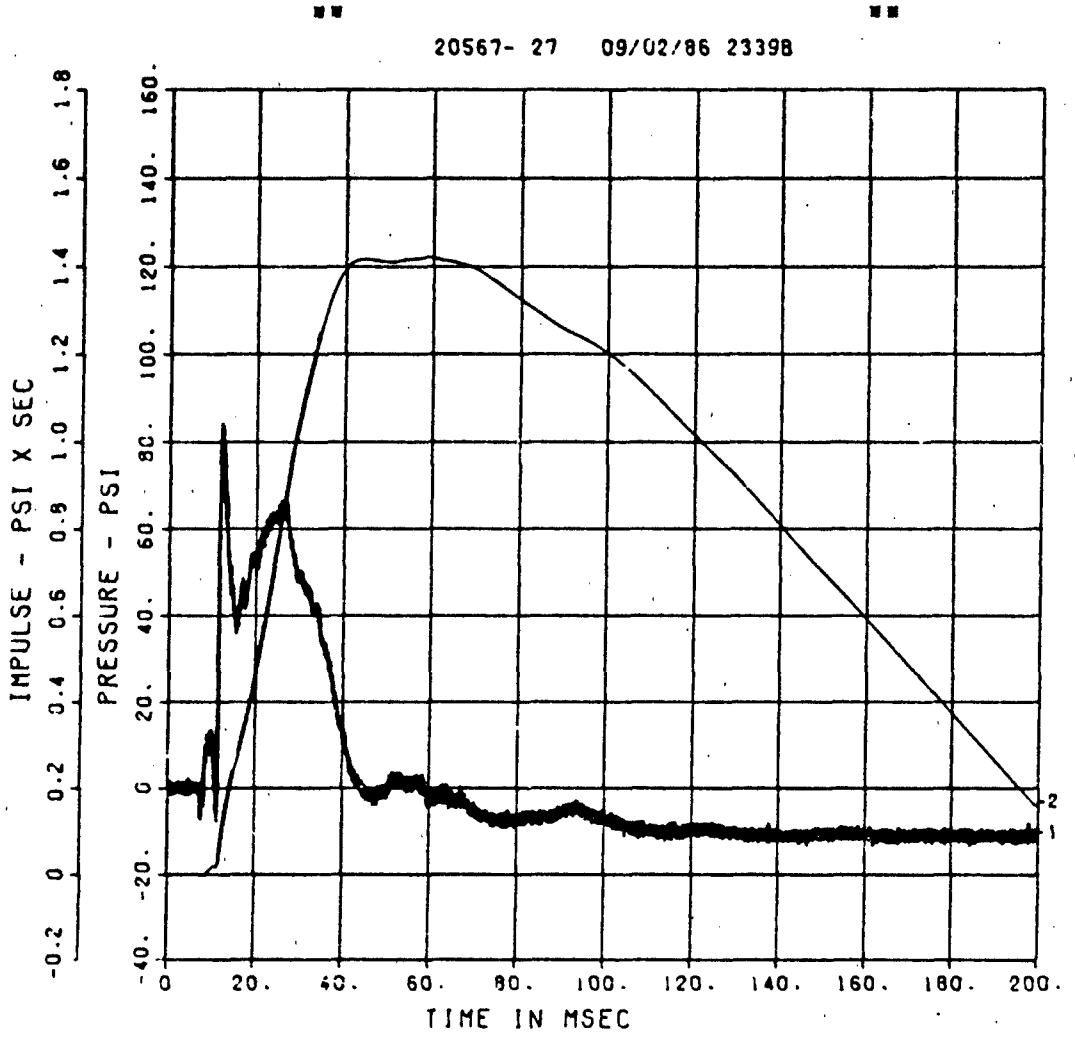

FEMA KEYWORKER
IF-20
200000. HZ CAL= 150.5

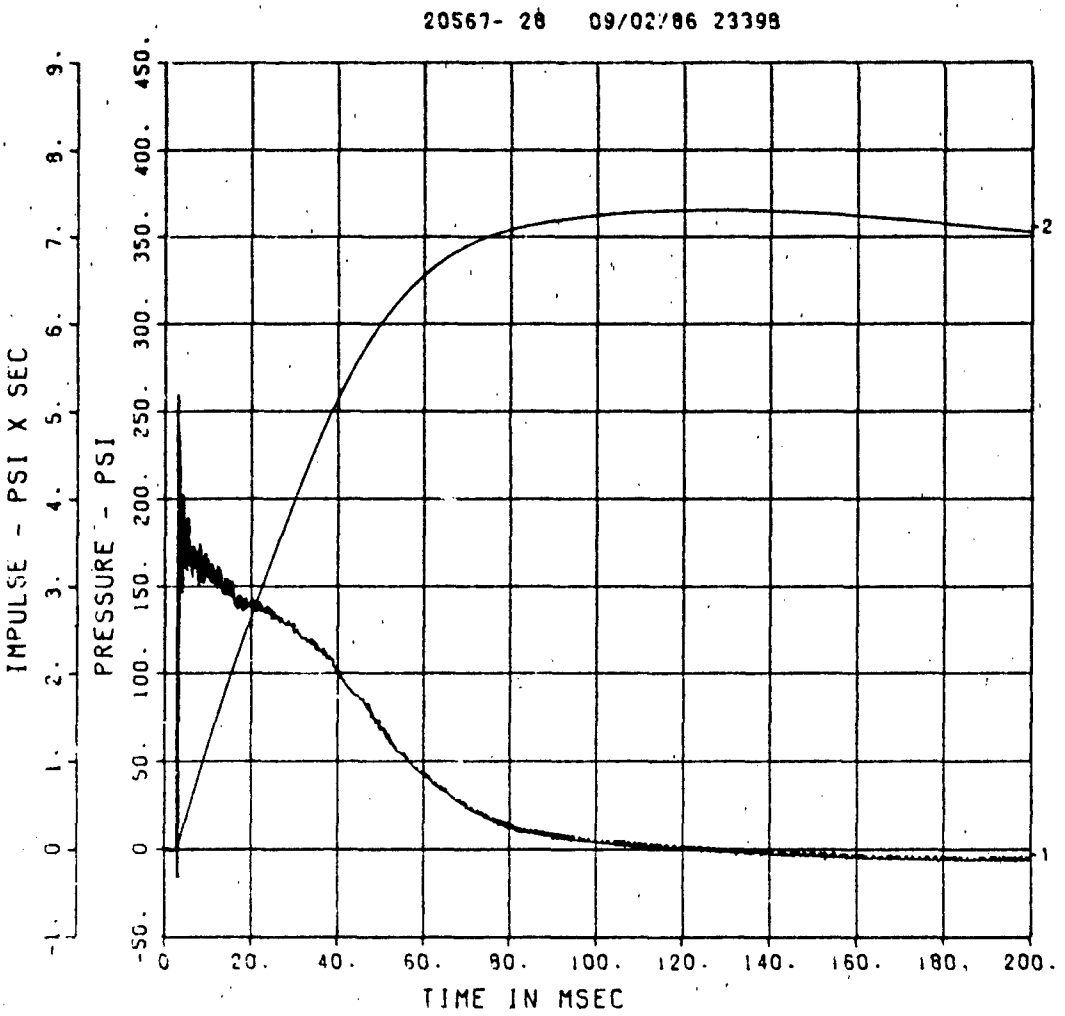

FEMA KEYWORKER
SE-1
200000. HZ CAL= 335.3

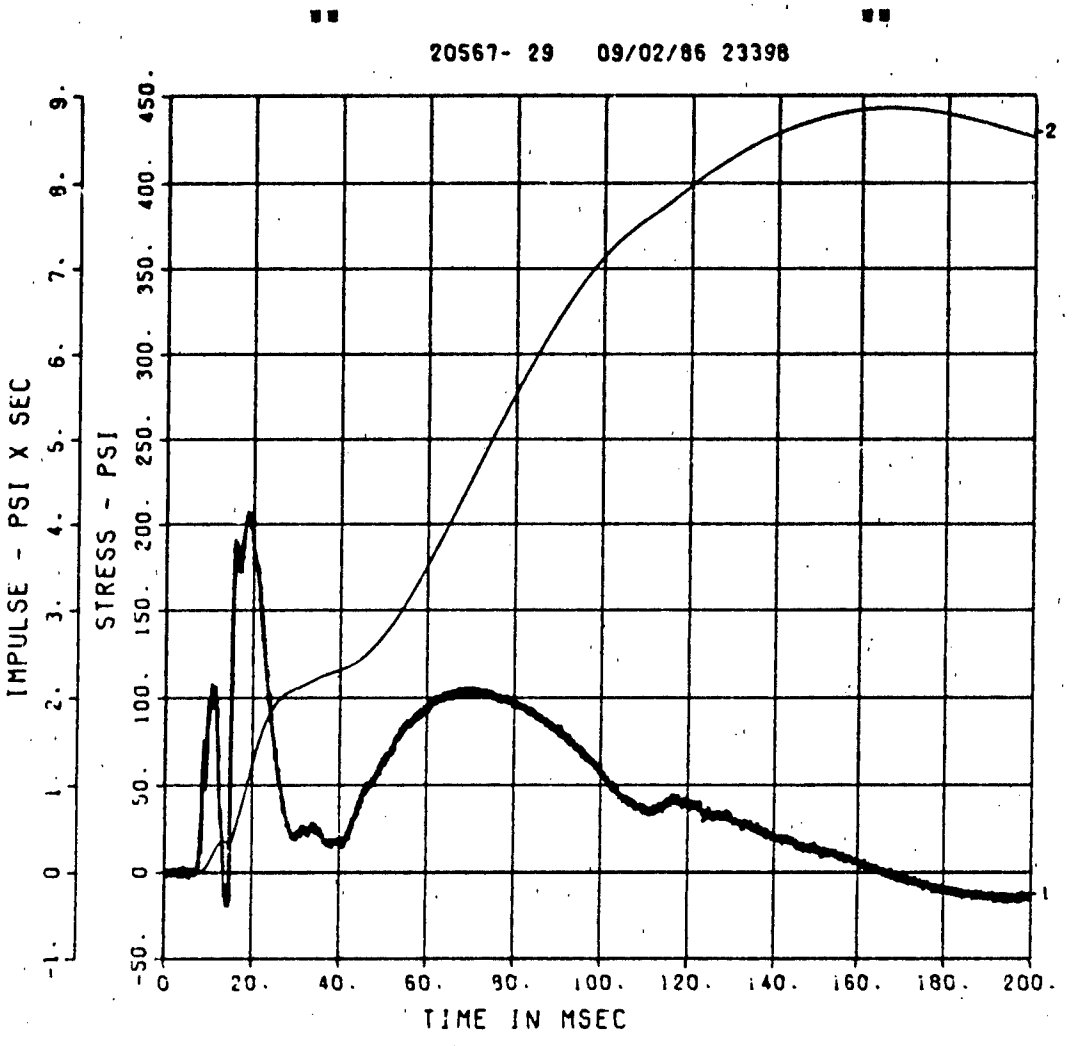

FEMA KEYWORKER
SE-2
200000. HZ CAL= 317.0

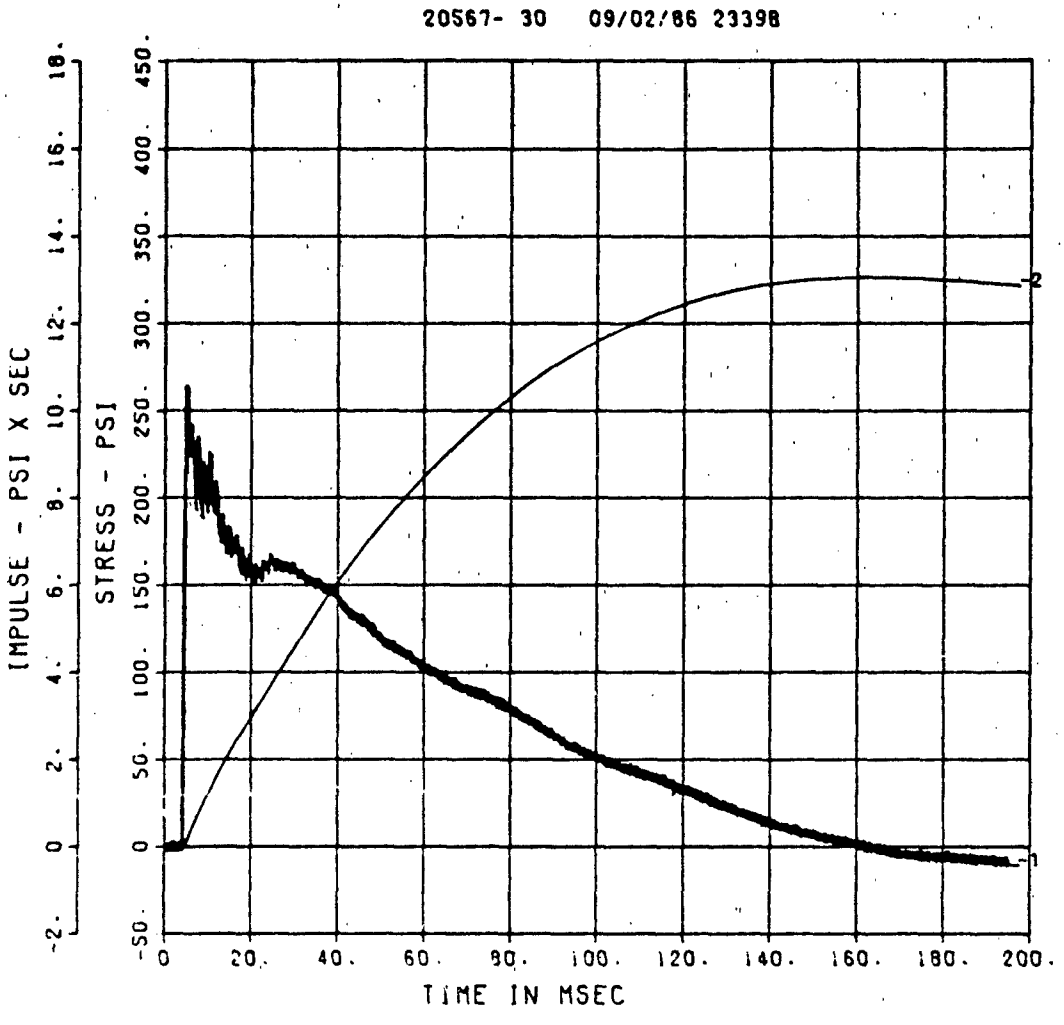

FEMA KEYWORKER
SE-3
200000. HZ CAL= 348.4

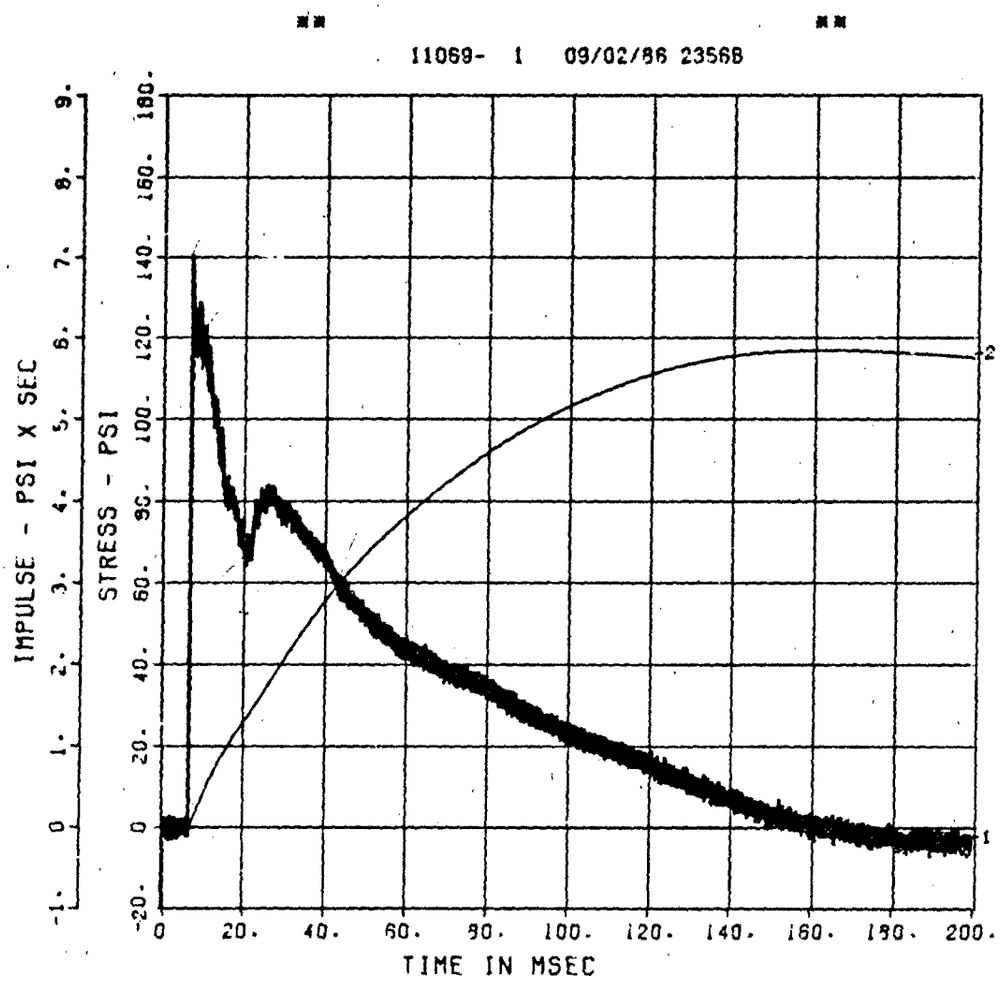

FEMA KEYWORKER
SE-4
200000. HZ CAL= 344.9

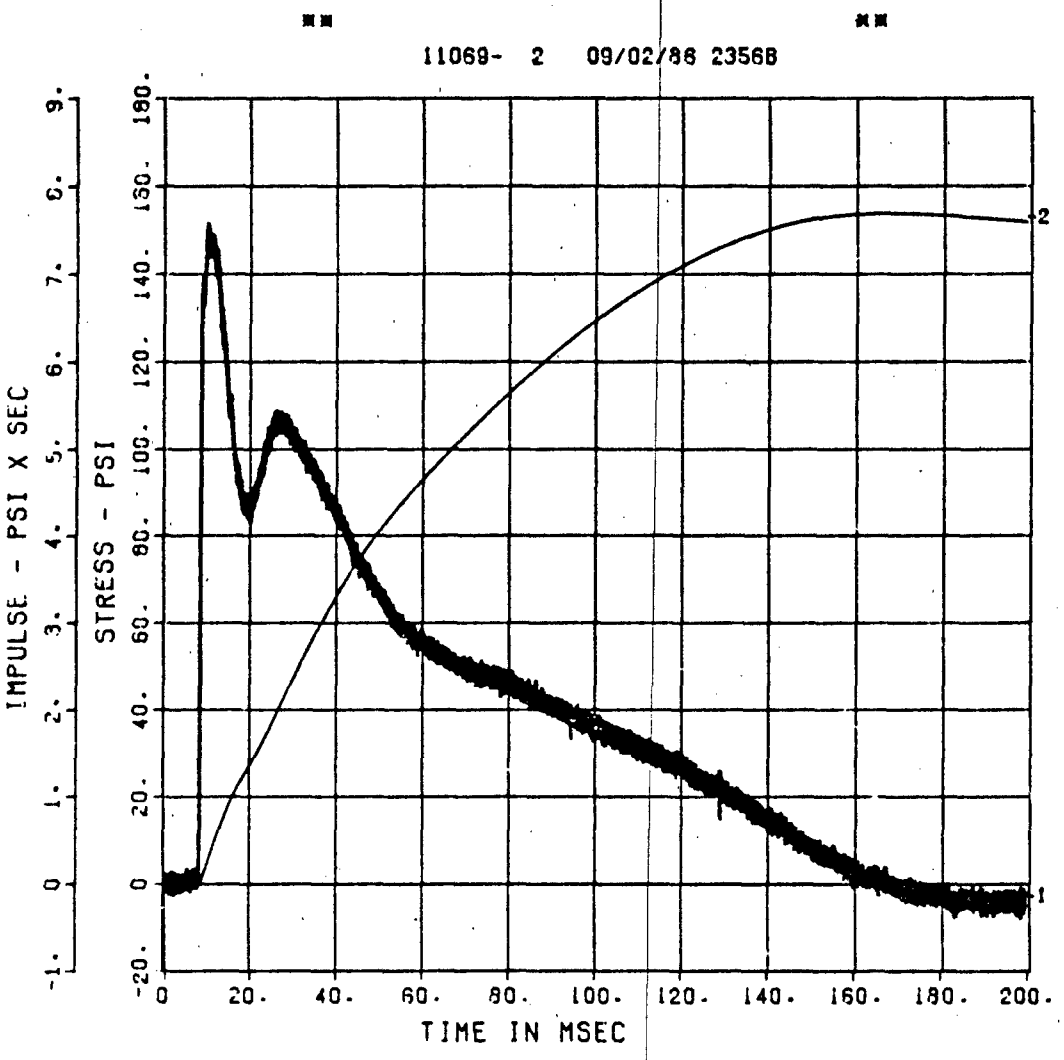

FEMA KEYWORKER
SE-5
200000. HZ CAL= 316.4

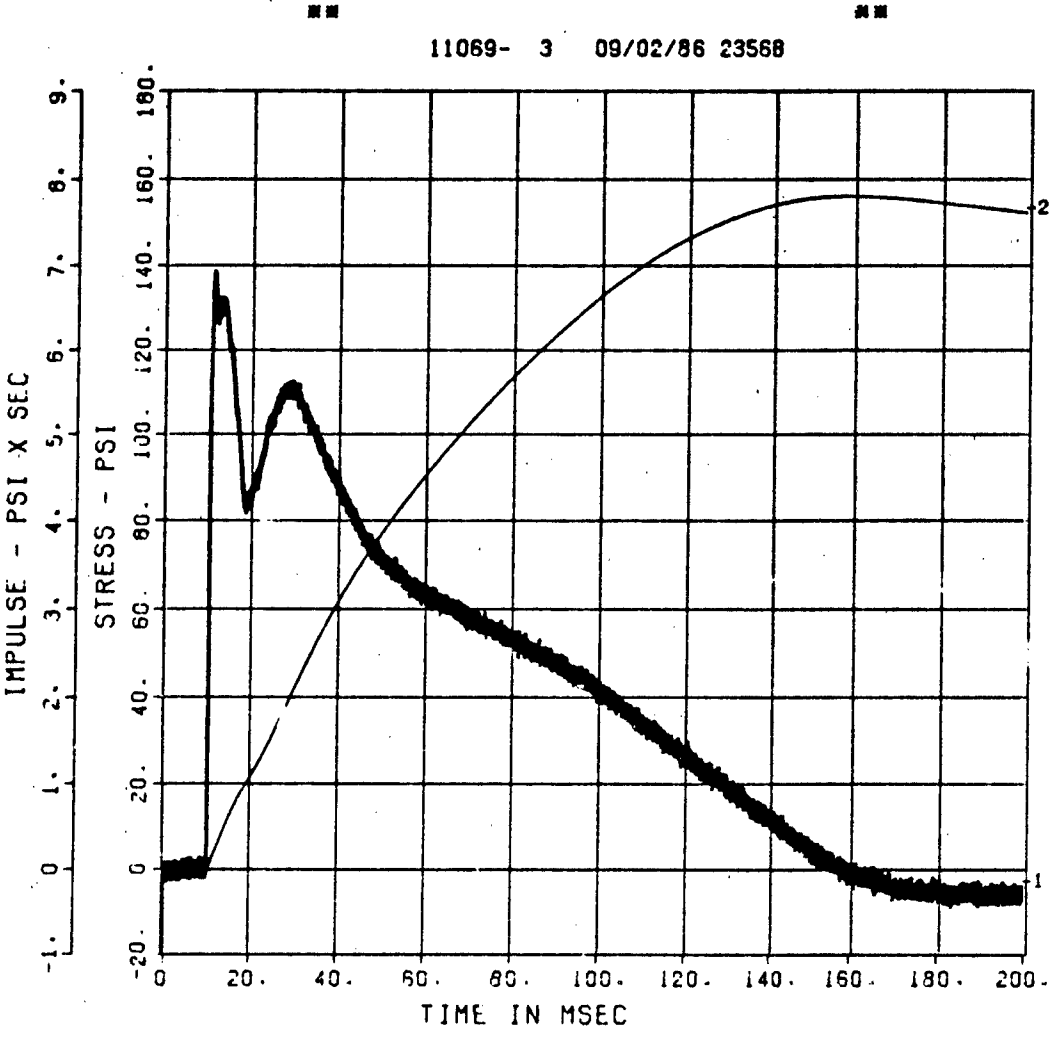

FEMA KEYWORKER
SE-6
200000. HZ CAL= 318.8

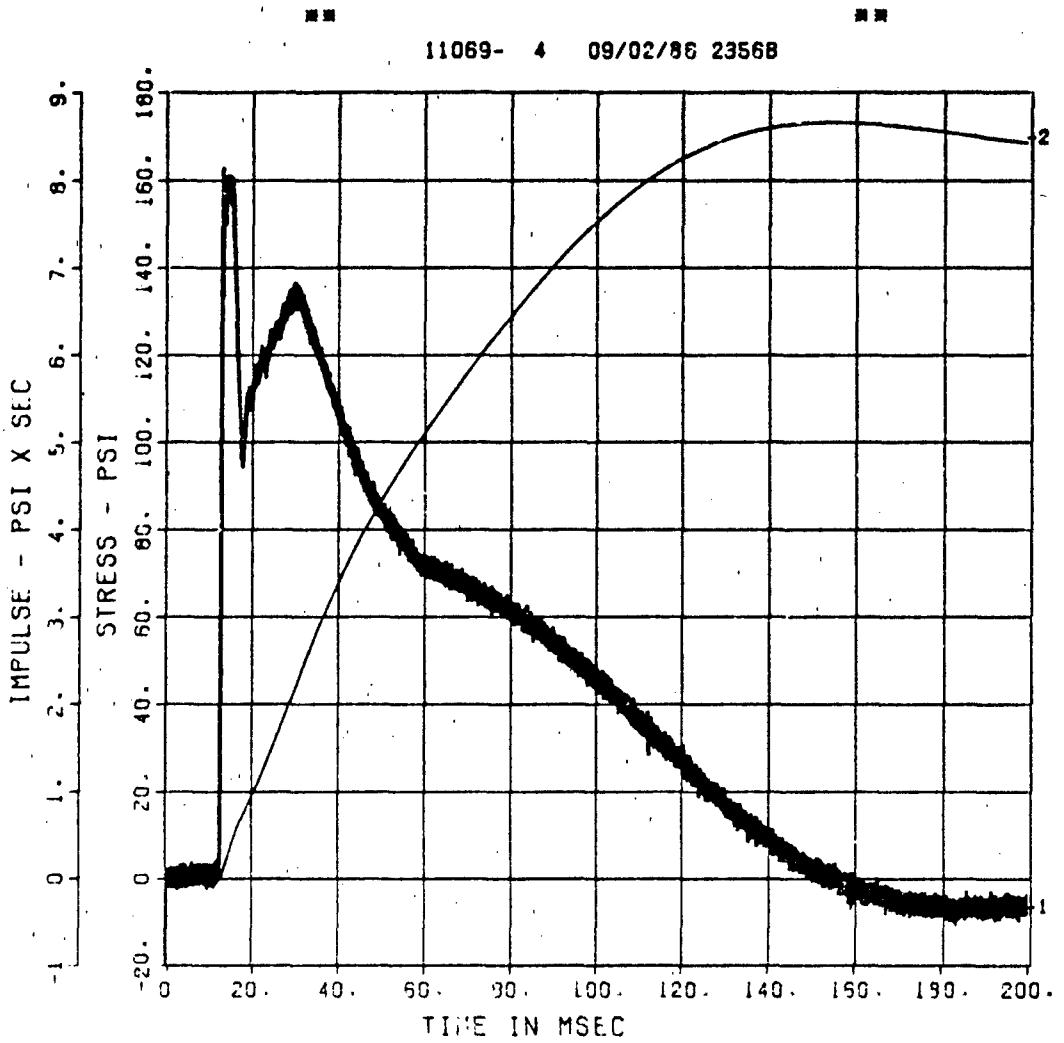

FEMA KEYWORKER
SE-7
200000. HZ CAL= 241.2
LP4/0 70% CUTOFF= 9000. HZ

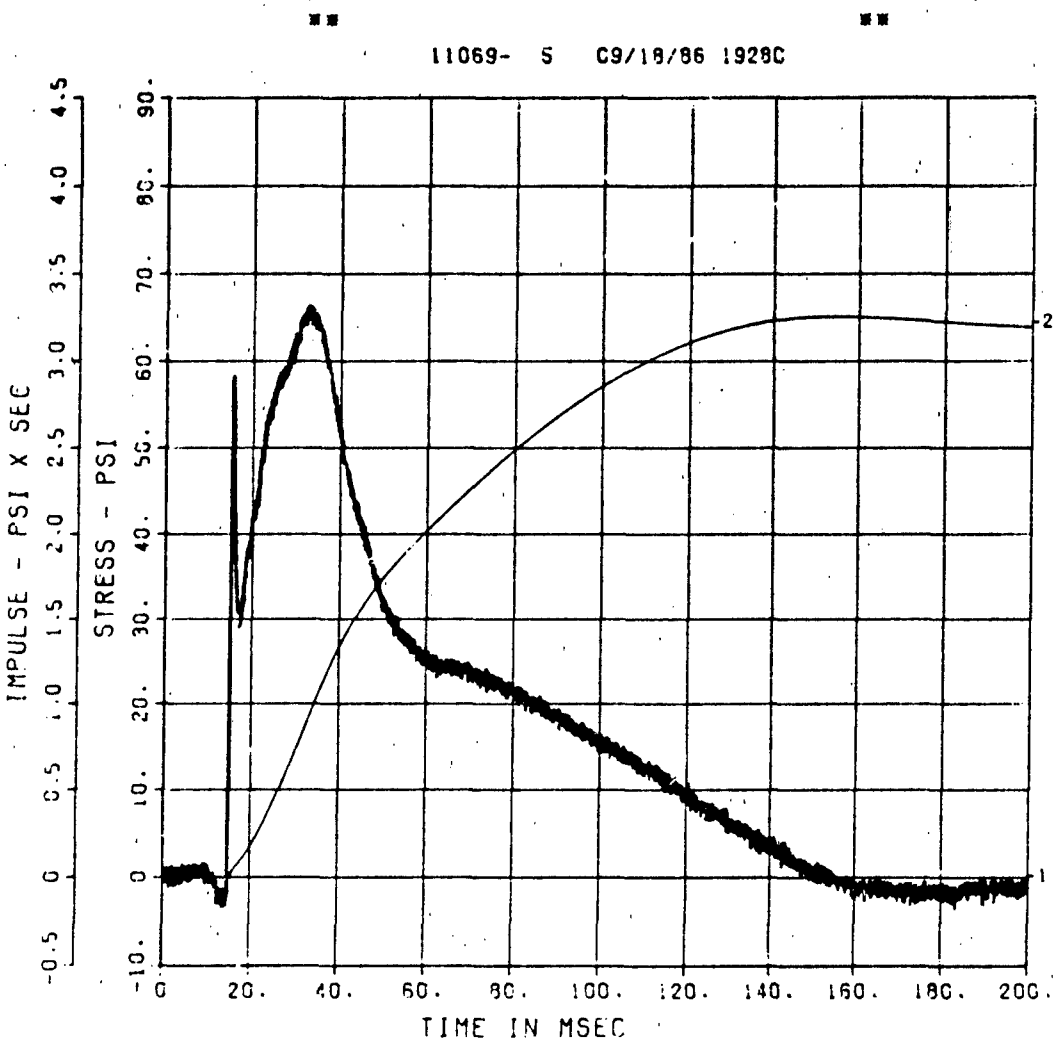

FEMA KEYWORKER
SE-8
200000. HZ CAL= 318.6

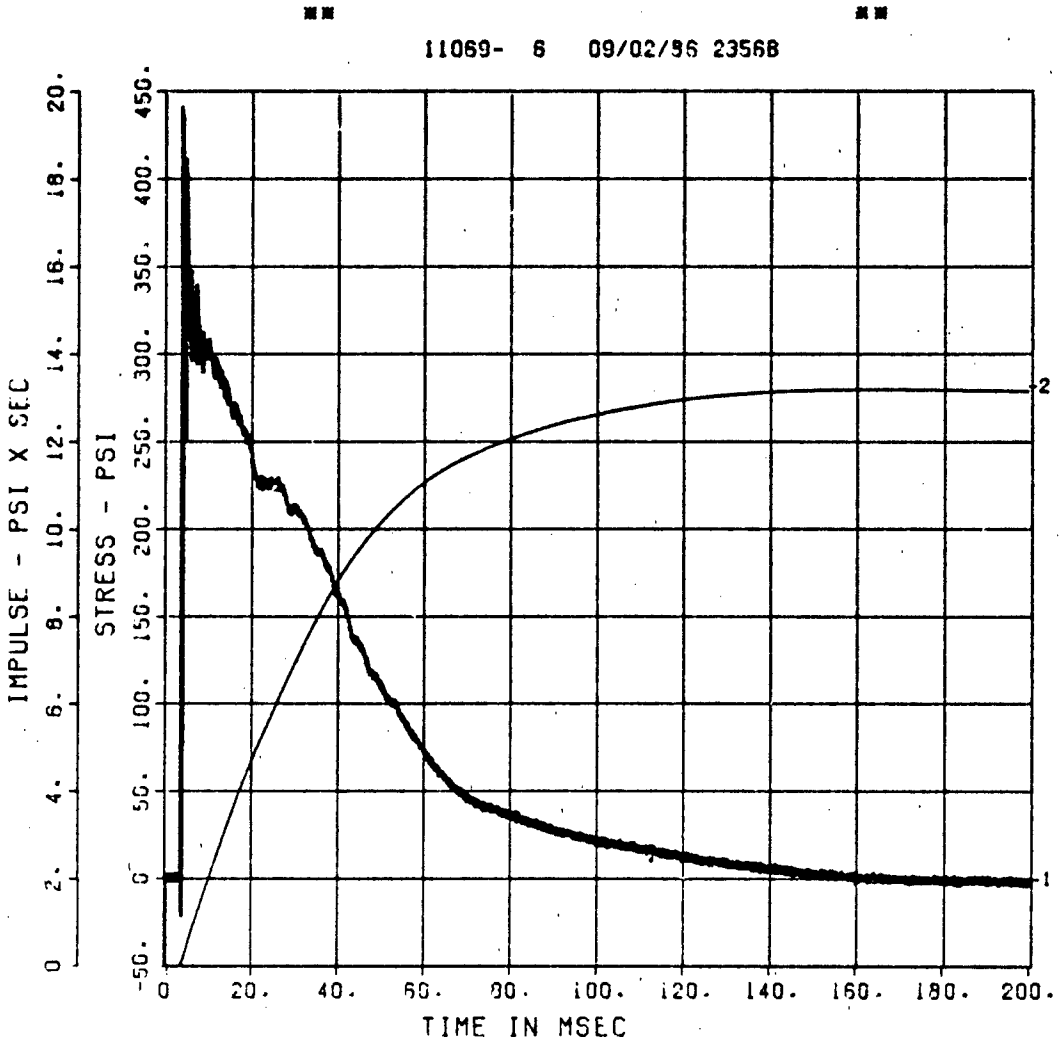

FEMA KEYWORKER
SE-9
200000. HZ CAL= 295.0

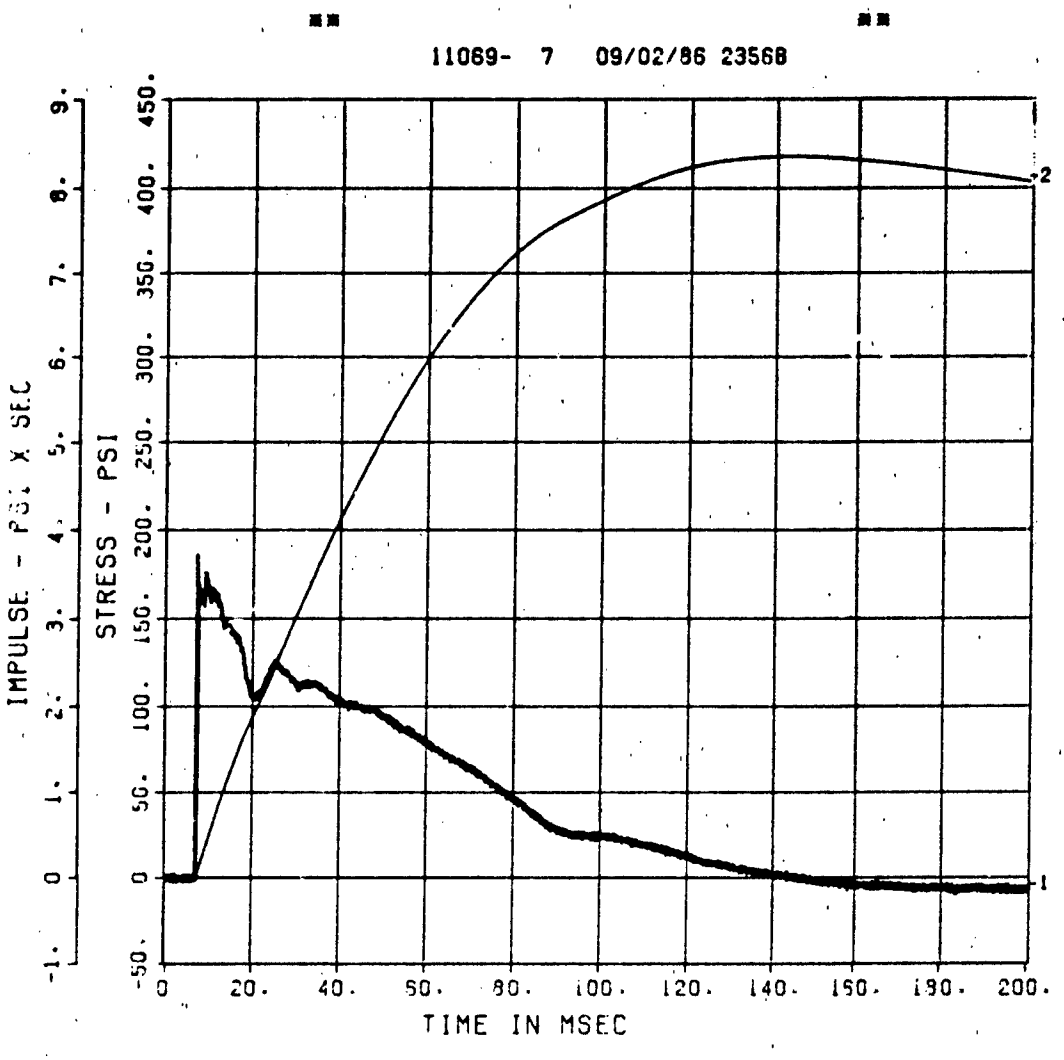

FEMA KEYWORKER
SE-10
200000. HZ CAL= 326.2

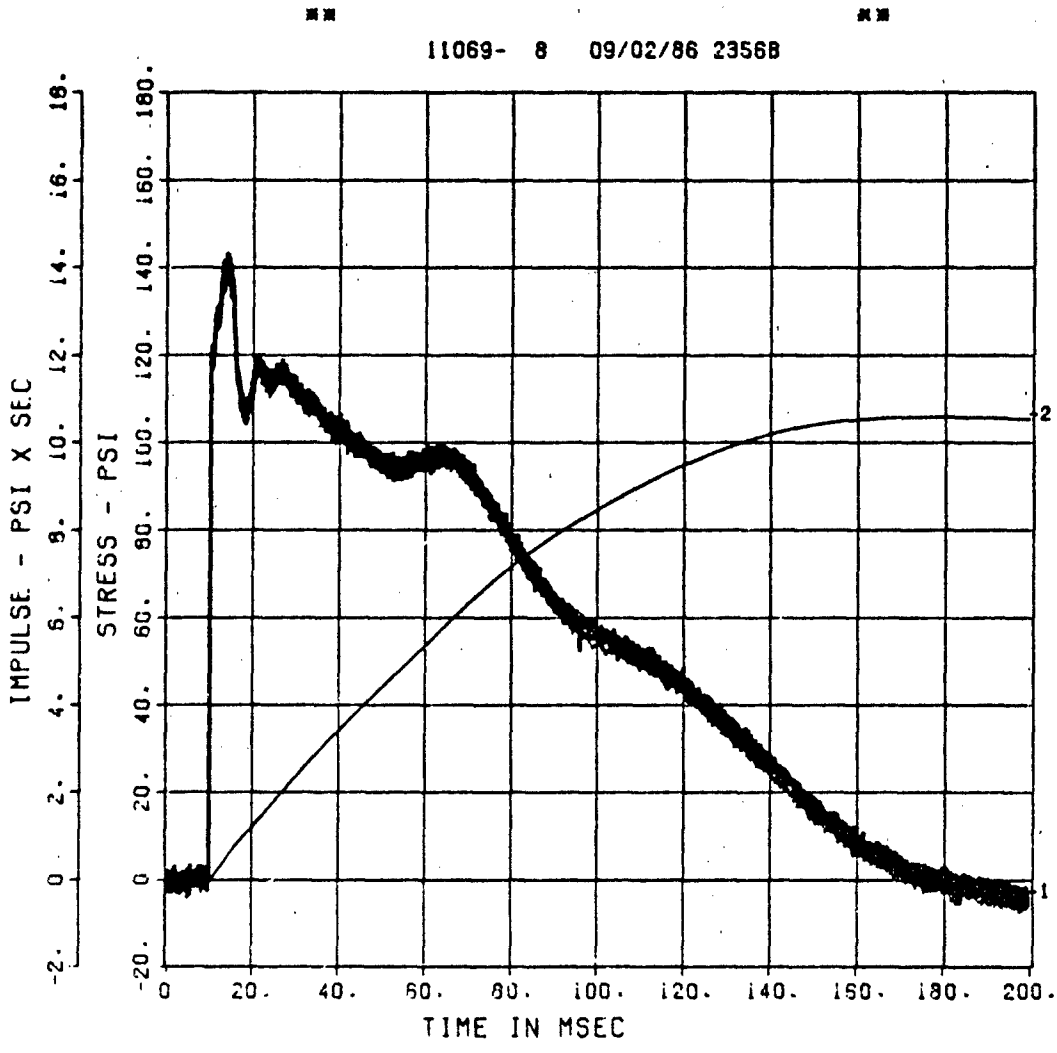

FEMA KEYWORKER
SE-11
200000. HZ CAL= 335.4

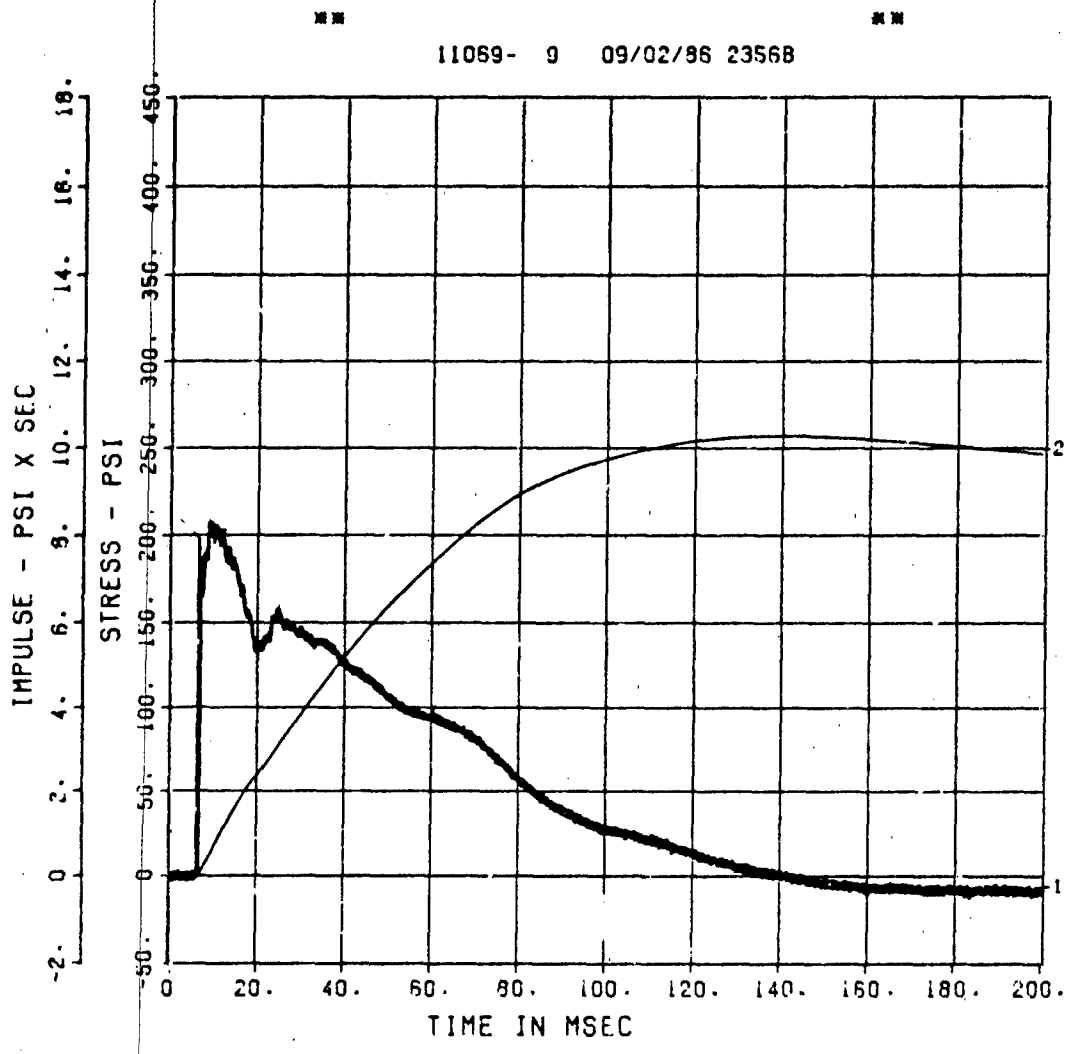

FEMA KEYWORKER
DW-1
50000. HZ CAL= 10.70
LP4/4 70% CUTOFF= 2250. HZ

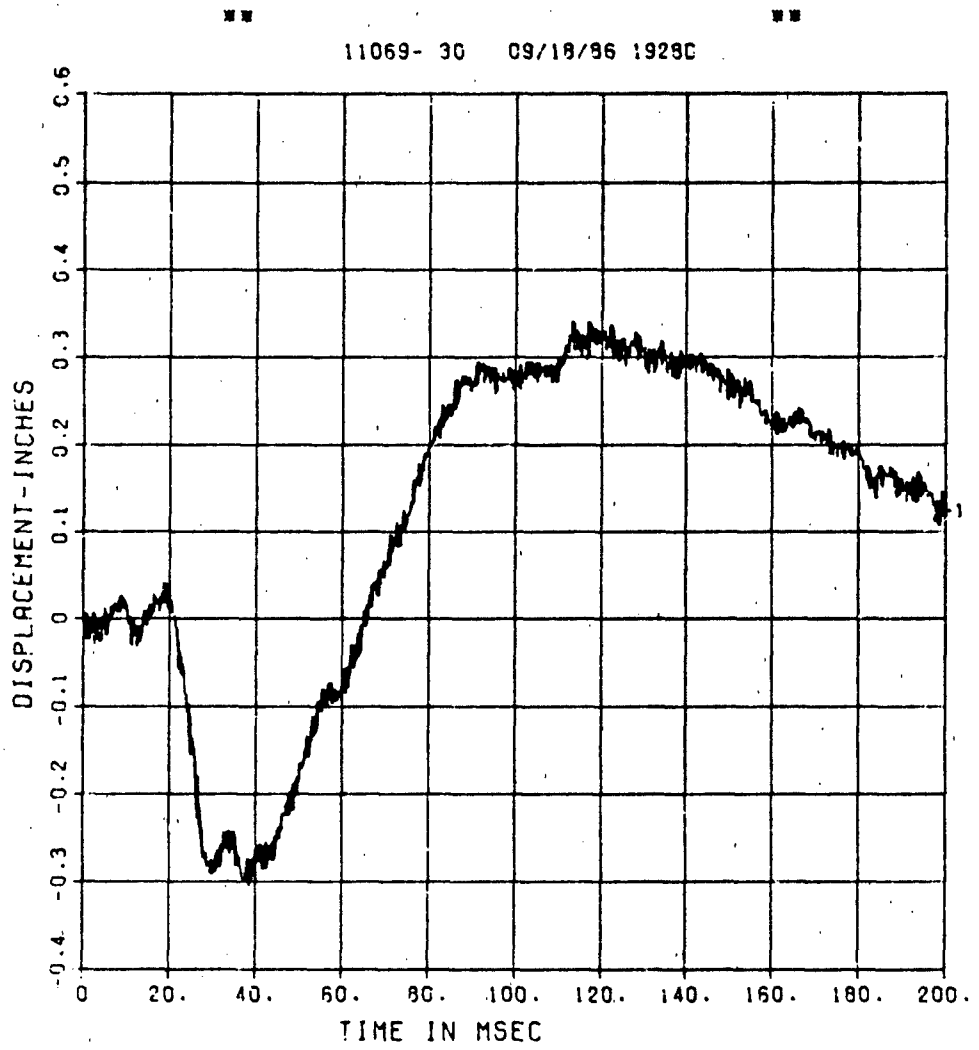

FEMA KEYWORKER
D-2
200000. HZ CAL= 10.80

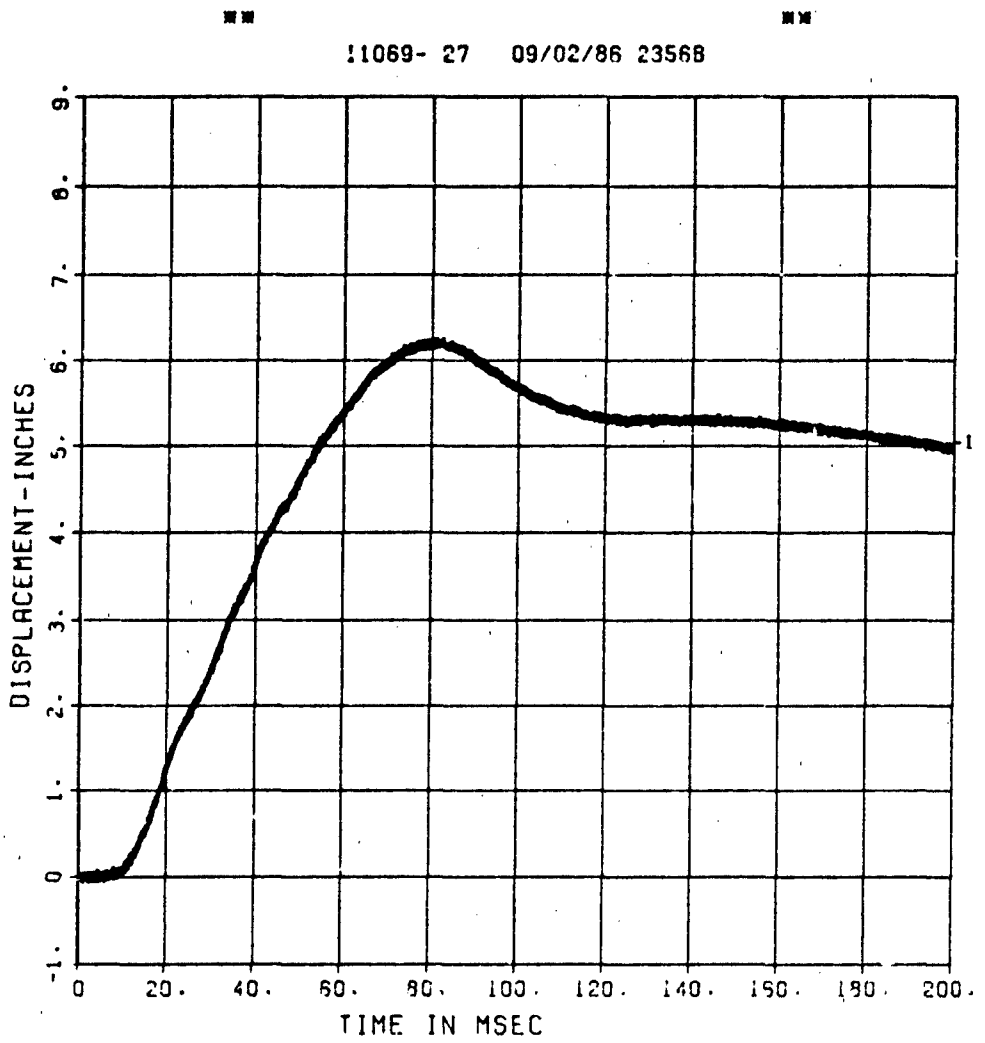

FEMA KEYWORKER
D-3
200000. HZ CAL= 10.70

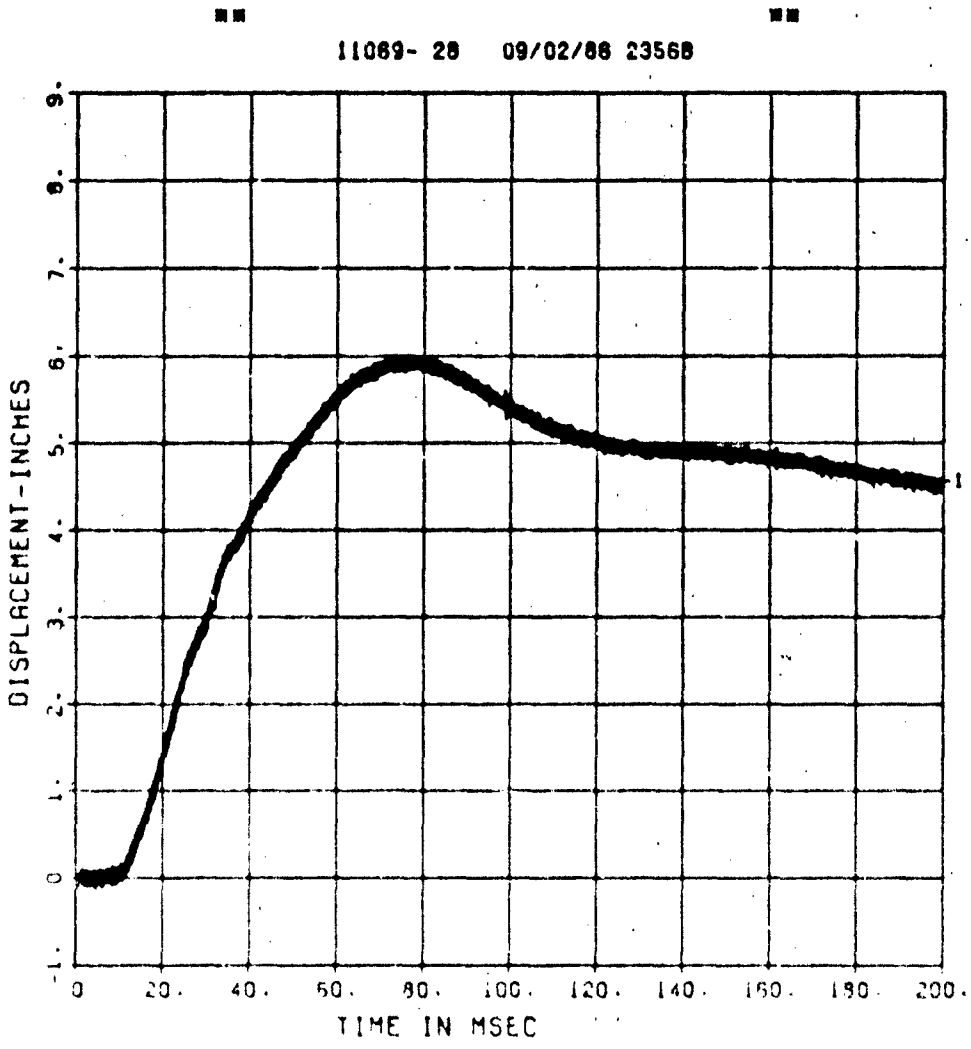

FEMA KEYWORKER
D-4
200000. HZ CAL= 10.70

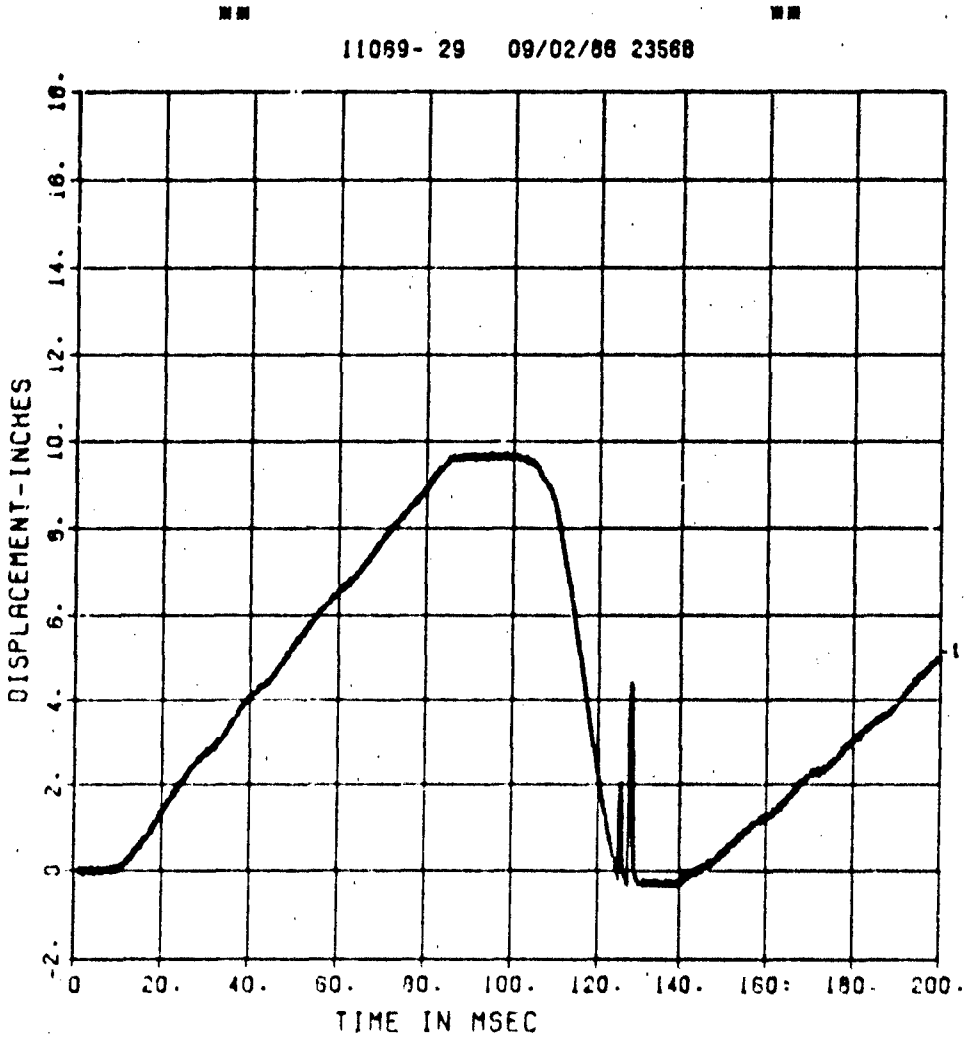

FEMA KEYWORKER
AR-1
50000. HZ CAL= 1363.
LP4/4 70% CUTOFF= 2250. HZ

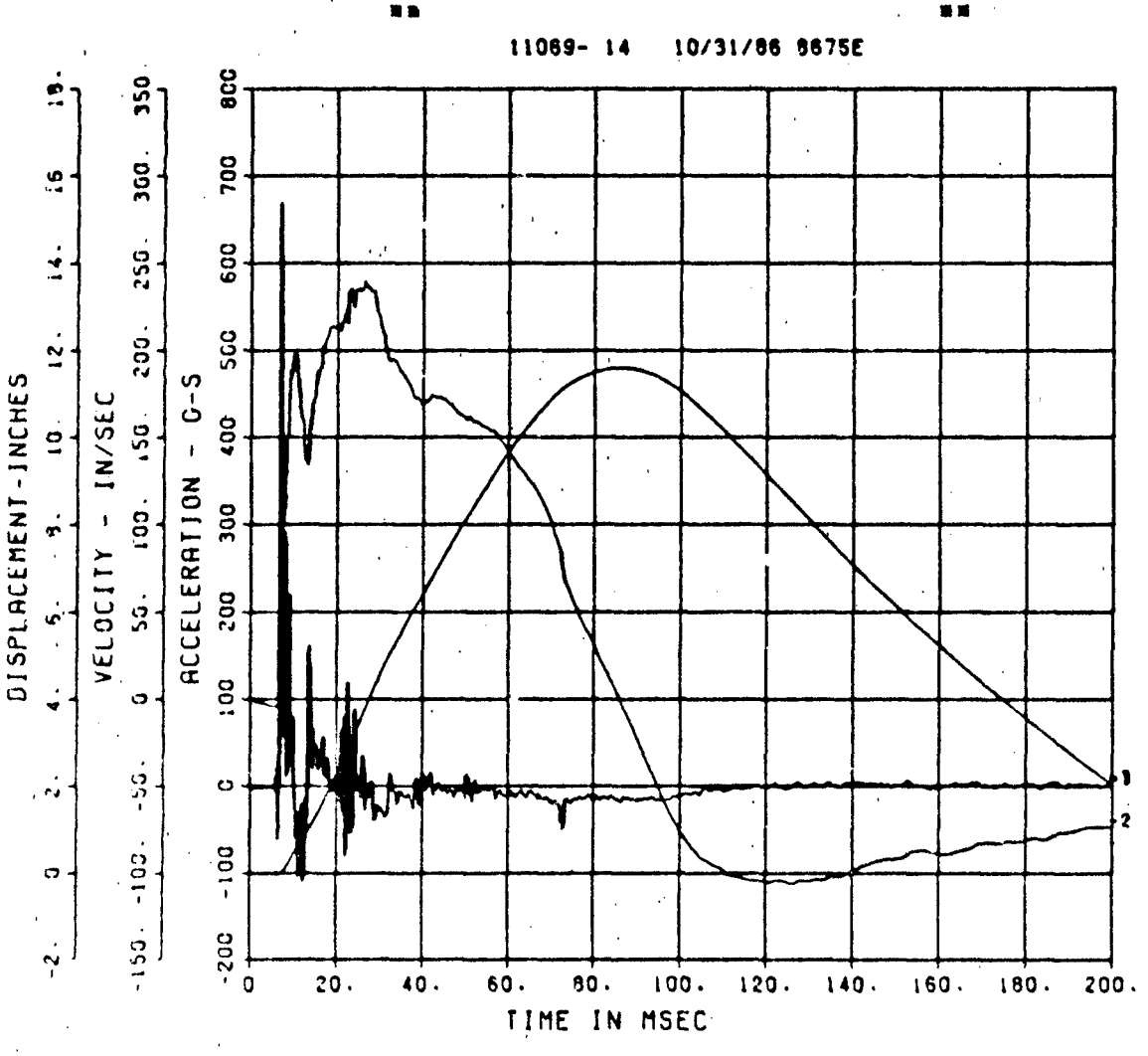

FEMA KEYWORKER
AR-2
50000. HZ CAL= 1417.
LP4/4 70% CUTOFF= 2250. HZ

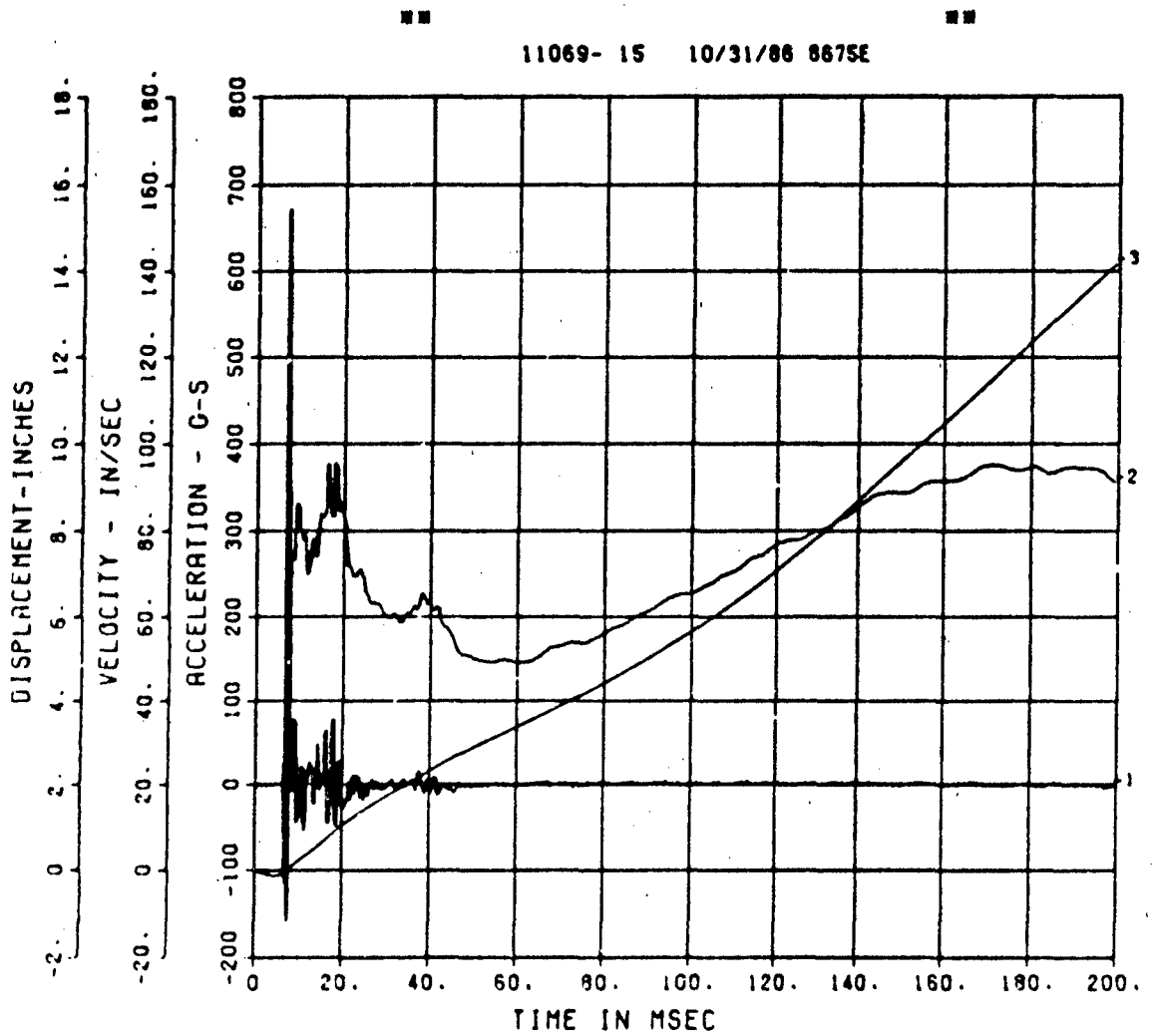

FEMA KEYWORKER
AR-3
50000. HZ CAL= 1382.
LP4/4 70% CUTOFF= 2250. HZ

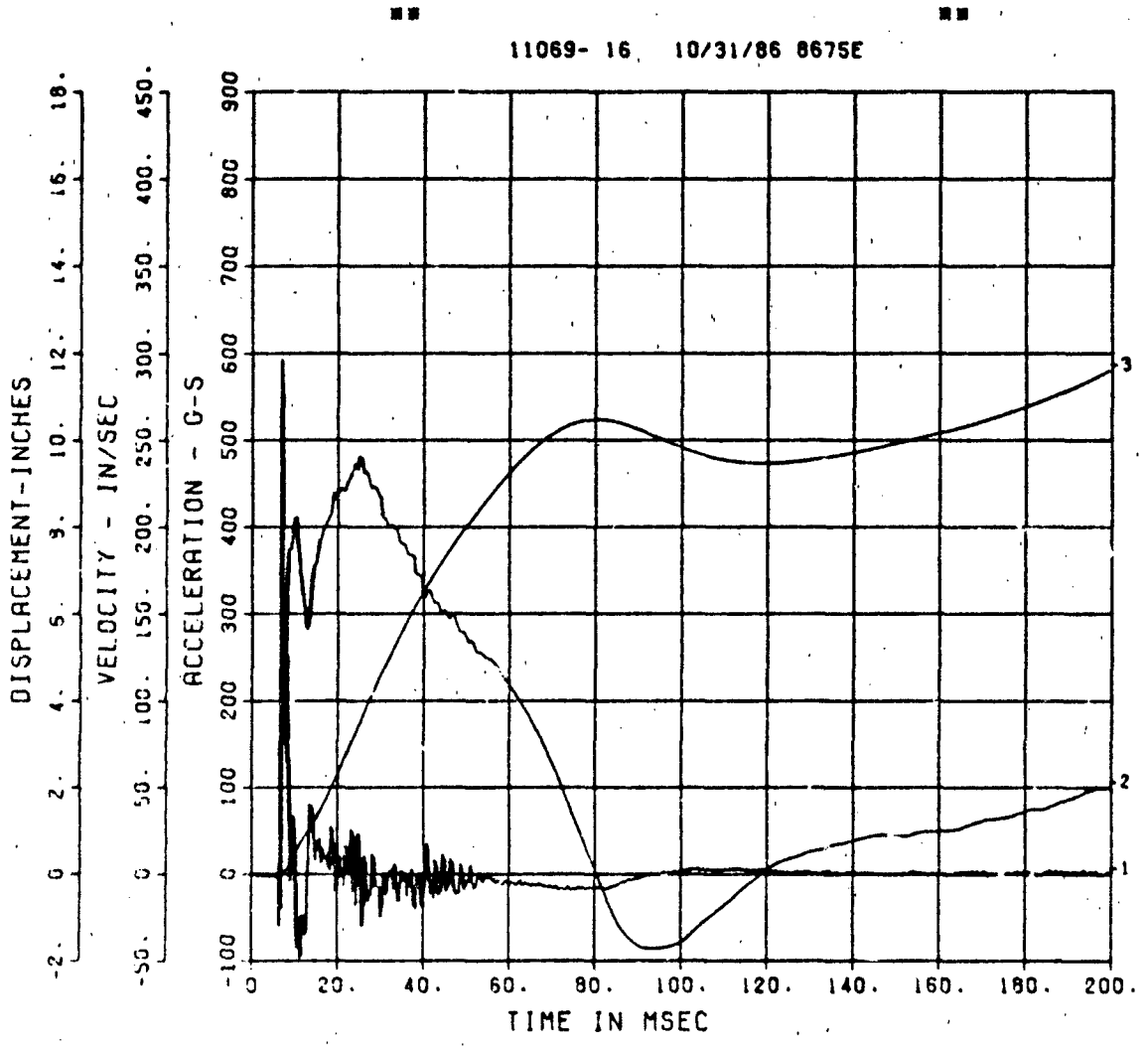

FEMA KEYWORKER
AR-4
50000. HZ CAL= 1248.
LP4/4 70% CUTOFF= 2250. HZ

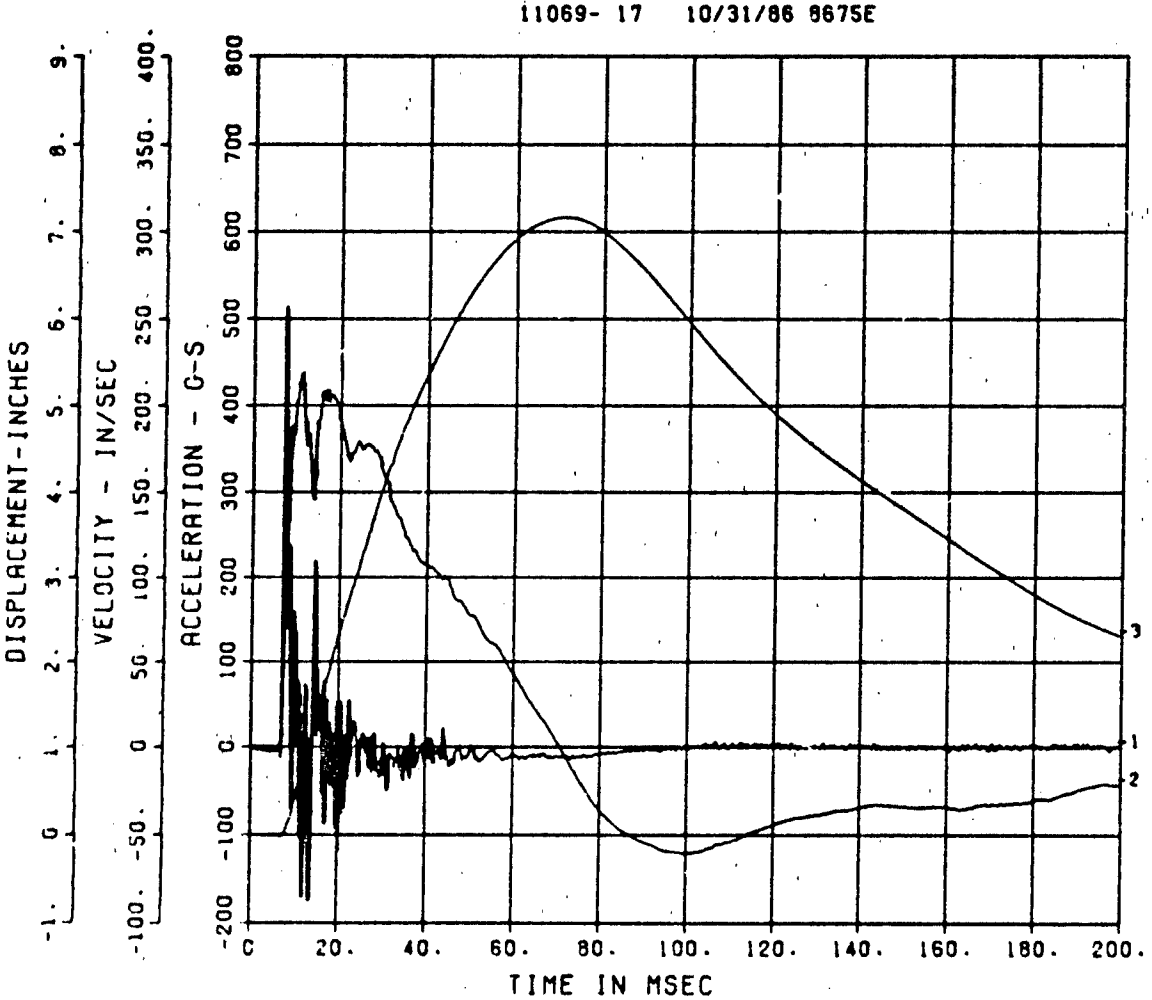

FEMA KEYWORKER
AF-1
50000. HZ CAL= 239.0
LP4/4 70% CUTOFF= 2250. HZ

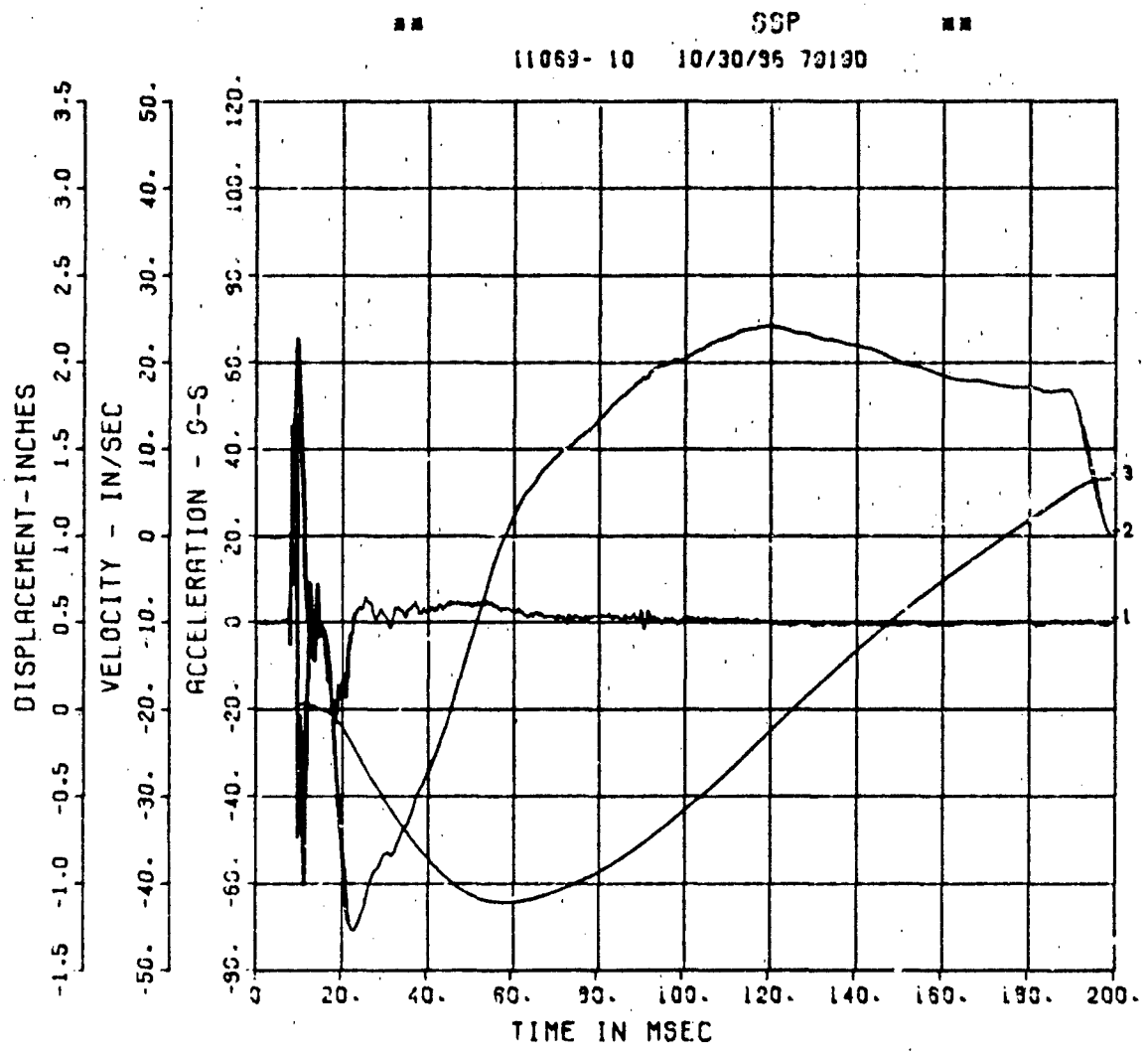

FEMA KEYWORKER
AF-2
50000. HZ CAL= 215.9
LP4/4 70% CUTOFF= 2250. HZ

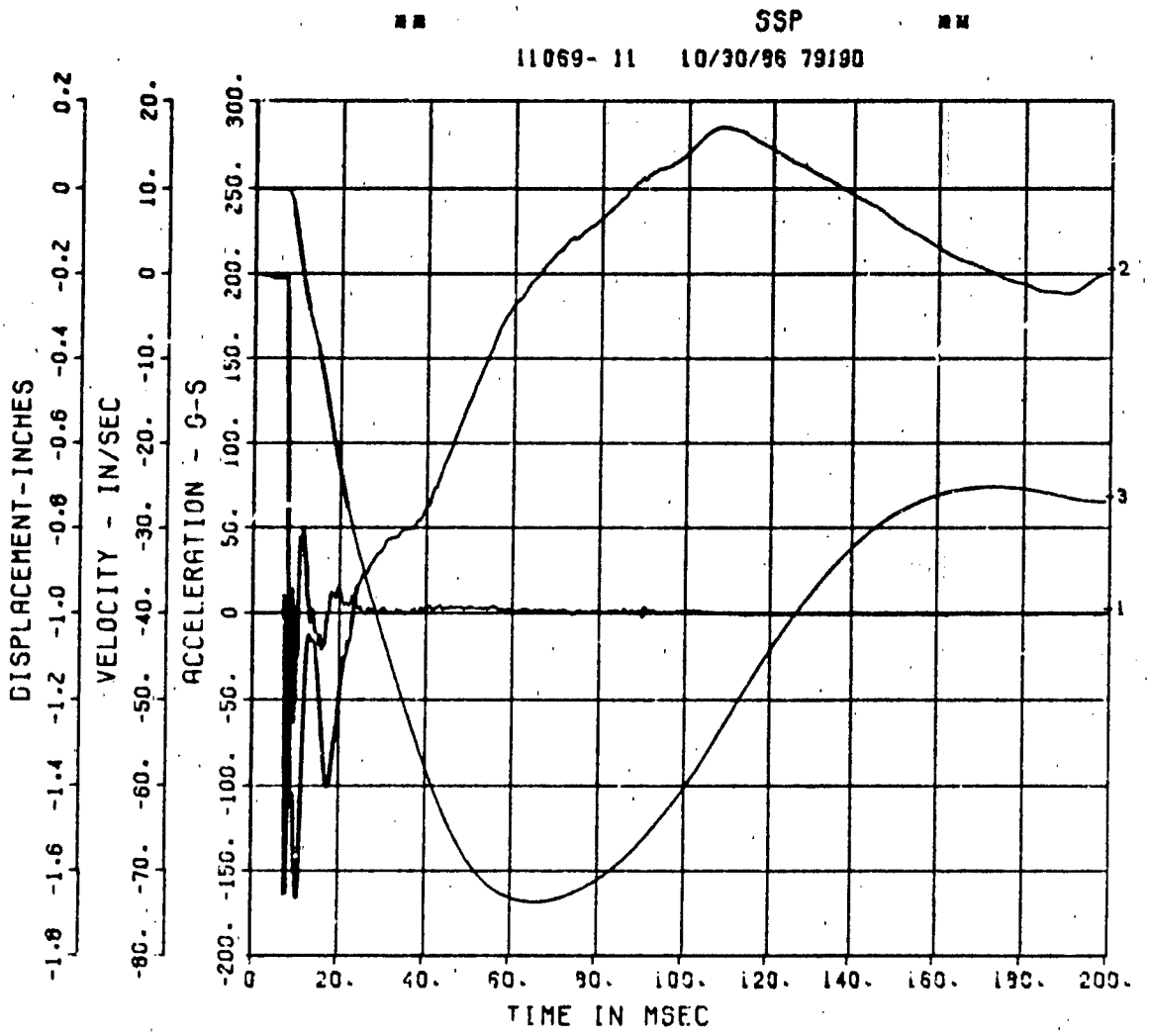

FEMA KEYWORKER
AF-3
50000. HZ CAL= 231.6
LP4/4 70% CUTOFF= 2250. HZ

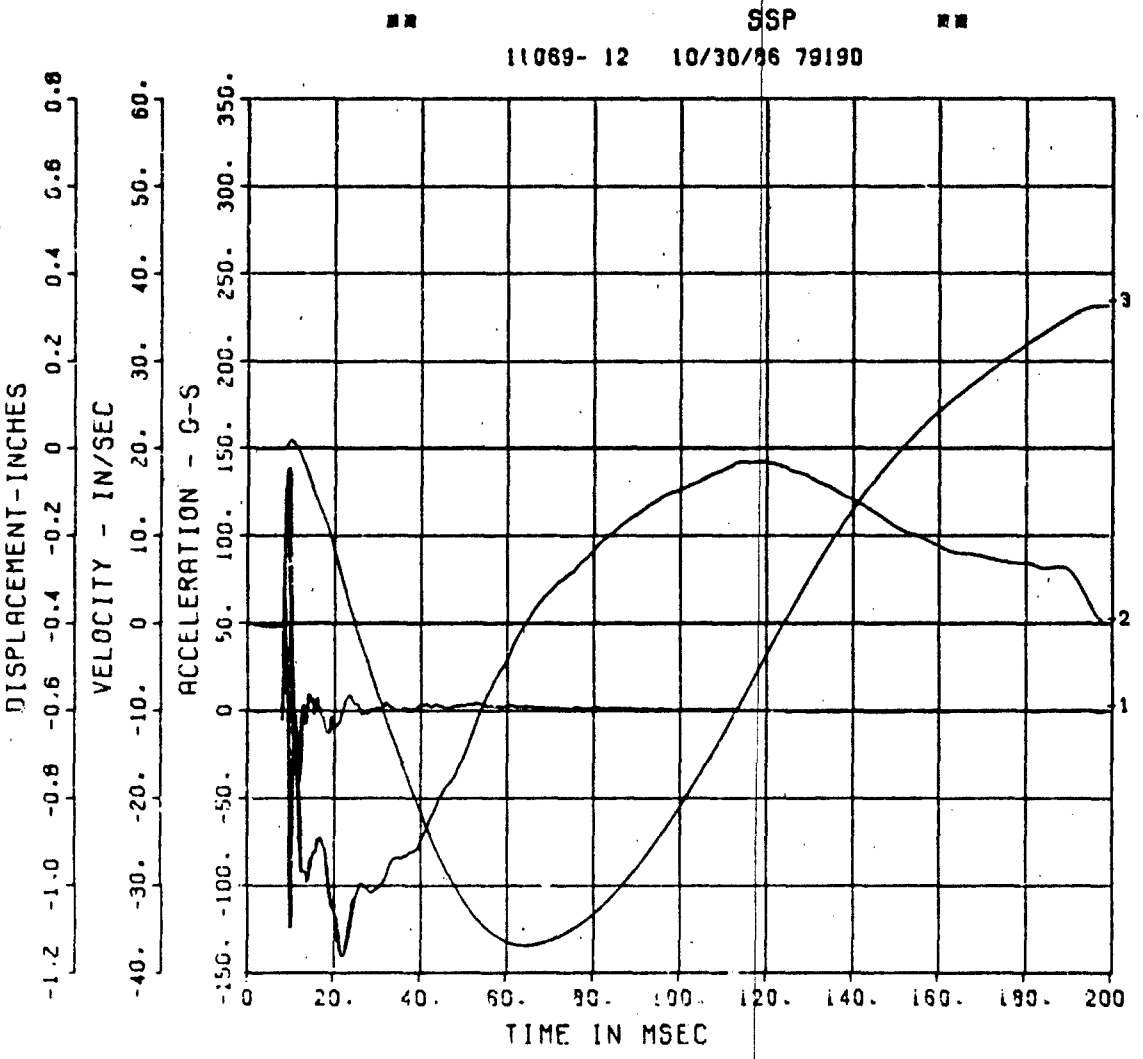

FEMA KEYWORKER
AF-4
50000. HZ CAL= 217.0
LP4/4 70% CUTOFF= 2250. HZ

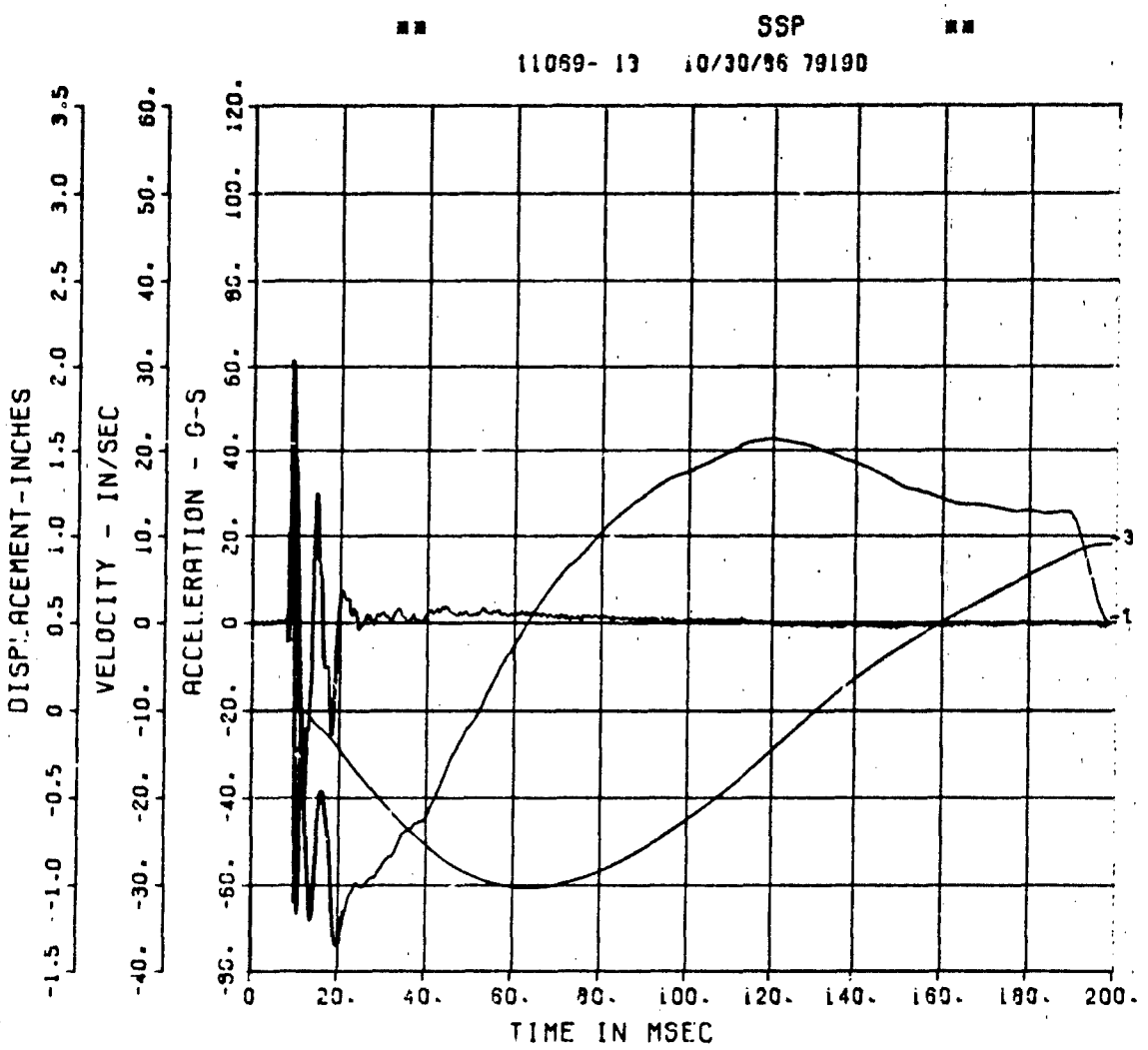

FEMA KEYWORKER
AFF-1
200000. HZ CAL= 432.8

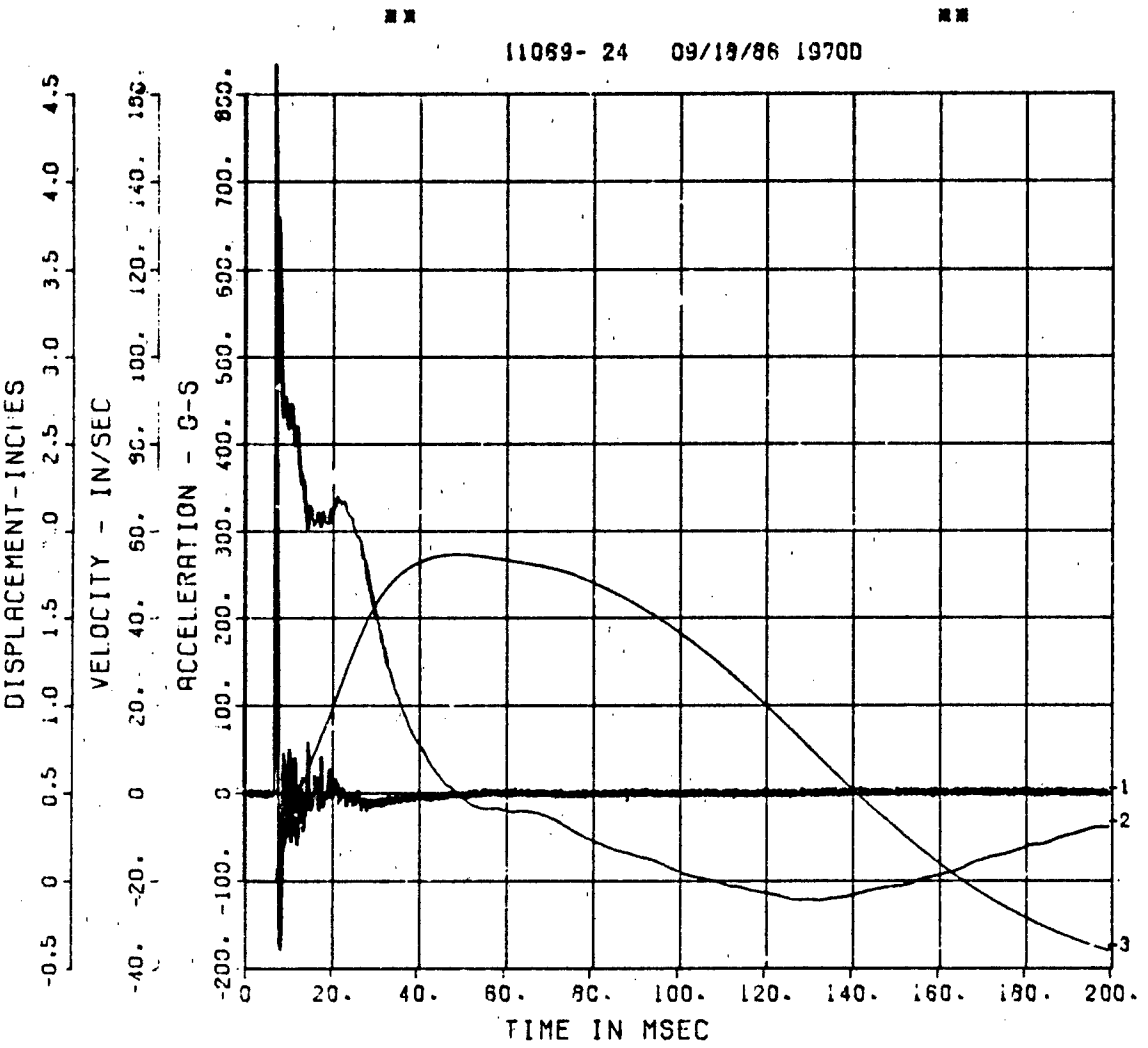

FEMA KEYWORKER
AFF-2
200000. HZ CAL= 194.2

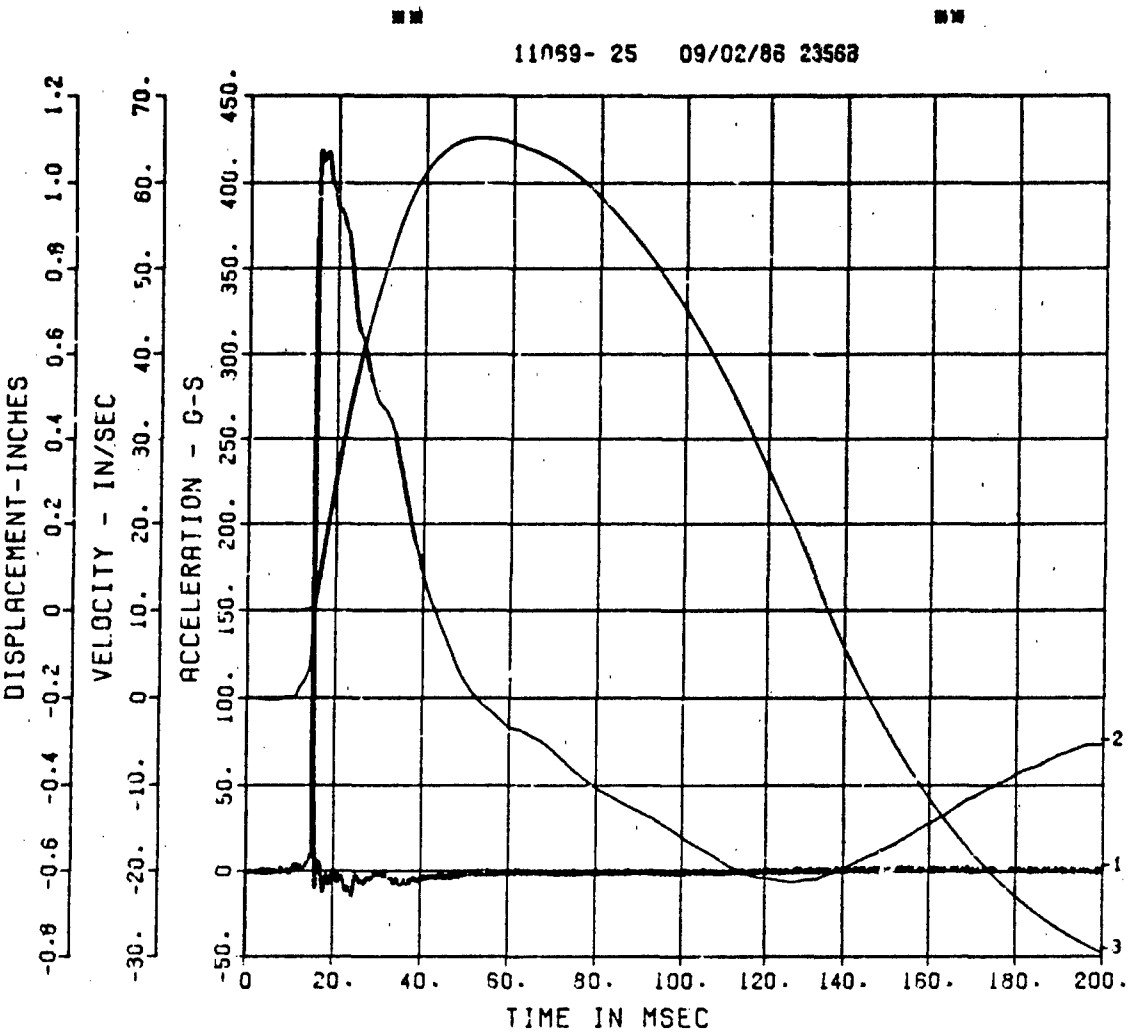

FEMA KEYWORKER
AM1-X
50000. HZ CAL= 8.360
LP4/4 70% CUTOFF= 2250. HZ

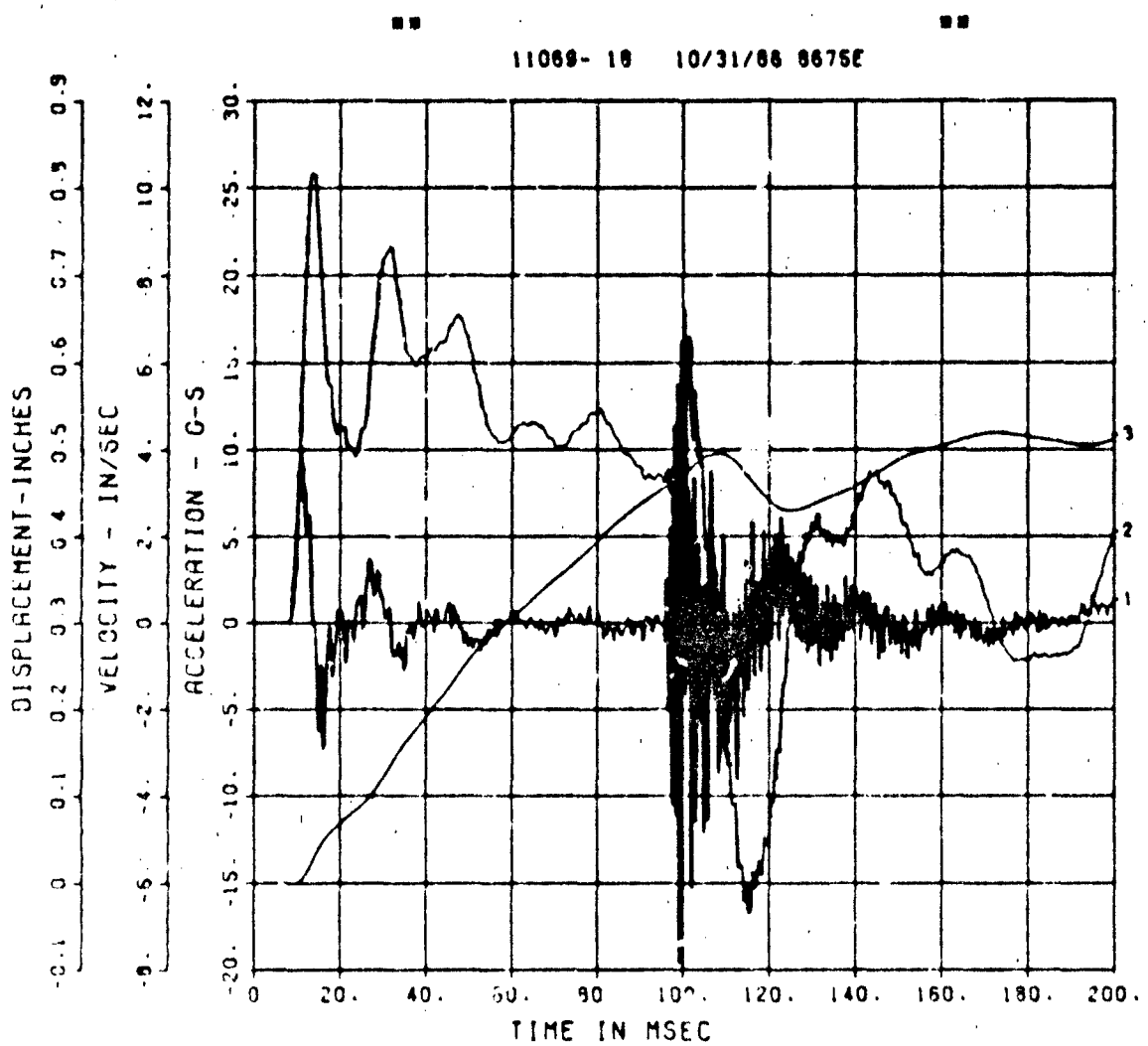

FEMA KEYWORKER
AM1-Y
50000. HZ CAL= 18.34
LP4/4 70% CUTOFF= 2250. HZ

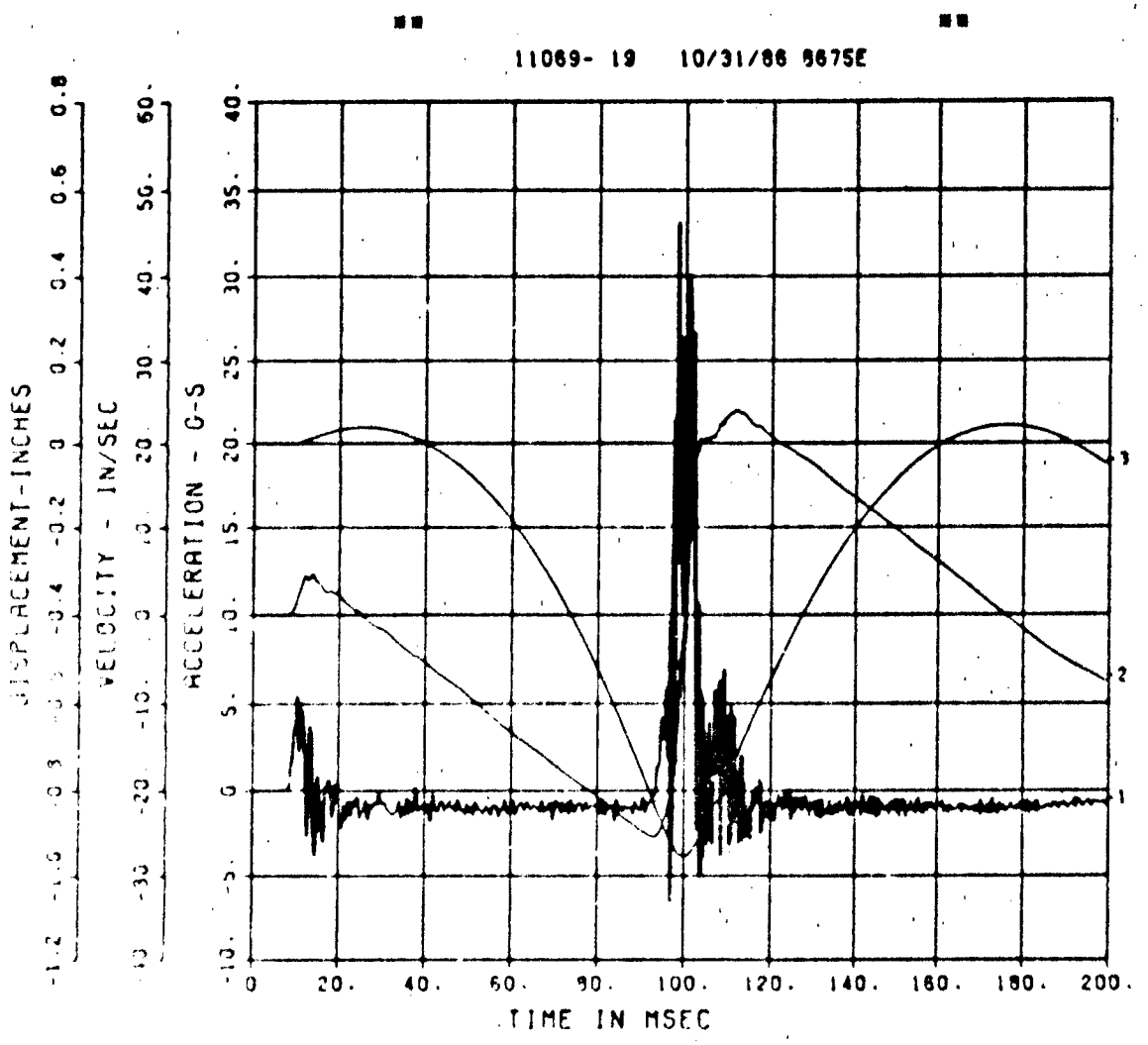

FEMA KEYWORKER
AM1-Z
50000. HZ CAL= 8.080
LP4/4 70% CUTOFF= 2250. HZ

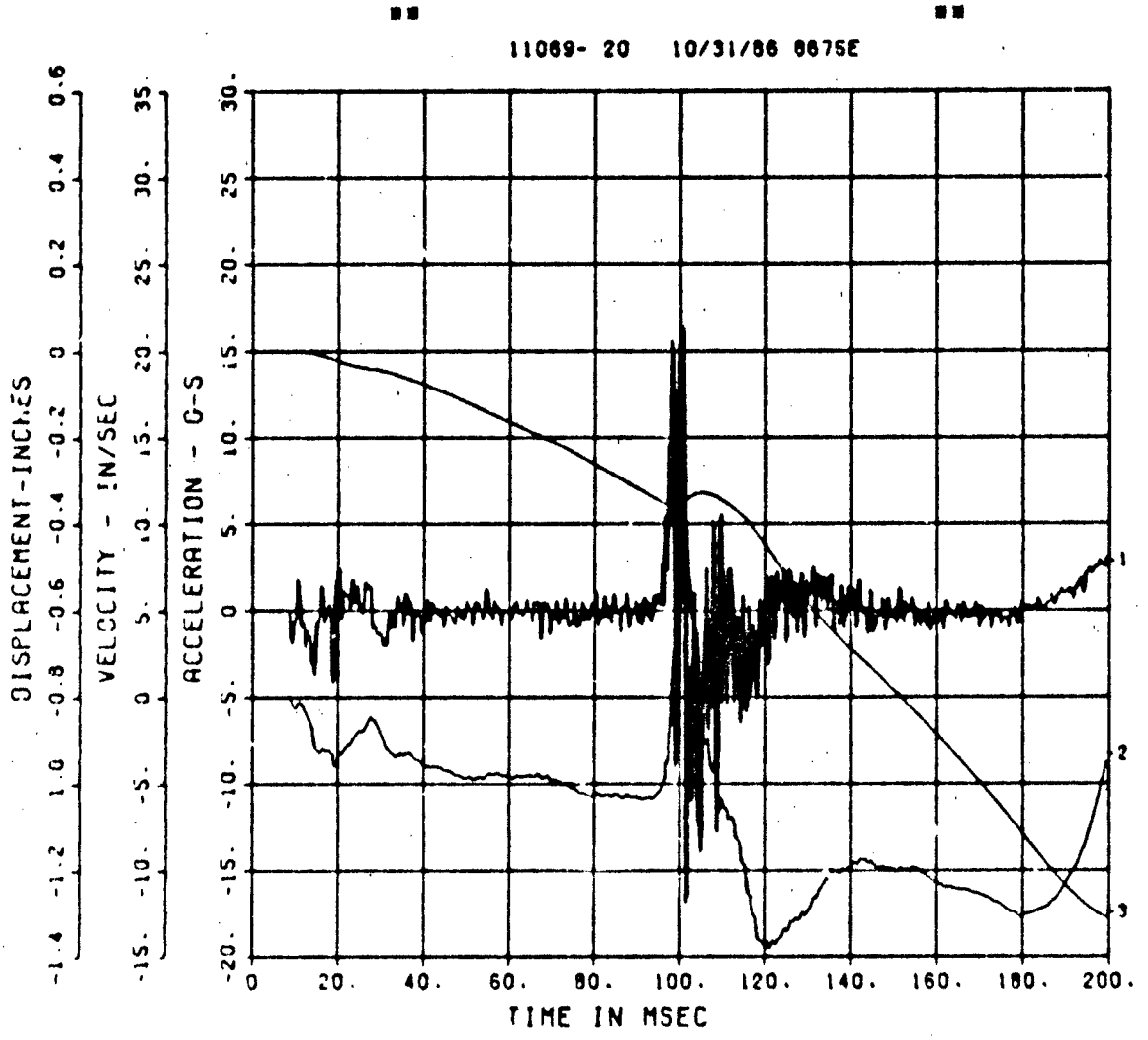

FEMA KEYWORKER
AM2-X
50000. HZ CAL= 7.520
LP4/4 70% CUTOFF= 2250. HZ

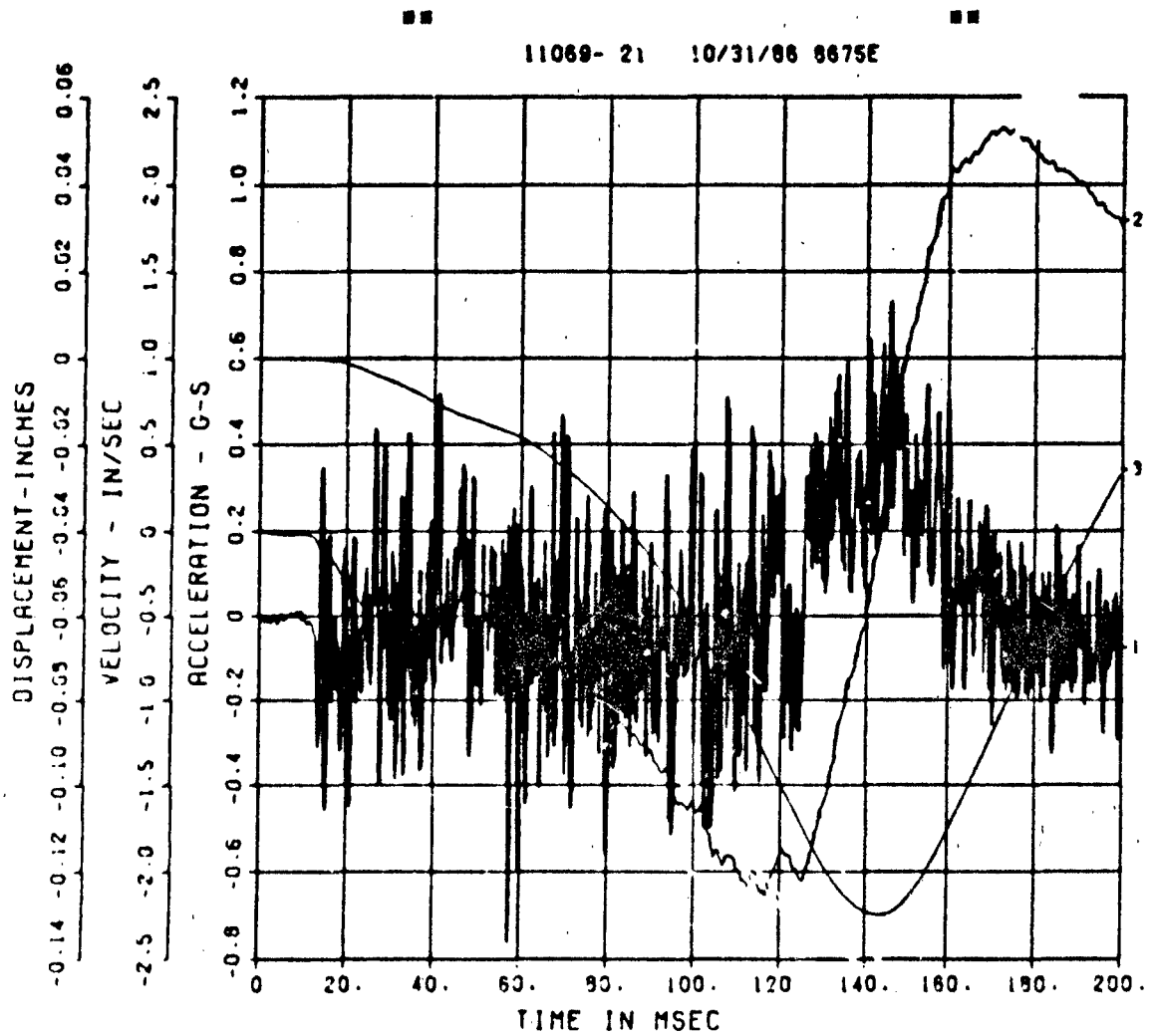

FEMA KEYWORKER
AM2-Y
50000. HZ CAL= 18.30
LP4/4 70% CUTOFF= 2250. HZ

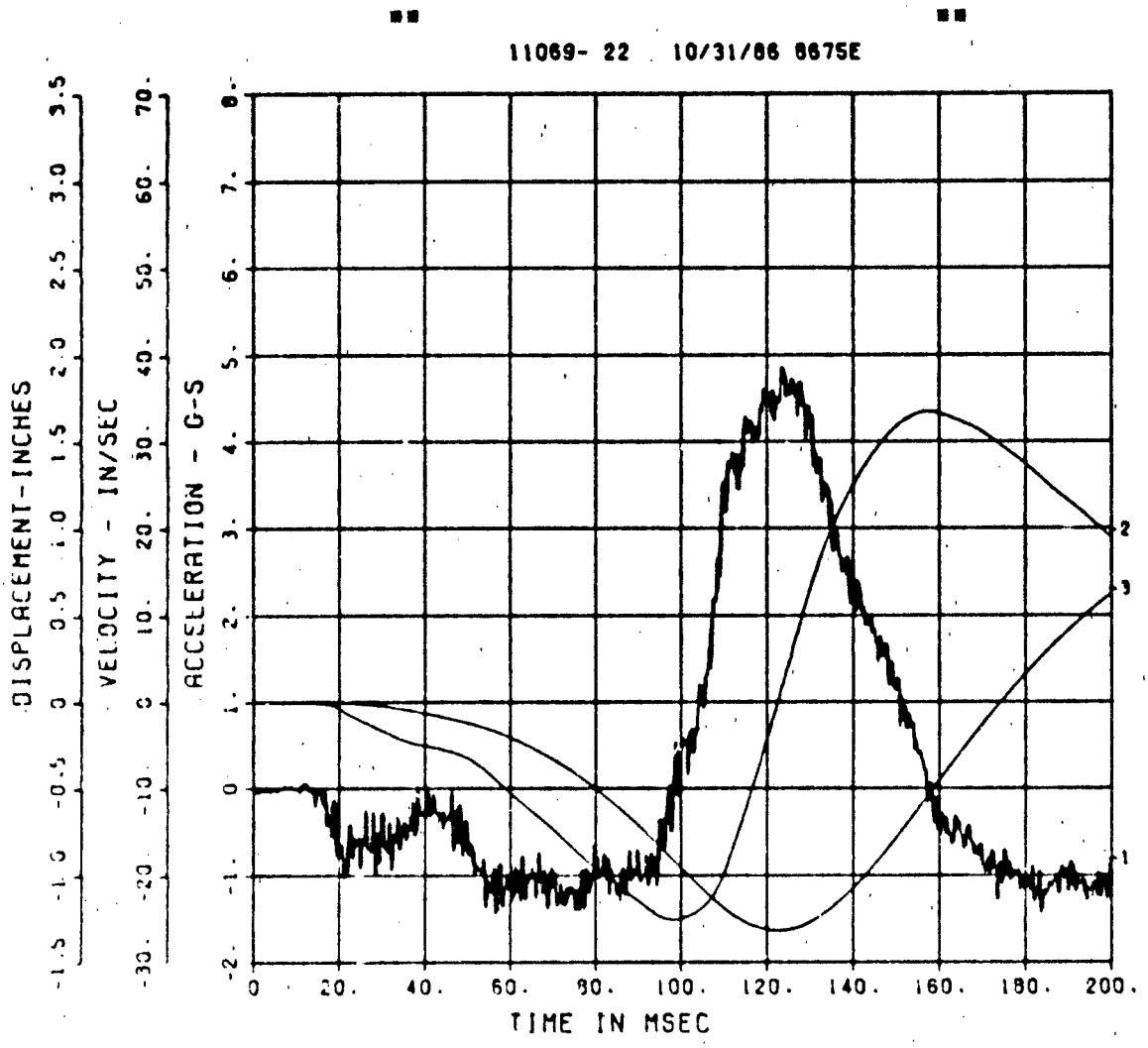

FEMA KEYWORKER
AM2-Z
50000. HZ CAL= 8.640
LP4/4 70% CUTOFF= 2250. HZ

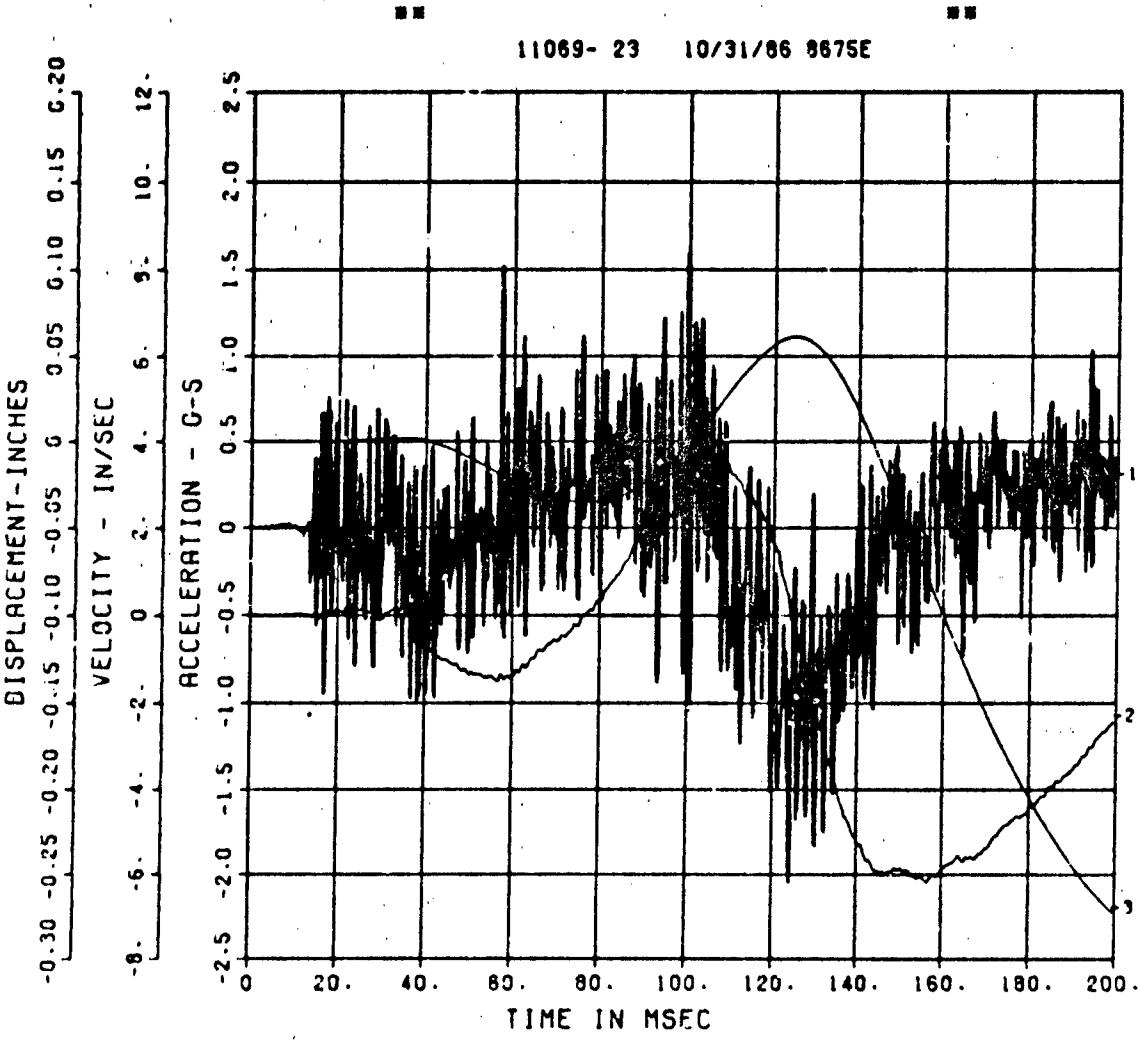

DISTRIBUTION LIST

Director, Federal Emergency Management Agency
10 cy ATTN: Mr. Jim Jacobs
500 C St. SW
Washington, DC 20472

Commander, US Army Engineer District, Wilmington
ATTN: Pat Burns/Library
PO Box 1890
Wilmington, N. C. 28402

Headquarters, Department of Energy
ATTN: Library/G-069 MA-232.2/GTN
Washington, DC 20545

National Bureau of Standards
ATTN: Mr. Samuel Kramer
Dr. Lewis V. Spencer
Washington, DC 20234

Associate Director, Natural Resources and
Commercial Services
Office of Science & Technology
ATTN: Mr. Phillip M. Smith
Executive Office Building
Washington, DC 20500

Director, Office of Administration
Program Planning and Control
Department of Housing and Urban Development
ATTN: Mr. Bert Greenglass
Washington, DC 20410

Director, Defense Nuclear Agency
ATTN: SPTD/Mr. Tom Kennedy
STTL/Technical Library
Washington, DC 20305

Director, Defense Intelligence Agency
ATTN: Mr. Carl Wiehle (DB-4C2)
Washington, DC 20301

Assistant Secretary of the Army (R&D)
ATTN: Assistant for Research
Washington, DC 20301

Office, Chief of Engineers,
Department of the Army
ATTN: DAEN-RDZ-A
DAEN-ECE-D
Washington, DC 20314

Sandia Corporation
ATTN: Dr. Clarence R. Mehl
Dept. 5230
Box 5800, Sandia Base
Albuquerque, N. Mex. 87115

Director, US Army Engineer Waterways
Experiment Station
ATTN: Dr. S. A. Kiger
Mr. Bill Huff
10 cy Mr. Tom Slawson
3 cy Library
PO Box 631
Vicksburg, Miss. 39180

Defense Technical Information Center
12 cy ATTN: (DTIC-DDAB/Mr. Myer B. Kahn)
Cameron Station
Alexandria, Va. 22314

Commander, US Army Materials and Mechanics
Research Center
ATTN: Technical Library
Watertown, Mass. 02172

Command and Control Technical Center
Department of Defense
Room 3E312 Pentagon
Washington, DC 20301

Oak Ridge National Laboratory
2 cy ATTN: Mr. Conrad Chester
Mr. Greg Zimmerman
PO Box X
Oak Ridge, Tenn. 37831

Los Alamos Scientific Laboratory
ATTN: Report Library MS-364
PO Box 1663
Los Alamos, N. Mex. 87544

Director, Ballistic Research Laboratory
ATTN: (DRXBR-TBD/Mr. George Coulter)
Aberdeen Proving Ground, Md. 21005

Commanding Officer, Office of Naval Research
Department of the Navy
Washington, DC 20390

Commanding Officer
US Naval Civil Engineering Laboratory
Naval Construction Battalion Center
ATTN: Library (Code L08A)
Port Hueneme, Calif. 93043

Commander, Air Force Weapons Laboratory/SUL
ATTN: Technical Library
Kirtland Air Force Base, N. Mex. 87117

Civil Engineering Center
AF/RECET
Tyndall AFB, Fla. 32403

University of Florida
Civil Defense Technical Services
College of Engineering
Department of Engineering
Gainesville, Fla. 32601

Technical Reports Library
Kurt F. Wendt Library
College of Engineering
University of Wisconsin
Madison, Wisc. 53706

Agbabian Associates
250 N. Nash Street
El Segundo, Calif. 90245

AT&T Bell Laboratories
ATTN: Mr. E. Witt
Whippany, N. J. 07981

James E. Beck & Associates
4216 Los Palos Avenue
Palo Alto, Calif. 94306

Chamberlain Manufacturing Corp.
GARD, Inc.
7449 N. Natchez Avenue
Niles, Ill. 60648

ITT Research Institute
ATTN: Mr. A. Longinow
10 West 35th Street
Chicago, Ill. 60616

H. L. Murphy Associates
Box 1727
San Mateo, Calif. 94401

RAND Corporation
ATTN: Document Library
1700 Main Street
Santa Monica, Calif. 90401

Research Triangle Institute
ATTN: Mr. Edward L. Hill
PO Box 12194
Research Triangle Park, N. C. 27709

Scientific Services, Inc.
517 East Bayshore Drive
Redwood City, Calif. 94060

US Army Engineer Division, Huntsville
10 cy ATTN: Mr. Paul Lahoud
PO Box 1600, West Station
Huntsville, Ala. 35807

VULNERABILITY EVALUATION OF THE KEYWORKER BLAST SHELTER, Unclassified, US Army Engineer Waterways Experiment Station, April 1987, 114 pp.

The 100-man Keyworker blast shelter that survived MINOR SCALE (a high explosive event) was retested using the High Explosive Simulation Technique (HEST) in August 1986. The test was conducted at White Sands Missile Range, N. Mex. The existing structure sustained minor damage (1/8-inch permanent midspan deflection) during MINOR SCALE at the predicted 75-psi peak overpressure level, and a retest was proposed to investigate the shelter's large deformation behavior.

The shelter was tested using a 1-MT nuclear weapon simulation at 130- to 160-psi (depending on the duration of the simulation). The shelter survived the test with large plastic roof deformations ranging from 8 to 17 inches at roof midspan. The failure mode of the shelter roof was very ductile, and the shelter had adequate reserve capacity to withstand large deformations without catastrophic failure.

Survivability of occupants and mechanical equipment at this overpressure was investigated. The mechnical equipment inside the shelter was fully functional after the test except for the roof-mounted fluorescent light fixtures. In-structure shock was within acceptable limits for shelter occupants, and high-speed movies of the mannequin movement reinforced this conclusion.

Based on this test result, it is concluded that the shelter performed as designed in the buried configuration under ideal backfill conditions. Additional scale model tests validated the shelter design in the bermed configuration and in various backfill types.

VULNERABILITY EVALUATION OF THE KEYWORKER BLAST SHELTER, Unclassified, US Army Engineer Waterways Experiment Station, April 1987, 114 pp.

The 100-man Keyworker blast shelter that survived MINOR SCALE (a high explosive event) was retested using the High Explosive Simulation Technique (HEST) in August 1986. The test was conducted at White Sands Missile Range, N. Mex. The existing structure sustained minor damage (1/8-inch permanent midspan deflection) during MINOR SCALE at the predicted 75-psi peak overpressure level, and a retest was proposed to investigate the shelter's large deformation behavior.

The shelter was tested using a 1-MT nuclear weapon simulation at 130- to 160-psi (depending on the duration of the simulation). The shelter survived the test with large plastic roof deformations ranging from 8 to 17 inches at roof midspan. The failure mode of the shelter roof was very ductile, and the shelter had adequate reserve capacity to withstand large deformations without catastrophic failure.

Survivability of occupants and mechanical equipment at this overpressure was investigated. The mechnical equipment inside the shelter was fully functional after the test except for the roof-mounted fluorescent light fixtures. In-structure shock was within acceptable limits for shelter occupants, and high-speed movies of the mannequin movement reinforced this conclusion.

Based on this test result, it is concluded that the shelter performed as designed in the buried configuration under ideal backfill conditions. Additional scale model tests validated the shelter design in the bermed configuration and in various backfill types.

VULNERABILITY EVALUATION OF THE KEYWORKER BLAST SHELTER, Unclassified, US Army Engineer Waterways Experiment Station, April 1987, 114 pp.

The 100-man Keyworker blast shelter that survived MINOR SCALE (a high explosive event) was retested using the High Explosive Simulation Technique (HEST) in August 1986. The test was conducted at White Sands Missile Range, N. Mex. The existing structure sustained minor damage (1/8-inch permanent midspan deflection) during MINOR SCALE at the predicted 75-psi peak overpressure level, and a retest was proposed to investigate the shelter's large deformation behavior.

The shelter was tested using a 1-MT nuclear weapon simulation at 130- to 160-psi (depending on the duration of the simulation). The shelter survived the test with large plastic roof deformations ranging from 8 to 17 inches at roof midspan. The failure mode of the shelter roof was very ductile, and the shelter had adequate reserve capacity to withstand large deformations without catastrophic failure.

Survivability of occupants and mechanical equipment at this overpressure was investigated. The mechnical equipment inside the shelter was fully functional after the test except for the roof-mounted fluorescent light fixtures. In-structure shock was within acceptable limits for shelter occupants, and high-speed movies of the mannequin movement reinforced this conclusion.

Based on this test result, it is concluded that the shelter performed as designed in the buried configuration under ideal backfill conditions. Additional scale model tests validated the shelter design in the bermed configuration and in various backfill types.